

Transport processes in the arbuscular mycorrhizal symbiosis

Dissertation

zur Erlangung des akademischen Grades

doctor rerum naturalium

(Dr. rer. nat.)

in der Wissenschaftsdisziplin

Molekulare Pflanzenphysiologie

eingereicht an der

Mathematisch-Naturwissenschaftlichen Fakultät

der Universität Potsdam

von

Nina Duensing

geboren am 06.05.1983 in Hannover

Potsdam, Mai 2013



MAX-PLANCK-GESELLSCHAFT

Published online at the
Institutional Repository of the University of Potsdam:
URL <http://opus.kobv.de/ubp/volltexte/2013/6821/>
URN <urn:nbn:de:kobv:517-opus-68210>
<http://nbn-resolving.de/urn:nbn:de:kobv:517-opus-68210>

TABLE OF CONTENTS

Table of Contents	I
Abbreviations	VI
Summary	VIII
Zusammenfassung	IX
1 Introduction	1
1.1 The arbuscular mycorrhizal symbiosis	1
1.1.1 Nutrient exchange in the AM symbiosis.....	3
1.1.2 AM-induced changes of plant gene expression and metabolite composition.....	5
1.1.3 Fungal transport processes involved in the AM symbiosis	6
1.2 Research objectives	9
2 Materials and Methods	10
2.1 Materials	10
2.1.1 Chemicals.....	10
2.1.1.1 Enzymes	10
2.1.1.2 Reaction kits	11
2.1.1.3 Antibiotics	11
2.1.1.4 Buffers and solutions	12
2.1.1.5 Other chemicals	14
2.1.2 Growth media.....	15
2.1.2.1 Bacterial growth media.....	15
2.1.2.2 Plant growth substrates, media and solutions	16
2.1.3 Biological material.....	18
2.1.4 Plasmids	18
2.1.5 Oligonucleotides	19
2.2 Methods	20
2.2.1 Plant growth and transformation of <i>Medicago truncatula</i>	20
2.2.1.1 Stratification, surface sterilization and germination of seeds	20
2.2.1.2 Inoculation with <i>Rhizophagus irregularis</i>	20
2.2.1.3 Nodulation of <i>Medicago truncatula</i> plants.....	20
2.2.1.4 Plant growth conditions.....	21
2.2.1.5 <i>Agrobacterium rhizogenes</i> mediated plant root transformation	21

2.2.1.6	<i>Nicotiana benthamiana</i> leaf infiltration with transformed <i>Agrobacterium tumefaciens</i>	21
2.2.2	In vitro cultivation of <i>Rhizophagus irregularis</i>	22
2.2.2.1	<i>Medicago truncatula</i> root organ culture	22
2.2.2.2	Isolation of fungal spores and hyphae	22
2.2.3	Biomolecular methods	22
2.2.3.1	Cloning strategies and preparation of plasmids	22
2.2.3.2	Transformation of microorganisms	24
2.2.3.3	DNA isolation methods	25
2.2.3.4	RNA isolation methods	25
2.2.3.5	cDNA synthesis	26
2.2.3.6	Polymerase-chain-reaction (PCR)	26
2.2.3.7	Sample preparation for Illumina sequencing	27
2.2.4	Biochemical methods	27
2.2.4.1	<i>MtHxt1 Tnt1</i> metabolic profiling analysis	27
2.2.4.2	GUS staining	29
2.2.4.3	Staining of fungal structures in roots	29
2.2.4.4	<i>In situ</i> hybridization	29
2.2.5	Microscopy	30
2.2.5.1	Cryosectioning and laser capture microdissection (LCM)	30
2.2.5.2	Vibratome sectioning	31
2.2.5.3	Epifluorescence and confocal microscopy	31
2.2.6	Bioinformatic methods	32
2.2.6.1	Processing of metabolic profiling data	32
2.2.6.2	Processing of Illumina SBS high-throughput sequencing data	32
3	Results	35
3.1	Characterization of cell type-specifically regulated <i>Medicago truncatula</i> genes involved in transport mechanisms	35
3.1.1	Selection and confirmation of candidate genes	36
3.1.1.1	Transcriptional regulation of the putative transporter genes in mycorrhizal roots	38
3.1.1.2	Cell-specific promoter activity of the transporter candidate genes	39
3.1.1.3	Potential transporter genes were confirmed to be cell-specifically regulated during AM symbiosis	43
3.1.2	Putative carbohydrate transporters with transcriptional regulation in mycorrhizal roots	43
3.1.2.1	Sugar transporters are cell-specifically regulated	43

3.1.2.2	Further genes involved in major carbohydrate metabolism with transcriptional regulation in mycorrhizal roots	47
3.2	The influence of the <i>MtHxt1</i> knock-out on the mycorrhizal interaction and primary metabolites in <i>M. truncatula</i>	49
3.2.1	Characterization of <i>MtHxt1</i> knock-out plants	49
3.2.2	Influence of the <i>MtHxt1</i> knock-out on the mycorrhizal symbiosis.....	51
3.2.2.1	Phenotypic and molecular characterization of <i>hxt1</i> plants	51
3.2.2.2	Primary metabolite changes in <i>hxt1</i> plants	54
3.3	Identification of <i>in planta</i> expressed <i>Rhizophagus irregularis</i> transporter genes	61
3.3.1	<i>Rhizophagus irregularis</i> transcriptome sequencing.....	61
3.3.1.1	Isolation of <i>Rhizophagus irregularis</i> RNA	61
3.3.1.2	Identification of differentially expressed genes.....	62
3.3.1.3	Identification and annotation of potential transporter gene candidates	64
3.3.2	Characterization of AM-specifically expressed <i>Rhizophagus irregularis</i> transporter genes	66
3.3.2.1	Confirmation of transcriptional regulation during root colonization.....	66
3.3.2.2	Identification of full length transcript sequences of transporter candidate genes...	68
3.3.2.3	<i>In situ</i> localization of candidate transcripts	70
3.3.2.4	Potential <i>Rhizophagus irregularis</i> transporter encoding genes are specifically regulated <i>in planta</i>	72
4	Discussion.....	73
4.1	AM-specifically regulated genes involved in transport processes and carbohydrate metabolism give new insight into transport processes during the symbiosis	73
4.1.1	Several transporter genes are AM-specifically regulated	73
4.1.2	Carbohydrates are mobilized and symplastically provided to the arbuscule-containing cells	75
4.1.3	AM-specifically regulated genes involved in carbohydrate metabolism and transport provide new insight into carbohydrate allocation in mycorrhizal roots	77
4.1.4	Outlook: AM specifically regulated transporter genes in <i>Medicago truncatula</i> .	78
4.2	<i>MtHxt1</i> influences the mycorrhizal interaction and primary metabolism of <i>Medicago truncatula</i>.....	79
4.2.1	Mycorrhizal colonization leads to metabolic changes in <i>hxt1</i> and WT <i>Medicago truncatula</i> plants	79
4.2.2	Mycorrhizal colonization of <i>hxt1</i> and WT <i>Medicago truncatula</i> plants leads to changes in the primary metabolite profile in roots and source leaves	82

4.2.3	Outlook: <i>hxt1</i> metabolite profiling.....	83
4.3	<i>Rhizophagus irregularis</i> transcriptome analyses reveal previously unknown fungal transporter genes involved in the AM symbiosis	84
4.3.1	Potential fungal transporter genes are specifically regulated <i>in planta</i>	84
4.3.2	SBS RNA sequencing of LCM-collected arbuscules identifies specifically regulated <i>Rhizophagus irregularis</i> transporter genes	87
4.3.3	Outlook: <i>in planta</i> transcriptome of <i>Rhizophagus irregularis</i>	87
5	Table of Figures.....	89
6	Literature.....	91
7	Supplementary	99
7.1	Oligonucleotides used in this study	99
7.2	<i>M. truncatula</i> transporter genes	103
7.2.1	<i>hxt1</i> phenotype	105
7.3	<i>R. irregularis</i> sequencing	108
7.3.1	The coding sequence of the following <i>R. irregularis</i> genes have been confirmed	111
8	Acknowledgements	113
9	Eidesstattliche Erklärung.....	114

Parts of this work were published in

Gaude N, Bortfeld S, Duensing N, Lohse M, Krajinski F (2012) Arbuscule-containing and non-colonized cortical cells of mycorrhizal roots undergo extensive and specific reprogramming during arbuscular mycorrhizal development. *Plant J* 69: 510-528

ABBREVIATIONS

AM	arbuscular mycorrhizal
ARB	arbuscule-containing cells
AS	acetosyringone
BCIP	5-bromo-4-chloro-3-indolyl phosphate
bp	base pairs
CDS	coding sequence
cDNA	complementary deoxyribonucleic acid
COR	cortical cells of non-mycorrhizal roots
Ct	threshold cycle
CTAB	hexadecyl-trimethyl-ammonium bromide
dATP	deoxyadenosine triphosphate
ddH ₂ O	double distilled water
DEPC	diethylpyrocarbonate
DIG	digoxigenin
DMF	dimethylformamide
DNA	deoxyribonucleic acid
DNase	deoxyribonuclease
dNTPs	deoxyribonucleotides
dpi	days post inoculation
dsRNA	double stranded ribonucleic acid
DTT	dithiothreitol
EDC	1-ethyl-3-(3-dimethylaminopropyl) carbodiimide
EDTA	ethylenediaminetetraacetic acid
ERM	extraradical mycelium
EST	expressed sequence tag
<i>et al.</i>	and others
EtBr	ethidium bromide
EtOH	ethanol
GC-EI/TOF-MS	gas chromatography coupled impact ionization/time-of-flight mass spectrometry
gDNA	genomic deoxyribonucleic acid
GFP	green fluorescent protein
GUS	β -glucuronidase
h	hour
IC	independent component
ICA	independent component analysis
IRM	intraradical mycelium
kb	kilo base pairs
LCM	laser capture microdissection
LFC	\log_2 -fold change
Mb	mega base pairs
MES	2-(N-morpholino) ethanesulfonic acid

MOPS	3-morpholinopropane-1-sulfonic acid
mRNA	messenger ribonucleic acid
MSTs	mass spectral tags of metabolites or metabolite derivatives
myc	mycorrhizal
NAC	non-arbuscule-containing cells of mycorrhizal roots
NBT/BCIP	nitro blue tetrazolium chloride/ 5-Bromo-4-chloro-3-indolyl phosphate, toluidine salt
NGS	next-generation sequencing
nt	nucleotides
nm	non-mycorrhizal
nonmyc	non-mycorrhizal
<i>nptII</i>	neomycin phosphotransferase II
ORF	open reading frame
PAM	periarbuscular membrane
PAS	periarbuscular space
PBS	phosphate buffered saline
PC	principal component
PCR	polymerase chain reaction
PFA	paraformaldehyd
P _i	orthophosphate
PPA	prepenetration apparatus
qRT-PCR	quantitative reverse transcription PCR
ROC	root organ culture
RNA	ribonucleic acid
RNA _i	RNA interference
RNase	ribonuclease
rpm	rotations per minute
rRNA	ribosomal ribonucleic acid
RT	room temperature
SBS	sequencing by synthesis
TAE	Tris-acetate-EDTA
TBS	Tris-buffered saline
TMD	transmembrane domain
Tris	Tris(hydroxymethyl)aminomethane
<i>Tnt1</i>	transposon 1 of <i>Nicotiana tabacum</i>
UTR	untranslated region
X-gal	5-bromo-4-chloro-indolyl-β-D-galactopyranoside
X-Gluc	5-Bromo-4-chloro-1 <i>H</i> -indol-3-yl β-D-glucopyranosiduronic acid
w/v	weight/volume
wpi	weeks post-inoculation
WT	wild-type
v/v	volume/volume
Vol	volume

SUMMARY

The nutrient exchange between plant and fungus is the key element of the arbuscular mycorrhizal (AM) symbiosis. The fungus improves the plant's uptake of mineral nutrients, mainly phosphate, and water, while the plant provides the fungus with photosynthetically assimilated carbohydrates. Still, the knowledge about the mechanisms of the nutrient exchange between the symbiotic partners is very limited. Therefore, transport processes of both, the plant and the fungal partner, are investigated in this study. In order to enhance the understanding of the molecular basis underlying this tight interaction between the roots of *Medicago truncatula* and the AM fungus *Rhizophagus irregularis*, genes involved in transport processes of both symbiotic partners are analysed here.

The AM-specific regulation and cell-specific expression of potential transporter genes of *M. truncatula* that were found to be specifically regulated in arbuscule-containing cells and in non-arbusculated cells of mycorrhizal roots was confirmed. A model for the carbon allocation in mycorrhizal roots is suggested, in which carbohydrates are mobilized in non-arbusculated cells and symplastically provided to the arbuscule-containing cells. New insights into the mechanisms of the carbohydrate allocation were gained by the analysis of hexose/H⁺ symporter *MtHxt1* which is regulated in distinct cells of mycorrhizal roots. Metabolite profiling of leaves and roots of a knock-out mutant, *hxt1*, showed that it indeed does have an impact on the carbohydrate balance in the course of the symbiosis throughout the whole plant, and on the interaction with the fungal partner. The primary metabolite profile of *M. truncatula* was shown to be altered significantly in response to mycorrhizal colonization.

Additionally, molecular mechanisms determining the progress of the interaction in the fungal partner of the AM symbiosis were investigated. The *R. irregularis* transcriptome *in planta* and in extraradical tissues gave new insight into genes that are differentially expressed in these two fungal tissues. Over 3200 fungal transcripts with a significantly altered expression level in laser capture microdissection-collected arbuscules compared to extraradical tissues were identified. Among them, six previously unknown specifically regulated potential transporter genes were found. These are likely to play a role in the nutrient exchange between plant and fungus. While the substrates of three potential MFS transporters are as yet unknown, two potential sugar transporters are might play a role in the carbohydrate flow towards the fungal partner.

In summary, this study provides new insights into transport processes between plant and fungus in the course of the AM symbiosis, analysing *M. truncatula* on the transcript and metabolite level, and provides a dataset of the *R. irregularis* transcriptome *in planta*, providing a high amount of new information for future works.

ZUSAMMENFASSUNG

In der arbuskulären Mykorrhiza (AM) Symbiose werden die Wurzeln fast aller Landpflanzen von Pilzen der Abteilung Glomeromycota besiedelt. Der Pilz erleichtert der Pflanze die Aufnahme von Mineralien, hauptsächlich Phosphat, und Wasser. Im Gegenzug versorgt die Pflanze ihn mit Photoassimilaten. Trotz der zentralen Bedeutung der Austauschmechanismen zwischen Pilz und Pflanze ist nur wenig darüber bekannt. Um die molekularen Grundlagen der Interaktion zwischen den Wurzeln der Leguminose *Medicago truncatula* und dem arbuskulären Mykorrhizapilz *Rhizophagus irregularis* besser zu verstehen, werden hier die Transportprozesse, die zwischen den Symbiosepartnern ablaufen, näher untersucht.

Die zellspezifische Regulation der Transkription potentieller *M. truncatula* Transporter Gene in arbuskelhaltigen und nicht-arbuskelhaltigen Zellen mykorrhizierter Wurzeln wird bestätigt. Ein Modell zur möglichen Verteilung von Kohlenhydraten in mykorrhizierten Wurzeln, nach dem Zucker in nicht-arbuskelhaltigen Zellen mobilisiert und symplastisch an arbuskelhaltige Zellen abgegeben werden, wird vorgestellt. Die Analyse eines Mykorrhiza-induzierten Hexose/H⁺ Symporter Gens, *MtHxt1*, liefert neue Einsichten in die Mechanismen der Kohlenhydratverteilung in mykorrhizierten Pflanzen. Metabolitanalysen von Wurzeln und Blättern einer *knock-out* Mutante dieses Gens zeigen dessen Einfluss auf den Kohlenhydrathaushalt der ganzen Pflanze und auf die Interaktion mit dem Pilz. Die Metabolitzusammensetzung von *M. truncatula* wird durch die Mykorrhiza Symbiose signifikant beeinflusst.

Darüber hinaus werden durch Transkriptomanalysen die molekularen Grundlagen der AM Symbiose auf der Seite des Pilzes analysiert. Arbuskeln wurden mittels *Laser Capture Mikrodisektion* direkt aus mykorrhizierten Wurzeln isoliert. Über 3200 pilzliche Transkripte weisen in diesen Arbuskeln im Vergleich zu extraradikalen Geweben ein deutlich verändertes Expressionslevel auf. Unter diesen Transkripten sind auch sechs zuvor unbekannte Gene, die für potentielle Transporter codieren und mit großer Wahrscheinlichkeit eine Rolle im Nährstoffaustausch zwischen Pilz und Pflanze spielen. Während die Substrate von drei potentiellen MFS Transportern noch unbekannt sind, spielen zwei potentiellen Zuckertransporter möglicherweise eine Rolle im Transport von Kohlenhydraten in Richtung des Pilzes.

Zusammengefasst bietet diese Arbeit neue Einsichten in Transportprozesse zwischen Pilz und Pflanze im Laufe der AM Symbiose. *M. truncatula* Transkript- und Metabolitlevel werden analysiert und die Transkriptomanalyse von *R. irregularis* liefert einen umfassenden Datensatz mit einer großen Menge an Informationen zu der noch unzureichend erforschten pilzlichen Seite der Symbiose für folgende Arbeiten.

1 INTRODUCTION

1.1 The arbuscular mycorrhizal symbiosis

The arbuscular mycorrhizal (AM) symbiosis is an ancient and very widespread interaction between arbuscular mycorrhizal fungi belonging to the phylum of *Glomeromycota* and the roots of the majority of all vascular plants. The origin of the AM symbiosis dates back approximately 500 million years, and it is considered to have played a major role in the colonization of land by plants (Smith and Read, 2008; Corradi and Bonfante, 2012). Due to a bidirectional nutrient exchange this mutual interaction is beneficial for both partners. The plant supplies the fungal partner with carbohydrates while in return the fungus facilitates the plant's uptake of water and mineral nutrients, especially phosphate (Graham, 2000; Strack *et al.*, 2001; Li *et al.*, 2013). Additionally, the symbiosis increases the plant's tolerance to biotic and abiotic stress (Strack *et al.*, 2003).

Next to the beneficial effects of the AM symbiosis on the plants, such as the better acquisition of immobile nutrients and water and the increased stress tolerance, it also has beneficial ecological effects. AM fungi play a role in the formation of stable soil aggregates, improving the water and air permeability of the soil and preventing erosion (Oehl *et al.*, 2003). It was even suggested that the AM symbiosis may serve as a filtration barrier for the transfer of metals to the shoot and therefore might be important for plant survival on heavy metal contaminated soils (Gaur and Adholeya, 2004). Moreover, the symbiosis can greatly contribute to crop productivity and ecosystem sustainability (Gianinazzi *et al.*, 2010). Most importantly, reduced amounts of phosphate fertilization are needed for mycorrhizal plants (Jakobsen, 1995). This is of particular importance since the phosphorus resources are limited. Latest estimations predict that the phosphate reserves worldwide might be depleted 100 to even only 50 years from now if the intensity of the currently applied phosphate fertilization is not reduced (Gilbert, 2009). Also, the excess use of phosphate fertilizers is an important cause of water eutrophication, therefore making the improvement of the phosphate uptake efficiency by plants a desired trait for both ecological and economic reasons (Gianinazzi *et al.*, 2010).

In the course of the AM symbiosis fungal hyphae grow into the apoplast of the plant roots, guided through the prepenetration apparatus (PPA), until they reach the cells of the inner cortex where they grow apoplastically along the root axis (Parniske, 2008). Here, the hyphae penetrate the inner cortical cells where they repeatedly branch dichotomously to form the name giving haustorium-like structures, the arbuscules (from the Latin *arbusculum* = small tree) (figure 1 B). These are considered

to be the actual site of the nutrient exchange between the fungus and the plant. An arbuscule will live for 4 to 5 days before it collapses. The cortex cell can then be colonized again by a new arbuscule. This makes the mycorrhizal interaction an asynchronous process with constant degradation of old arbuscules and re-infection of previously colonized cortex cells, so that arbuscules of all developmental stages are present in one mycorrhizal root at all times (Bonfante and Genre, 2010).

The colonisation by the fungus leads to drastic changes in the cytoplasmic organization of the host cell. The vacuole of arbuscule-containing cells is compartmented, the amount of cell organelles increases, and the nucleus is moved to a central position (Gianinazzi-Pearson, 1996; Hause and Fester, 2005). The arbuscule takes up the largest part of the host cell but stays separated from its cytoplasm by the periarbuscular membrane (PAM) which is continuous with the plant cell membrane (Parniske, 2008) (figure 1 A). The PAM completely surrounds the arbuscule and even though it is derived from the plasma membrane it is characterized by an altered composition (Hause and Fester, 2005; Pumplin and Harrison, 2009). The periarbuscular space (PAS) is the apoplastic space between the PAM and the fungal membrane. It is composed of cell wall material of both the plant and the fungus (Parniske, 2008). Phosphate and other mineral nutrients as well as nitrogen and carbon are exchanged across this symbiotic interface (Delano-Frier and Tejeda-Sartorius, 2008). The H^+ -ATPase activity in the PAM is high to supply the energy for active transport. It accounts for the acidic conditions in the PAS (Guttenberger, 2000; Hause and Fester, 2005)

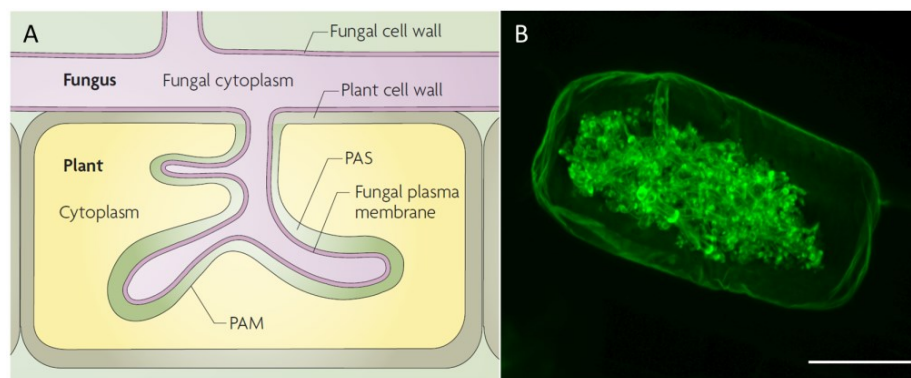


Figure 1: The arbuscule. Fungal hyphae grow into the cells of the inner cortex and form the branched arbuscules. A: Schematic overview. The arbuscule is completely surrounded by the plant derived periarbuscular membrane (PAM) (figure from Parniske, 2008). B: WGA Alexa fluor 488 stained arbuscule of *R. irregularis* in a *M. truncatula* root cell. Scale bar: 20 μ m (Julia Tepy, MPIMP, unpublished).

Still, little is known about the development and the exact composition of the PAM (Pumplin and Harrison, 2009) but given the large surface and the close proximity to the fungus, it appears ideal for the exchange of nutrients between both symbiotic partners. A high amount of genes involved in transport processes have been found to be specifically induced in mycorrhizal roots and in arbuscule-containing cells (Gomez *et al.*, 2009; Hogekamp *et al.*, 2011; Gaude *et al.*, 2012) and AM-specifically expressed transporters have been characterized and shown to be localized in the PAM (Harrison *et al.*, 2002; Pumplin and Harrison, 2009).

1.1.1 Nutrient exchange in the AM symbiosis

The nutrient exchange between the symbiotic partners is the key element of this mutualistic interaction. While AM fungi are obligate biotrophs and cannot complete their life cycle without the host plant, the plants do survive without the fungal partner, but the symbiotic interaction leads to a massive improvement of their growth and fitness (Delano-Frier and Tejeda-Sartorius, 2008).

Besides nitrogen, phosphorus is the most limiting macro nutrient for plant growth and development. It is taken up by plants as inorganic phosphate. Phosphate forms pH-dependent insoluble complexes with positively charged mineral and organic ions, is often adsorbed to soil particles, and diffuses very slowly in the soil as compared to the uptake rate by plants, leading to a depletion zone of soluble phosphate in the rhizosphere (Marschner and Dell, 1994). Therefore, it is scarcely available to the plants, even if the total amount of phosphate in the soil may be high (Smith and Read, 2008). The association with mycorrhizal fungi is one major strategy to facilitate the plant's phosphate acquisition. Through their extensive and far-reaching hyphal network, AM fungi can access higher amounts of phosphate, thus improving the phosphate-status of the plant (Smith and Smith, 2012). Phosphate is taken up from the soil by fungal transporters (Harrison and van Buuren, 1995; Maldonado-Mendoza *et al.*, 2001; Benedetto *et al.*, 2005). It is thought to be moved to the intraradical mycelium (IRM) in the form of polyphosphate and released into the PAS as free phosphate (Bapaume and Reinhardt, 2012). AM-induced plant phosphate transporters like the *Medicago truncatula* MtPT4 are localized in the PAM, importing phosphate into the plant cell (Harrison *et al.*, 2002; Delano-Frier and Tejeda-Sartorius, 2008) (figure 2).

The AM symbiosis is also considered to be an important part of the plant's nitrogen metabolism. Nitrogen is taken up by the extraradical hyphae from the soil primarily as nitrate (NO_3^-) or ammonium (NH_4^+) and translocated toward the IRM as arginine (Govindarajulu *et al.*, 2005; Tian *et al.*, 2010). It is then most likely released into the PAS as ammonium which can be taken up via

ammonium transporters such as GmAMT4;1 in soybean (*Glycine max*) (Kobae *et al.*, 2010) or LjAMT2;2 which is specifically induced in mycorrhizal *Lotus japonicus* roots (Guether *et al.*, 2009). AMT2;2 releases NH_3 instead of NH_4^+ , leading to the suggestion that ammonium might be bound and get deprotonated in the PAS and is released into the plant cell as neutral NH_3 (Guether *et al.*, 2009) (figure 2).

It has been shown that minerals like sulphur and micronutrients like copper and zinc are also made more easily available to the plant by the fungus (Smith and Read, 2003; Parniske, 2008). While the AM-specific regulation of the transcription of *M. truncatula* sulphur transporters has been shown recently (Casieri *et al.*, 2012; Sieh *et al.*, 2013), only little is known about the mechanisms of the transfer of the micronutrients (Smith and Read, 2003). However, an AM-induced putative copper transporter has been identified in *M. truncatula* (Frenzel *et al.*, 2005).

Mineral nutrient transporters mostly require an active transport mechanism, using the energy of the proton electrochemical gradient. Therefore, H^+ -ATPases are induced in mycorrhizal roots (Gianinazzi-Pearson *et al.*, 2000; Krajinski *et al.*, 2002) and are thought to be localized in the PAM to provide the energy for the nutrient uptake from the symbiotic interface (Bapaume and Reinhardt, 2012) (figure 2).

The plant supplies the fungus with up to 20 % of its photosynthetically assimilated carbon (Delano-Frier and Tejeda-Sartorius, 2008). Being an obligate biotroph, the fungus is completely dependent on the carbon supply from the plant. It was shown that the CO_2 assimilation of host plants is enhanced upon mycorrhizal colonization of the roots, ensuring the demand for carbon of the fungus (Boldt *et al.*, 2011). The sink strength of the roots is increased upon mycorrhizal colonization (Blee and Anderson, 1998; Wright *et al.*, 1998) and increasing amounts of carbohydrates are transported to the roots. Sucrose synthase and invertase activity as well as the expression of the corresponding genes were shown to be up-regulated in mycorrhizal roots in *M. truncatula* and other species (Hohnjec *et al.*, 2003; Schaarschmidt *et al.*, 2006; Tejeda-Sartorius *et al.*, 2008). Carbohydrates are primarily taken up into the IRM in the form of hexoses (Shachar-Hill *et al.*, 1995), very small amounts of the transferred carbon may also be transported as sucrose (Delano-Frier and Tejeda-Sartorius, 2008). The exact place and mechanism of the carbon transfer to the fungus are still unknown. A fungal monosaccharide transporter, RiMST2, has recently been identified in *Rhizophagus irregularis*. It can take up glucose and some other hexoses and was shown to be essentially important for a functional symbiosis (Helber *et al.*, 2011). Once inside the IRM, hexoses are either metabolized directly or transported into the extraradical mycelium (ERM) in the form of glycogen (Bago *et al.*, 2000; Bago *et al.*, 2003) (figure 2).

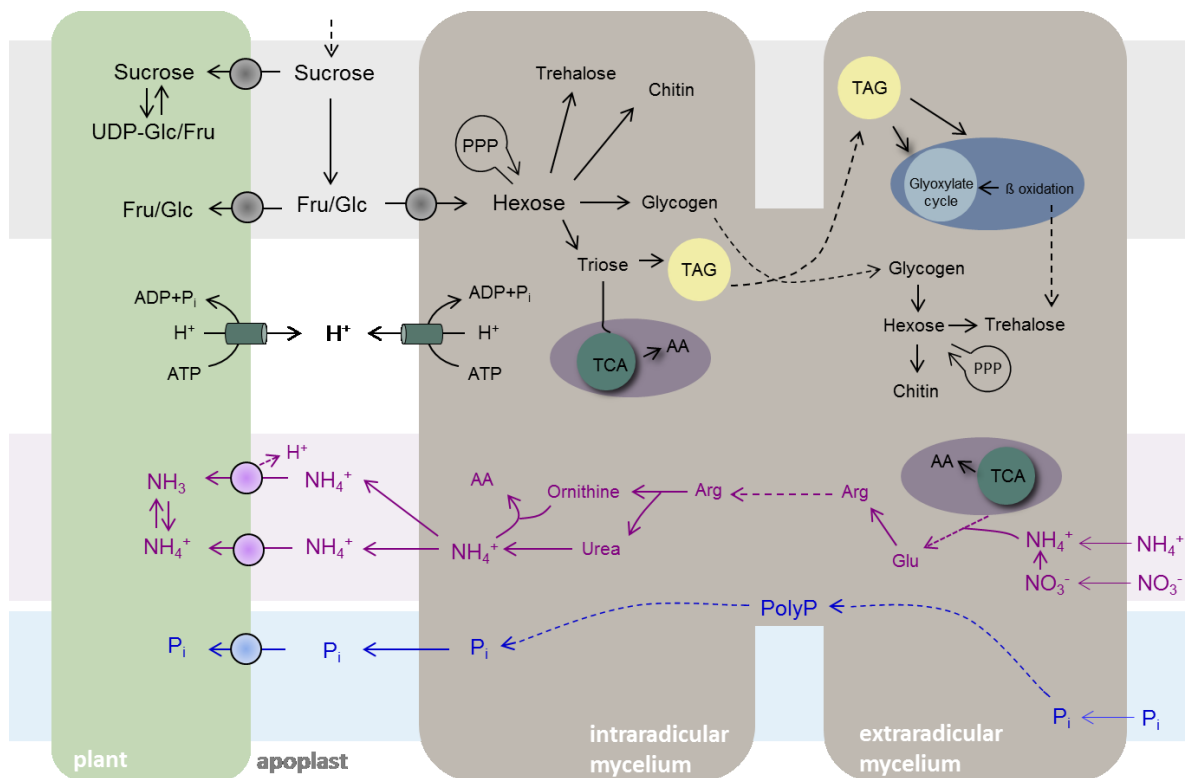


Figure 2: Schematic overview over the nutrient flow in the AM symbiosis. AA: amino acids; PolyP: polyphosphate; PPP: pentose phosphate pathway; TAG: triacylglyceride; TCA: tricarboxylic acid cycle. Modified from Bago *et al.* (2000), Bago *et al.* (2003).

1.1.2 AM-induced changes of plant gene expression and metabolite composition

In the last years, transcriptome and metabolite analyses resulted in a better overview of the effects of the mycorrhizal interaction on the plant. Gomez *et al.* (2009) reported the AM-responsive regulation of over 600 genes in *M. truncatula* roots that were identified via Affymetrix GeneChip hybridization. On a cell-specific level, separately assessing different cell types of mycorrhizal roots and thereby increasing the special resolution, 1951 genes differentially regulated upon mycorrhizal colonization of *M. truncatula* roots were identified (Gaude *et al.*, 2012). It was shown that even cells that do not harbour arbuscules undergo drastic transcriptional changes, indicating a substantial reprogramming of mycorrhizal roots that is not directly linked to arbuscule development, or may also indicate the preparation of cells in the vicinity of fungal structures for subsequent colonization. Hoge Kamp *et al.* (2011) compared roots colonized with different AM fungi, *R. irregularis* and *Glomus mosseae*. The overlap of the specifically regulated genes of *M. truncatula* roots interacting with either of these fungi lead to the identification of 512 genes related to root colonization by AM fungi.

In all these approaches, genes of a variety of functional classes, including transcription regulation, transport, lipid metabolism, and signalling, were found to be regulated, indicating the importance of these cellular functions for the development and maintenance of the symbiosis. Hogenkamp *et al.* (2011) divide the progress of the symbiosis development into four distinct stages, each defined by the activity of distinct genes: first, an activation of signalling cascades in epidermal cells for the exchange of diffusible signals, secondly the direct physical contact, PPA formation and penetration by the fungal hyphae, then their spreading in the apoplast and finally the formation of arbuscules.

Metabolite profiling of *M. truncatula* roots revealed a number of metabolic differences between mycorrhizal and non-mycorrhizal conditions (Schliemann *et al.*, 2008). It was shown that there are clear differences in development-, nutritional- and mycorrhiza-dependent effects in the primary and secondary metabolism of *M. truncatula* roots. Not only were the phosphate levels found to increase in mycorrhizal roots compared to non-mycorrhizal conditions, but also the levels of certain amino acids and, at later stages, isoflavonoids were shown to increase upon mycorrhizal colonization. The analysis of specific proteomic changes in arbuscule-containing root cells of *M. truncatula* (Gaude *et al.*, 2012) showed an increased number of proteins involved in lipid metabolism which are likely to be related to the synthesis of the PAM.

1.1.3 Fungal transport processes involved in the AM symbiosis

All AM fungi belong to the phylum of the Glomeromycota, a monophyletic group diverged from the same common ancestor as Ascomycota and Basidiomycota (Schüßler *et al.*, 2001). They are obligate biotrophic fungi that have co-evolved with their host plants for an extremely long period of time, probably up to 500 million years (Corradi and Bonfante, 2012). AM fungi are characterized by coenocytic hyphae, forming a continuous cytoplasm in which the nuclei are freely distributed (Corradi and Bonfante, 2012) and each spore contains multiple nuclei, varying mostly between 100 and 200 nuclei per spore (Marleau *et al.*, 2011).

Rhizophagus irregularis (DAOM197198) was recently reclassified from its previous clade and therefore renamed from *Glomus intraradices* (Stockinger *et al.*, 2009; Krüger *et al.*, 2012). It is widely used as a model AM fungus as it colonizes a wide range of host plants relatively fast, but as all other AM fungi it cannot be grown without the plant partner, even if carbohydrates are provided with the growth medium (Bonfante and Genre, 2010). *R. irregularis* produces big spores containing multiple nuclei and has a comparatively big genome. Latest estimations indicate that with >150 Mb, the size of the genome space might be much higher than the amount of DNA in each nucleus (Martin *et al.*,

2008). The genome is sequenced for the most part, but due to a large amount of repetitive sequences and the genetic differences even between the nuclei of one spore it has not been successfully assembled (Martin *et al.*, 2008) until very recently. In a new approach, genomic DNA isolated from single nuclei of one spore was sequenced and the genome of each nucleus was assembled individually. A relatively high genetic difference of approximately 3 % was shown between the genomes of each spore (Francis Martin, INRA, Nancy, personal communication). Also, an EST database is available online (GlomusDB, INRA) albeit a vast majority of the sequences are as yet incomplete and not annotated.

Transcriptome analyses of extraradical tissues of *R. irregularis* and mycorrhizal roots recently gave a first glimpse of the molecular basis of symbiosis-related traits (Tisserant *et al.*, 2012). Transcripts from germinated spores, ERM and symbiotic roots were used for Sanger and 454 sequencing to obtain nonredundant virtual transcripts for the construction of an oligoarray. Subsequent gene expression analyses showed an induced expression of genes coding for membrane transporters and small secreted proteins in the IRM, but no expression of hydrolytic enzymes acting on plant cell wall polysaccharides, all features of *R. irregularis* that are shared with ectomycorrhizal symbionts and obligate biotrophic pathogens. Also, transcripts coding for the meiotic recombination machinery and meiosis-specific proteins were identified. This suggests that major deletions of genes essential for sexual reproduction and meiosis are not the reason for the lack of a known sexual cycle in *R. irregularis*. Genes of different functional classes were found to be up-regulated in the IRM in comparison to germinating hyphae. Among these, numerous genes involved in transport mechanisms were identified, but also several genes involved in lipid metabolism and signal transduction were found to up-regulated in the IRM.

Since until recently only incomplete genomic information for *R. irregularis* was available, and due to the difficult process of culturing AM fungi, only a few fungal transcripts that are directly involved in the interaction with the plant partner during the AM symbiosis have been found in previous works.

Among those is a sugar transporter, *RiMst2*, which was shown to be expressed in arbuscules and to play an essential role in the AM symbiosis (Helber *et al.*, 2011). RiMST2 was characterized in detail, including expression analyses and a functional characterization of the protein. It was shown to be a high affinity monosaccharide transporter, able to transport glucose, xylose, mannose, and fructose. Its expression is closely correlated with the AM-specific *M. truncatula* phosphate transporter *MtPt4* and a reduction of the *RiMst2* expression leads to impaired mycorrhiza formation and deformed arbuscules. The transcripts of *RiMst2* were shown to accumulate in arbuscules and intraradical hyphae.

Also, two fungal ammonium transporters were identified recently. While the high affinity transporter RiAMT1 is substrate-inducible and is expressed preferentially in the extraradical mycelium, RiAMT2 is preferentially expressed in the intraradical mycelium and is not substrate-regulated (Lopez-Pedrosa *et al.*, 2006; Perez-Tienda *et al.*, 2011). Both are expressed in arbuscule-containing cells and it was suggested that they might modulate the amount of delivered nitrogen by re-uptake (Perez-Tienda *et al.*, 2011).

Recently, two *R. irregularis* aquaporin genes, GintAQPF1 and GintAQPF2, were identified and cloned by Li *et al.* (2013). In yeast, GintAQPF1 was shown to be localized at the plasma membrane and GintAQPF2 is localized at the plasma membrane and intracellular membranes. Both aquaporins are hypothesized to be localized at the plant-fungal interface, but they are also expressed in the ERM. Since they are up-regulated both *in planta* and in extraradical tissues under drought conditions, they highlight the important role of AM fungi in plant drought tolerance.

On the other hand, a phosphate transporter, RiPt, is expressed in the ERM during symbiotic interactions of *R. irregularis* with *M. truncatula* and *Dracys carota* (Maldonado-Mendoza *et al.*, 2001). It is regulated in response to phosphate concentrations surrounding the extraradical hyphae and modulated by the overall phosphate status of the mycorrhiza. According to the authors, these data imply that *R. irregularis* can perceive phosphate levels in the external environment and suggest the presence of an internal phosphate sensing mechanism.

1.2 Research objectives

The nutrient exchange between plant and fungus is the key element of the arbuscular mycorrhizal symbiosis, probably one of the most ecologically essential symbioses between eukaryotes. This work is mainly concerned with the elucidation of transport processes between plant roots of *Medicago truncatula* and the fungal partner *Rhizophagus irregularis* during the AM symbiosis in order to enhance the understanding of the molecular basis underlying this tight interaction.

Two main projects associated with different aspects of the nutrient exchange during the AM symbiosis will be addressed:

Potential transporter genes of *Medicago truncatula* that were found to be specifically regulated in arbuscule-containing cells and in non-arbusculated cells of mycorrhizal *M. truncatula* (Gaude *et al.*, 2012) will be analysed. The mycorrhiza-specific regulation and cell-specific expression of these genes will be confirmed. Since so far very little is known about the allocation and transfer of carbohydrates in the course of the symbiosis, the carbohydrate transfer from the plant to the fungus will be studied in particular. The two most interesting candidates, the mycorrhiza-responsively expressed sucrose transporter MtSUT4-1 and the hexose transporter MtHXT1, will be analysed further to get deeper insight into the molecular mechanisms of the carbon transfer. Metabolite profiling will be performed for a knock-out mutant of *MtHxt1* to elucidate its role in the symbiosis and to increase the knowledge of the influence of the mycorrhizal colonization on the metabolite profile of *M. truncatula*.

The second project is aimed to deepen the as yet limited knowledge of the molecular mechanisms determining the interaction between the symbiotic partners on the fungal side of the AM symbiosis. The isolation of *R. irregularis* arbuscules from mycorrhizal roots via laser capture microdissection (LCM) will be established. The *R. irregularis* transcriptome *in planta* and in extraradical tissues will be sequenced in order to get a more detailed insight into genes that are differentially expressed in these two states of the fungal growth. Fungal transcripts with an altered level in arbuscules as compared to extraradical tissues will be identified. The setup is focused on finding genes, i.e. transporter genes, which are specifically regulated in the arbuscule stage and are therefore likely to play a role in the nutrient exchange between plant and fungus.

2 MATERIALS AND METHODS

2.1 Materials

2.1.1 Chemicals

Lab chemicals, solvents, buffering agents, detergents, nutrient ingredients and antibiotics were obtained from Merck (Darmstadt), Sigma-Aldrich (München), Duchefa (Haarlem, Netherlands), Biozym (Hessisch Oldendorf), BD Becton, Dickinson and Company (Heidelberg), and Carl Roth (Karlsruhe).

2.1.1.1 Enzymes

Restriction enzymes

If available, the restriction enzymes used in this study were obtained from Fermentas (St. Leon-Rot, Germany) as Fast Digest® Restriction enzymes. Non Fast Digest® restriction enzymes were obtained from NEB (Frankfurt a.M., Germany).

The following additional enzymes were used

Advantage® 2 DNA Polymerase	Clontech (Saint-Germain-en-Laye, France)
BP-Clonase	Life Technologies (Darmstadt, Germany)
GoTaq® Flexi DNA Polymerase	Promega (Mannheim, Germany)
LR-Clonase	Life Technologies (Darmstadt, Germany)
Lysozym	Carl Roth (Karlsruhe, Germany)
Proteinase K	Life Technologies (Darmstadt, Germany)
RevertAid Premium Reverse Transcriptase	Thermo Scientific (Karlsruhe, Germany)
RiboLock™ RNase Inhibitor	Thermo Scientific (Karlsruhe, Germany)
RNase A	Thermo Scientific (Karlsruhe, Germany)
<i>SuperScript® III Reverse Transcriptase</i>	Life Technologies (Darmstadt, Germany)
T4 DNA Ligase	Promega (Mannheim, Germany)
TURBO DNase™	Life Technologies (Darmstadt, Germany)

2.1.1.2 Reaction kits

Advantage® 2 DNA Polymerase Kit	Clontech (Saint-Germain-en-Laye, France)
Agilent RNA 6000 Pico Kit	Agilent Technologies (Waldbronn, Germany)
Gateway® BP Clonase® II Enzyme Kit	Life Technologies (Darmstadt, Germany)
Gateway® LR Clonase® II Enzyme Kit	Life Technologies (Darmstadt, Germany)
GoTaq® Flexi DNA Polymerase Kit	Promega (Mannheim, Germany)
InviTrap® Spin Plant RNA Mini Kit	Stratec Molecular (Berlin, Germany)
Maxima™ SYBR Green/ROX qPCR Master Mix (2x)	Thermo Scientific (Karlsruhe, Germany)
pENTR™/D-TOPO® Cloning Kit	Life Technologies (Darmstadt, Germany)
RNase-Free DNase Set	QIAGEN (Hilden, Germany)
RNeasy Micro Kit	QIAGEN (Hilden, Germany)
RNeasy Mini Kit	QIAGEN (Hilden, Germany)
TOPO® TA Cloning® Cloning Kit for subcloning	Life Technologies (Darmstadt, Germany)
TURBO DNA-free™	Life Technologies (Darmstadt, Germany)
ZR Fungal/Bacterial RNA MicroPrep™	Zymo Research (Freiburg, Germany)

2.1.1.3 Antibiotics

Table 1: Antibiotics

Antibiotic	Stock concentration	Final concentration (bacteria cultures)	Final concentration (plant cultures)
Kanamycin	50 mg/ml	50 µg/ml	25 µg/ml
Streptomycin	150 mg/ml	600 µg/ml	
Spectinomycin	50 mg/ml	50 - 100 µg/ml	
Gentamycin	200 mg/ml	40 µg/ml	
Ampicillin	50 mg/ml	100 µg/ml	
Rifampicin	50 mg/ml (in DMSO)	50 µg/ml	
Beta Bactyl	125 mg/ml		187.5 µg/ml

The stock solutions were filter sterilized and stored at -20 °C.

2.1.1.4 Buffers and solutions

If not mentioned otherwise, all buffers and solutions were prepared with bi-distilled H₂O (ddH₂O).

Plasmid mini preparation: alkaline lysis

Solution 1	125 mM	Tris-HCl pH 8
	10 mM	EDTA
	5 mg/ml	Lysozym (added after autoclaving)
Solution 2	0.2 mM	Sodium hydroxide (NaOH)
	1 % [w/v]	Sodium dodecylsulfate (SDS)
Solution 3	3 M	Potassium acetate, pH 5.2 with acetic acid

Leaf infiltration

AS Medium	10 mM	MES-KOH buffer (pH 5.6)
	10 mM	MgCl ₂
	150 µM	Acetosyringone (dissolved in DMSO) pH 5.6 (KOH)

Extraction of genomic DNA

CTAB buffer	2 % [w/v]	CTAB
	1.4 M	NaCl
	20 mM	EDTA pH 8
	100 mM	Tris-HCl pH 8
	0.2 % [v/v]	β-Mercaptoethanol (added directly before use)

Gel electrophoresis

50 x TAE buffer	242 g	Tris base
	57.1 ml	Glacial acetic acid
	100 ml	0.5 M EDTA (pH 8)
	ad to 1 l	ddH ₂ O

Ethidium bromide (EtBr) solution

0.01 % [w/v] 0.01 mg EtBr in 100 ml 0.5 x TAE

DEPC-H₂O 0.1 % [v/v] in ddH₂O, stirred over night, autoclaved twice

10 x MOPS buffer	200 mM	MOPS
	50 mM	Sodium acetate
	20 mM	EDTA (pH 7)

RNA sample buffer	100 µl	Formamide
	38 µl	Formaldehyde
	20 µl	10 x MOPS buffer
	42 µl	DEPC-H ₂ O
RNA loading buffer	99 µl	6 x loading dye
	1 µl	10 mg/ml EtBr

GUS assay

GUS staining solution	100 mM	Sodium phosphate buffer pH 7.2
	5 mM	K ₃ (Fe(CN) ₆)
	5 mM	K ₄ (Fe(CN) ₆)
	10 mM	EDTA
	0.5 mg/1ml	X-Gluc. Dissolved in DMF and added directly before use.
Sodium phosphate buffer	423 ml/l	1 M Na ₂ HPO ₄
	577 ml/l	1 M NaH ₂ PO ₄ , pH 7.2

Staining of fungal structures

Trypan blue solution	0.1 % [w/v]	Trypan blue in lactophenol (25% [w/v] phenol in water/glycerol/lactic acid in the ratio 1:1:1)
WGA Alexa Flour 488 staining	5 µg/ml	WGA Alexa fluor in 1 x PBS buffer, pH 7.5

Isolation of spores from solid medium (Declerck *et al.*, 2005)

0.01 M Citrate buffer	0.082 vol.	0.1 M Trisodium citrate
	0.018 vol.	0.1 M Citric acid pH 6 (NaOH)

In-situ hybridization

1 M Tris-HCl	121.1 g	Tris-HCl, pH 8 adjust with HCl
1 x PBS	137 mM	Sodium chloride (NaCl)
	2.7 mM	Potassium chloride (KCl)
	12 mM	di-sodium hydrogen phosphate (Na ₂ HPO ₄)/potassium di-hydrogen phosphate (KH ₂ PO ₄) pH 7.4
PBST		1 x PBS with 0.1 % [w/v] Tween-20
1 x TBS	50 mM	Tris-HCl
	150 mM	Sodium chloride (NaCl) adjust to pH 7.5 with HCl

TBST		1 x TBS with 0.1 % [w/v] Tween-20
Fixative	10 ml 2.5 ml	10 % [w/v] para formaldehyde 10 x PBS add ddH ₂ O to 25 ml, adjust to pH 7
20 x SSC	3 M 0,3 M	NaCl NaCitrate pH 7 with 1 M HCl
10 % PFA	10 g 2 pieces ad 100 ml	Paraformaldehyde NaOH Dissolved in H ₂ O, pH 7 with 1 M H ₂ SO ₄ H ₂ O
Blocking Sol A	100 mM 150 mM 0.1 % 1.5 % 2 %	Maleic acid NaCl Tween20 Blocking Reagent (Roche) BSA (Serum albumin fraction V)
NBT/BCIP detection buffer	0.1 M 0.1 M	Tris-HCl pH 9.5 NaCl

Other buffers

TE buffer	10 mM 1 mM	Tris-HCl EDTA, pH 8
-----------	---------------	------------------------

2.1.1.5 Other chemicals

6x DNA Loading Dye	Fermentas (St. Leon-Rot, Germany)
Midori Green Advanced	Biozym (Hessisch Oldendorf, Germany)
Bacto™ Agar	Becton Dickinson (Heidelberg, Germany)
Biozyme LE Agarose	Biozym Scientific (Hessisch Oldendorf, Germany)
Blocking Reagent for nucleic acid hybridization and detection	Roche (Mannheim, Germany)
DEPC	Carl Roth (Karlsruhe, Germany)
GeneRuler™ 100bp Plus DNA Ladder	Fermentas (St. Leon-Rot, Germany)
GeneRuler™ 1kb DNA Ladder	Fermentas (St. Leon-Rot, Germany)
GeneRuler™ 1kb Plus DNA Ladder	Fermentas (St. Leon-Rot, Germany)
<i>In situ</i> hybridization buffer	ENZO® life science (Lörrach, Germany)
Phytigel	Sigma-Aldrich (Munich, Germany)
MOPS	Sigma-Aldrich (Munich, Germany)
Nuclease free water (not DEPC-treated)	Ambion (Austin, TX, USA)

Select Agar [®]	Invitrogen (Darmstadt, Germany)
TFM Tissue Freezing Medium	Electron Microscopy Sciences (Hatfield, PA, USA)
Wheat Germ Agglutinin Alexa Fluor [®] 488	Invitrogen (Darmstadt, Germany)

2.1.2 Growth media

2.1.2.1 Bacterial growth media

LB medium

10 g/l Bacto™ Tryptone, 5 g/l Yeast extract, 10 g/l NaCl, pH 7 (NaOH)

YT medium

0,8 % (w/v) Peptone, 0,5 % (w/v) Yeast extract, 0,5 % (w/v) NaCl

YEB medium

5 g/l Bacto™ Beef extract, 5 g/l Bacto™ Peptone, 1 g/l Yeast extract, 5 g/l Sucrose, 2 ml of 1 M Mg₂SO₄/ 1 l medium, pH 7.2 (NaOH)

TY/Ca medium

5 g/l Bacto™ Tryptone, 3 g/l yeast extract, pH 7.2 (NaOH), 4.5 mM CaCl₂ (added after autoclaving)

All media are autoclaved for 20 min at 121 °C. For solid media 15 g/l Select Agar[®], or Bacto™ Agar for TY medium, were added before autoclaving.

2.1.2.2 Plant growth substrates, media and solutions

Modified Fahraeus medium (Barker *et al.*, 2006)

0.8 mM	Na ₂ HPO ₄ x H ₂ O
0.7 mM	KH ₂ PO ₄
0.5 mM	MgSO ₄ x 7H ₂ O
0.5 mM	NH ₄ NO ₃
50 µM	FeSO ₄ x 7H ₂ O
50 µM	Na ₂ EDTA x 2H ₂ O
0.1 mg/l	CuSO ₄
0.1 mg/l	H ₃ BO ₃
0.1 mg/l	MnSO ₄ x H ₂ O
0.1 mg/l	Na ₂ MoO ₄ x 2H ₂ O
0.1 mg/l	ZnSO ₄ x H ₂ O
15 g/l	Bacto™ Agar
1 mM	CaCl ₂ (added after autoclaving) pH 6.5 (KOH)

The calcium chloride and the antibiotics for selection of transgenic plants were added after autoclaving and cooling down of the medium.

M medium for root organ cultures (Bécard and Fortin, 1988)

Stock solutions:		Final concentration:	
Macro elements:	3.2 g/l	KNO ₃	0.79 mM
	29.2 g/l	MgSO ₄ x 7H ₂ O	3.0 mM
	2.6 g/l	KCl	0.87 mM
Micro elements:	6 g/l	MnCl ₂ x 4H ₂ O	30.3 µM
	1.5 g/l	H ₃ BO ₃	24.0 µM
	2.65 g/l	ZnSO ₄ x 7H ₂ O	9.2 µM
	0.75 g/l	KI	4.5 µM
	0.0024 g/l	Na ₂ MoO ₄ x 2H ₂ O	0.01 µM
	0.13 g/l	CuSO ₄ x 5H ₂ O	0.5 µM
Calcium:	57.6 g/l	Ca(NO ₃) ₂ x 4H ₂ O	1.22 mM
Phosphate:	4.8 g/l	KH ₂ PO ₄	35.0 µM
FeEDTA:	1.6 g/l	NaFe-EDTA	21.7 µM

Vitamins:	0.3 g/l	Glycin	40 μ M
	5 g/l	Myo-Inositol	277 μ M
	50 mg/l	Niacin	4.0 μ M
	10 mg/l	Pyridoxin HCl	0.5 μ M
	10 mg/l	Thiamin HCl	0.3 μ M
	filter sterilize		

Add from stock solutions:

25 ml/l Macro elements, 1 ml/l Micro elements, 5 ml/l Calcium, 1 ml/l Phosphate, 5 ml/l Fe-EDTA, 10 ml/l Vitamins (after autoclaving), 10 g/l Sucrose, 3.5 g/l Phytigel.

The vitamins were added after autoclaving and cooling down of the medium.

Modified 0.5 x Hoagland's solution (Hoagland and Arnon, 1950)

2.5 mM	$\text{Ca}(\text{NO}_3)_2 \times 4\text{H}_2\text{O}$
2.5 mM	KNO_3
1 mM	$\text{MgSO}_4 \times 7\text{H}_2\text{O}$
50 μ M	NaFeEDTA
20 μ M	$\text{KH}_2\text{PO}_4/\text{K}_2\text{HPO}_4$ pH 6.8
10 μ M	H_3BO_3
2 μ M	$\text{MnCl}_2 \times 4\text{H}_2\text{O}$
1 μ M	$\text{ZnSO}_4 \times 7\text{H}_2\text{O}$
0.5 μ M	$\text{CuSO}_4 \times 5\text{H}_2\text{O}$
0.2 μ M	$\text{CoCl}_2 \times 6\text{H}_2\text{O}$
0.2 μ M	$\text{Na}_2\text{MoO}_4 \times 2\text{H}_2\text{O}$
0.2 μ M	$\text{NiSO}_4 \times 6\text{H}_2\text{O}$

The phosphate concentration ($\text{KH}_2\text{PO}_4/\text{K}_2\text{HPO}_4$ pH 6.8) was adjusted to the respective experiments. For -Pi conditions, 20 μ M $\text{KH}_2\text{PO}_4/\text{K}_2\text{HPO}_4$ were added, for moderate phosphate 400 μ M and for +Pi 1 mM were added to the fertilizer.

For nitrogen limiting conditions, $\text{Ca}(\text{NO}_3)_2$ and KNO_3 were replaced by equimolar amounts of CaCl_2 and KCl, respectively.

2.1.3 Biological material

Table 2: Plants, fungi and bacteria

Organism	Strain/cultivar	Reference
<i>Medicago truncatula</i>	A17 cv Jemalong	Max Planck Institute MP (Golm)
<i>Medicago truncatula</i>	R108	Tadege <i>et al.</i> (2008)
<i>Nicotiana benthamiana</i>	TW16	Max Planck Institute MP (Golm)
<i>Rhizophagus irregularis</i>	Strain BB-E	Agrauxine, Dijon, France
<i>Echerichia coli</i>	DB3.1	Agilent Technologies, Waldbronn
<i>Echerichia coli</i>	TOP 10	Invitrogen, Karlsruhe
<i>Echerichia coli</i>	TOP 10F'	Invitrogen, Karlsruhe
<i>Echerichia coli</i>	DH5 α	Stratagene, Agilent Technologies, Waldbronn
<i>Agrobacterium rhizogenes</i>	ARqua 1	Quandt <i>et al.</i> (1993)
<i>Agrobacterium tumefaciens</i>	GV2260	Deblaere <i>et al.</i> (1985)
<i>Sinorhizobium meliloti</i> WT	2011 (expR+)	Provided by Prof. Dr. Helge Küster (University of Hannover)

The *Tnt1* insertion mutants were produced in the R108 background. For all other experiments, A17 cv Jemalong was used.

2.1.4 Plasmids

Table 3: Plasmids

Name	Description	Reference
pENTR™/ D-TOPO®	GATEWAY™ Cloning vector for PCR products	Invitrogen, Karlsruhe
pCR2.1	GATEWAY™ Cloning vector for PCR products	Invitrogen, Karlsruhe
pDONR207	GATEWAY™ Cloning vector for PCR products	Invitrogen, Karlsruhe
pGWB433	GATEWAY™ Cloning vector for Entry vectors, promoter GUS fusion	Karimi <i>et al.</i> (2002), Nakagawa <i>et al.</i> (2007)
pK7WGF2	GATEWAY™ Cloning vector for Entry vectors, C-terminal GFP fusion	Karimi <i>et al.</i> (2002)
pK7FWG2	GATEWAY™ Cloning vector for Entry vectors, N-terminal GFP fusion	Karimi <i>et al.</i> (2002)
pK7FWGF2	GATEWAY™ Cloning vector for Entry vectors, C- and N-terminal GFP fusion	Karimi <i>et al.</i> (2002)
pKDSR(I)GFP ₁	RNA _i vector with 384 bp GFP fragment insertion, constitutive DsRed expression as visible marker	Dr. Igor Kryvoruchko (Ardmore, OK, USA)
VakRK_CD3-975	mCherry tonoplast marker	Nelson <i>et al.</i> (2007)

2.1.5 Oligonucleotides

All primers used in this study were obtained from Eurofins MWG (Ebersberg). They were synthesized on a 0.01 μ mol scale and lyophilized. For regular PCRs they were used in a 10 mM solution, for qRT PCR the concentration was 0.05 mM.

All oligonucleotides used in this study are listed in the supplemental data (supplementary tables S1.1 to S1.6). The stated melting temperatures (T_m) were calculated with the Promega BioMath calculator (<http://www.promega.com/techserv/tools/biomath/calc11.htm?origUrl=http%3a%2f%2fwww.promega.com%2fbiomath%2fcalc11.htm>).

For the in situ hybridization, 20mer 5'DIG labelled RNA oligos were used (Apara Bioscience). Probe and sense control were designed for the same area of *RiMfs2* (Comp2270_c0) (table 4).

Table 4: 5'DIG labeled RNA oligos for in situ hybridization.

Name/ target	Sequence 5' - 3'	T_m
RiMFS2 probe	CCAGUAGCCUUAUAUGCAUC	45,3 °C
RiMFS2 sense control	GAUGCAUAUAAGGCUACUGG	45,3 °C

2.2 Methods

2.2.1 Plant growth and transformation of *Medicago truncatula*

2.2.1.1 Stratification, surface sterilization and germination of seeds

Medicago truncatula cv. Jemalong line A17 seeds were covered with concentrated sulphuric acid for 8 to 10 min followed by 8 washing steps with distilled water. Afterwards, surface sterilization was carried out using 6 % [v/v] sodium hypochlorite for 6 min. After rinsing with sterile water, seeds were germinated on 0.8 % (w/v) water agar at 4 °C for 48 h followed by an overnight incubation at room temperature for the root transformation or two days of incubation before planting the seedlings in soil.

For *Medicago truncatula* R108 the incubation times in sulphuric acid and NaOCl were reduced to 3 min and 1.5 min, respectively.

2.2.1.2 Inoculation with *Rhizophagus irregularis*

Seedlings or small plants obtained from root transformation were placed in a quartz sand (0.6-1.2 mm), expanded clay and vermiculite mix (1:1:1).

For inoculation with the AM fungus *R. irregularis*, inoculum (substrate from mycorrhizal *Allium porrum* plants) was added to the substrate at 10 % [v/v]. For inoculum production *R. irregularis* (strain BB-E, provided by Agrauxine, Dijon, France) was propagated on *A. porrum* plants, which were fertilized twice a week with half strength Hoagland's solution containing 20 µM phosphate. After 4 months, the *A. porrum* plants were harvested and the growth substrate was used as inoculum for the *M. truncatula* seedlings.

2.2.1.3 Nodulation of *Medicago truncatula* plants

For the nodulation of *M. truncatula* roots with *Sinorhizobium meliloti*, the plants were kept under nitrogen starvation conditions for the whole treatment by equimolar replacement of NO₃⁻ with Cl⁻ in the Hoagland's solution. *S. meliloti* WT was grown in liquid culture (TY medium) to an optical density of 0.5 (λ = 600 nm) and diluted 1:10 [v/v] with ddH₂O prior to inoculation by watering the plants with the bacterial suspension.

2.2.1.4 Plant growth conditions

Growth conditions in the greenhouse

M. truncatula plants were grown at 21 °C during the day and 17 °C at night. A 16 h light period was used in the greenhouse. The relative humidity was 60 %. The plants were fertilized according to the experimental conditions.

Growth conditions in the phytotron

After root transformation and 3 to 4 weeks of *in vitro* cultivation, the plants were grown in a phytotron (200 $\mu\text{E m}^2\text{s}^{-1}$, 22 °C, 65 % humidity, 8 h dark, 16 h light). The plants were fertilized according to the experimental condition.

2.2.1.5 Agrobacterium rhizogenes mediated plant root transformation

For the *M. truncatula* root transformations, seeds were surface sterilized as mentioned above. The following protocol is based on axenic transformation developed by Boisson-Dernier *et al.* (Boisson-Dernier *et al.*, 2001).

After an overnight germination, the root tip of each seedling was cut off with a sterile razor blade and discarded. The fresh wound of the seedling was dipped on a 2 day old culture of *A. rhizogenes* strain ARqua-1 containing the appropriate destination vector. The seedlings were placed on water agar and kept in the dark at room temperature for two days for efficient transformation of the roots. The seedlings were then transferred onto selective Fahraeus-medium and grown in a growth chamber (200 $\mu\text{E m}^2\text{s}^{-1}$, 21 °C, 65 % humidity, 8 h dark, 16 h light) for 3 to 4 weeks. If necessary, the plants were then transferred into soil with or without *R. irregularis* inoculum and grown in the phytotron.

2.2.1.6 Nicotiana benthamiana leaf infiltration with transformed Agrobacterium tumefaciens

Transformed *A. tumefaciens* GV2278 (Deblaere *et al.*, 1985) were grown at 28 °C for 2 days in selective YEB medium to produce a thick Agrobacteria stock. 1 ml of the stock solution was added to 4 ml of selective YEB medium and shaken for 4 h at 28 °C. The cultures were pelleted by centrifuging for 15 min at 2880 x g. The supernatant was discarded and the pellet resuspended in 1 ml freshly prepared AS-medium. The optical density (OD600) of the culture was adjusted to 1.0 and the culture was incubated for further 2 to 3 h at room temperature. 4 - 6 weeks old *N. benthamiana* plants were well watered and then infiltrated after 4 h. The bacterial solution was injected into the abaxial side of the tobacco leaves using a syringe without a needle (1 ml). The plants were incubated for 2 to 3

days in the phytotron. For the co-infiltration of different constructs, these were mixed in a 1:1 ratio before infiltration.

2.2.2 In vitro cultivation of *Rhizophagus irregularis*

2.2.2.1 *Medicago truncatula* root organ culture

For the *in vitro* cultivation of *R. irregularis*, *M. truncatula* root organ cultures were used. The roots therefore need to be transformed with *A. rhizogenes*. As a vector, pKDSR(I)GFP_i was used, a Gateway-compatible RNAi vector with constitutively expressed DsRed as a visible selection marker and the *nptII* gene for kanamycin selection of successfully transformed roots. A 384 bp fragment of GFP was cloned into the vector to replace the cytotoxic *ccdB* gene.

2.2.2.2 Isolation of fungal spores and hyphae

To obtain extraradical hyphae of *R. irregularis*, *M. truncatula* root organ cultures were grown on a compartmented petri dish and inoculated with *R. irregularis* spores from older root organ cultures (ROCs). After the roots were well colonized, one half of the solid medium was removed from the petridish and it was refilled with liquid M-Medium without sucrose. After approximately 2 weeks, hyphae had grown into the liquid compartment and were harvested using a sterile tip. In order to obtain enough material, hyphae of several plates were pooled for one RNA isolation.

Spores were isolated from well colonized *M. truncatula* ROCs. The medium was dissolved in 0.01 M citrate buffer. The spores were washed several times and incubated in sterile water at room temperature for 2 to 3 days to germinate. They were then disrupted with a small pistil in lysis buffer (RLT Buffer, Qiagen RNeasy Micro Kit) with 8.75 µl RNase Inhibitor (RNaseOUT) and 3,5 µl β-Mercaptoethanol prior to the RNA isolation.

2.2.3 Biomolecular methods

2.2.3.1 Cloning strategies and preparation of plasmids

Gateway™ cloning

Promoter-GUS fusions of *M. truncatula* transporter candidates and C- and/or N- terminal GFP fusions for the intracellular localization of *M. truncatula* sugar transporters were created via directional TOPO® cloning (pENTR™ Directional TOPO® Cloning Kit, Invitrogen) into the pENTR™/D-

TOPO vector or into pDONR207 via Gateway BP-reaction (Invitrogen) according to the manufacturer's instructions. The PCRs to produce the fragments were performed with Advantage[®] 2 Polymerase (Clontech) and the appropriate overhang was added to the respective primers: a CACC sequence at the 5' end of the forward primer for pENTR cloning, and the Invitrogen *attB1* site to the forward primer and the *attB2* site to the reverse primer for the BP cloning into pDONR207. cDNA was derived from RNA of mycorrhizal *M. truncatula* roots for the protein localization fusions, while template gDNA for the amplification and cloning of the promoter regions was isolated from *M. truncatula* leaves. PCR fragments were cloned into the respective vector and transformed into OneShot[®] TOP10 *E. coli* (Invitrogen) or *E. coli* DH5alpha (Stratagene) cells from which the respective entry vector was then isolated. Constructs were checked via PCR and restriction of the plasmids. Positive constructs were sequenced at LGC Genomics (Berlin, Germany) using the Donr-F and SeqL-E sequencing primers. Positive clones were used for recombination with the respective destination vectors: pGWB433 (Karimi *et al.*, 2002; Nakagawa *et al.*, 2007) for the promoter-GUS fusions, pK7WGF2 and pK7FWG2 for the C- or N-terminal GFP fusion, respectively, and pK7FWGF2 (Karimi *et al.*, 2002) for a GFP fusion to both ends of the resulting protein for the intracellular localization studies. For this recombination, the LR-Clonase II Mix (Invitrogen) was used according to the manual.

Regions that needed to be sequenced, such as the full-length CDS of the *R. irregularis* transporter candidates, were TA-cloned into pCR2.1 (Invitrogen). cDNA of mycorrhizal roots (for *R. irregularis* sequences highly expressed *in planta*) or from germinating spores and hyphae were used as a template for the PCR amplification of the fragments. After the PCR with Advantage[®] 2 Polymerase, GoTaq Polymerase (Fermentas) and additional dATPs were added and a 10 min 72 °C step was performed to add A-overhangs at the end of the amplified fragments. These were then cloned according to the manufacturer's instructions and transformed into OneShot[®] TOP10 *E. coli* cells. After the blue/white selection, white colonies were picked, checked via PCR and restriction analysis, and sequenced using the M13F and M13R sequencing primers delivered with the TA-cloning Kit.

Plasmid preparation

A liquid *E. coli* culture (5 ml) was grown over night at 37 °C in LB medium with the respective antibiotics for selection. 2 ml of the culture were centrifuged for 2 min at 10000 rpm to pellet the bacteria. The supernatant was discarded and the pellet was resuspended in 100 µl mini prep solution 1 and 5 µl RNaseA (10 mg/ml). After the mixture was incubated for 5 min at room temperature, 200 µl of solution 2 and 150 µl of solution 3 were added followed by an incubation time of 5 min on ice after each step. The solutions were mixed carefully by inverting the tube. The samples were then centrifuged at maximum speed for 10 min and the supernatant (V = 450 µl) was

transferred into a new tube. 1 ml of 96 % [v/v] ethanol and 50 µl of 3 M sodium acetate pH 5.2 were added and the samples were incubated for at least 30 min on ice to precipitate the plasmid DNA. Then the plasmids were pelleted by 10 min centrifugation at full speed and the pellet was washed with 70 % [v/v] ethanol prior to drying. The plasmids were resuspended in 20 µl of sterile ddH₂O.

Restriction analysis of constructs

Prior to sequencing for construct validation, a restriction analyses were performed. If appropriate enzymes were available, the Fast Digest system (Fermentas) was used. The digest reaction was performed in a 10 µl volume including 1 u of the respective enzyme(s) and 1 µg plasmid DNA at 37 °C for 10 min, and was analysed by gel electrophoresis.

2.2.3.2 Transformation of microorganisms

Transformation of Escherichia coli

50 µl chemically competent *E. coli* cells were thawed on ice and incubated on ice for 30 min with 2 µl of the appropriate vector. For the heat shock transformation, the cells were incubated at 42 °C for 30 s, then immediately chilled on ice for 2 min. 200 µl SOC medium were added and the transformed cells were shaken (650 rpm) for 1 h at 37 °C. Positive clones were selected by plating 50 - 150 µl of the cells on solid LB medium containing the appropriate antibiotic and, if blue-white screening was possible, 40 µl X-Gal (40 mg/ml). The cells were grown over night at 37 °C.

Transformation of Agrobacterium strains

50 µl electro-competent *A. rhizogenes* or *A. tumefaciens* cells were thawed on ice and mixed with 2 µl of the appropriate vector in an electroporation cuvette (1 mm). The cells were incubated on ice for 30 min. After the electroporation (2.5 kV), 500 µl YT or YEB medium were added. The transformed cells were shaken for 2 - 3 h at 28 °C and 50 - 100 µl of the cell suspension were plated on solid YT or YEB medium containing appropriate antibiotics. The cells were grown for 2 days at 28 °C.

2.2.3.3 DNA isolation methods

CTAB gDNA extraction

100 mg of frozen and grinded plant material were mixed with 800 μ l preheated (65 °C) CTAB DNA extraction buffer. The samples were incubated for 30 min at 60 °C. Afterwards, an equal volume of phenol:chloroform:isoamylalcohol (25:24:1) was added and mixed by inverting the tube. The samples were centrifuged for 2 min at maximum speed, the upper phase was transferred into a new tube and RNaseA (final conc. 20 μ g/ml) was added. After 15 min at 37 °C, the P:C:I extraction step was repeated. The upper phase was mixed with an equal volume of chloroform. After centrifugation, the upper phase was recovered. The DNA was precipitated by adding 1/10 vol NaOAc (0.3 M stock, pH 5.2) and 0.6 vol isopropanol and incubation of the samples at - 20 °C for at least 60 min. After 15 min of centrifugation at maximum speed, the pellet was washed with 70 % ethanol, air dried, and resuspended in 50 μ l 1 x TE buffer (pH 8.0).

gDNA extraction with alkaline lysis

For the screen of *Tnt1* insertion plants, a young leaf was removed from each plant and gDNA was extracted with alkaline lysis (Wang *et al.* (1993), modified). The leaves were frozen in liquid nitrogen and retched with small glass beads in a 2 ml reaction tube. 60 μ l of 0.5 M NaOH were added, the reaction was mixed thoroughly and incubated for 1 min at RT before 980 μ l 1.0 M Tris pH 8.0 were added. 1 μ l of this solution was directly used in a 10 μ l PCR reaction.

2.2.3.4 RNA isolation methods

RNA was isolated from *M. truncatula* roots using the InviTrap® Spin Plant RNA Mini Kit (Stratec Molecular). The isolation was performed according to the manufacturer's instruction, using the RP Lysis Buffer with β -Mercaptoethanol. The lysis was performed at 56 °C, shaking (14000 rpm) for 3 min. The RNA was eluted with 30 μ l of Elution Buffer. Afterwards, the samples were treated with TURBO DNase (Ambion) as described in the manual to remove all DNA contaminations. The quality and quantity of the RNA was analysed using the NanaDrop photospectrometer.

Due to the low amount of starting material, the RNeasy Micro Kit (QIAGEN) was used for the RNA isolation from LCM collected *R. irregularis* arbuscules. *R. irregularis* hyphae and spores were harvested from a two-compartment petridish and RNA was isolated with the Fungal/Bacterial RNA Microprep™ Kit (ZYMO Research Corp). Additionally, spores were isolated from mycorrhizal *M.*

truncatula ROCs, incubated in water for 3 days to germinate, disrupted manually by squeezing with a small pistil in a 1.5 ml reaction tube, and RNA was isolated using the RNeasy Micro Kit (QIAGEN).

2.2.3.5 cDNA synthesis

Superscript™ III Reverse transcription kit (Invitrogen) and oligo (dT)₁₈ primer (Fermentas) were used for the cDNA synthesis of mycorrhizal and non-mycorrhizal roots for the verification of the symbiosis-related regulation of the *M. truncatula* transporter candidate genes. First strand synthesis was performed with 1 µg of total RNA (in a reaction volume of 20 µl) according to the manufacturer's protocols.

For the cDNA synthesis for the *Mthxt1-Tnt1* samples and the validation of the differential regulation of the *R. irregularis* transporter candidate genes, the RevertAid Reverse Transcriptase (Thermo Scientific) and oligo (dT)₁₈ were used. First strand synthesis was performed with 1 µg of total RNA (in a reaction volume of 20 µl) according to the manufacturer's protocols.

2.2.3.6 Polymerase-chain-reaction (PCR)

Standard PCR

For standard PCR amplification the Advantage®2 proofreading polymerase (Clontech) or GoTaq™ DNA polymerase (Promega) was used according to the manufacturer's instruction. For each primer pair the specific annealing temperature was determined in a PCR temperature gradient. For efficient DNA amplification 30 PCR cycles were applied (table 5).

Table 5: Standard PCR programme

Step	Temperature	Time	Cycles
	GoTaq/Adv.2 Polymerase		
1. Denaturation	95 °C	2 min	
2. Denaturation	95 °C	30 s	
3. Annealing	T _m -3 °C	1 min	30
4. Elongation	72 °C/68 °C	1 min/kb	
5. Final elongation	72 °C/68 °C	5 min	
6. Hold	4 °C	∞	

Quantitative real-time PCR (qRT-PCR)

qRT-PCRs were performed in a reaction volume of 10 µl with 1 µl of 1:10 diluted cDNA, 4 µl of 2 mM primer-pair mix and 5 µl of Maxima™ SYBR Green/ROX qPCR Master Mix (Fermentas). For the measurement, the qRT-PCR machine ABI Prism 7900 HT (Applied Biosystems) was used with the following programme: one cycle 95 °C for 10 min, 40 cycles 95 °C for 15 s and 60 °C for 60 s. An additional dissociation stage for analysing melting curves was included. The data was analysed using SDS 2.3 (Applied Biosystems) and MS Excel 2003 (Microsoft). The Ct-threshold was set to 0.2. The average of the Ct-values of the measured plant or fungal housekeeping genes, respectively, was used as a housekeeping gene-index (HK-index) to normalize transcript abundance. The relative expression level of each transcript was calculated.

$$\Delta Ct = Ct_{Gene} - Ct_{HK}$$
$$\text{Relative expression level} = 2^{-\Delta Ct}$$

Alternatively, 40-ΔCt was calculated to visualize the relative transcript abundance in measurements with very diverse relative expression levels, since the qPCR runs 40 cycles. For this reason, also undetermined Ct values were set to 40 prior to the calculations. Student's t-test was used to determine the statistical significance of the difference between the calculated expression levels.

2.2.3.7 Sample preparation for Illumina sequencing

For the Illumina sequencing, two different *R. irregularis* tissues were sampled: LCM collected arbuscules from *M. truncatula* roots and extraradical *R. irregularis* tissues from *M. truncatula* ROCs as described (2.2.2.2, 2.2.3.4, and 2.2.5.1). RNA was isolated and the quantity and quality of each sample were assessed with an Agilent 2100 Bioanalyzer, and only samples with highest RNA content and an RNA integrity number (RIN) above 6 were sent for RNAseq. Several isolations of one tissue were pooled to obtain at least 100 ng of RNA for sequencing.

2.2.4 Biochemical methods

2.2.4.1 MtHxt1 Tnt1 metabolic profiling analysis

Root and leaf samples of mycorrhizal and non-mycorrhizal *M. truncatula* (R108) WT and *Tnt1* insertion plants were harvested, weighed, and immediately frozen in liquid nitrogen to stop plant metabolism.

Metabolite profiling was performed by Ines Fehrlé and Alexander Erban (AG Kopka, MPIMP) by gas chromatography coupled impact ionization/time-of-flight mass spectrometry (GC-EI/TOF-MS) (Agilent 6890N24 gas chromatograph, Agilent, Böblingen, with splitless injection onto a FactorFour VF-5ms capillary column, 30-m length, 0.25-mm inner diameter, 25 μm film thickness (varian-Agilent Technologies) connected to a Pegasus III time-of-flight mass spectrometer, LECO Instrumente GmbH, Mönchengladbach). A polar metabolite fraction was profiled as described earlier (Sanchez *et al.*, 2012). Briefly, for the polar phase extraction, the samples were homogenized under liquid nitrogen, metabolites were extracted from 120 mg \pm 5 % of plant tissue. 360 μl of a premix from 300 μl of 100 % methanol and 60 μl of internal standards (30 μl nonadecanoic acid methylester [2 mg/ml stock in CHCl_3], 30 μl of $^{13}\text{C}_6$ -sorbitol [0.2 mg/ml in MeOH], and d4-alanine [1 mg/ml in water]) were cooled and added to the homogenized tissues. The samples were shaken at 70 $^\circ\text{C}$ for 15 min, 200 μl CHCl_3 were added and shaken at 37 $^\circ\text{C}$ for 5 min. After the addition of 400 μl H_2O , the samples were vortexed and centrifuged for 5 min at 14000 rpm. Two 160 μl aliquots of the upper polar phase were transferred to a 1.5 ml reaction tube and dried in the vacuum centrifuge over night (Erban *et al.*, 2007). Metabolites were methoxyaminated and trimethylsilylated prior to GC-EI/TOF-MS. Retention indices were calibrated by addition of a C_{10} , C_{12} , C_{15} , C_{18} , C_{19} , C_{22} , C_{28} , C_{32} , an C_{36} n-alkane mixture to each sample (Strehmel *et al.*, 2008).

GC-EI/TOF-MS chromatograms were acquired, visually controlled, baseline corrected and exported in NetCDF file format using ChromaTOF software (Version 4.22, LECO, St. Joseph, USA). The GC-MS data processing into a standardized numerical data matrix and compound identification were performed using the TagFinder software (Luedemann *et al.*, 2008; Allwood *et al.*, 2009). Compounds were identified by mass spectral and retention time index matching to the reference collection of the Golm metabolome database (GMD, <http://gmd.mpimp-golm.mpg.de/>) (Kopka *et al.*, 2005; Schauer *et al.*, 2005; Hummel *et al.*, 2010). Guidelines for manually supervised metabolite identification were the presence of at least three specific mass fragments per compound and retention index deviation $<1.0\%$ (Strehmel *et al.* 2008).

The mass features were normalized by sample fresh weight and internal standard and were maximum scaled. For quantification purposes all mass features were evaluated for best specific, selective and quantitative representation of observed analytes. Laboratory and reagent contaminations were eliminated by non-sample control experiments. Metabolite pool sizes were assessed by relative changes expressed as response ratios, i.e. x-fold factors in comparison to a control condition. For independent component analyses (ICAs), the ratio to the mean of the control condition was calculated for all samples.

2.2.4.2 GUS staining

Mycorrhizal and non-mycorrhizal roots transformed with the appropriate promoter-GUS construct via *A. rhizogenes* mediated root transformation were harvested 4 wpi, washed carefully and covered with freshly prepared GUS buffer containing 0.5 mg/ml X-Gluc. They were incubated over night in darkness at 37 °C. Once blue areas were visible, they were embedded in 4 % agarose for subsequent sectioning.

2.2.4.3 Staining of fungal structures in roots

Trypan blue staining

The trypan blue staining is suitable for a wide range of AM fungi and was carried out as described in Phillips and Hayman (1970). Mycorrhizal roots were covered with 10 % KOH and incubated at 90 °C for 20 min. After decanting the KOH the roots were washed twice with distilled water, placed in trypan blue staining solution (25 ml 2 % trypan blue and 1000 ml lactoglycerol solution), and incubated at 90 °C for 3-5 min. The roots were washed with water, cut into 1 cm fragments, and were then mounted on glass slides in 10 % glycerol for the light microscopic analysis.

WGA Alexa Fluor 488 staining

Mycorrhizal roots were treated with KOH as described above. After washing thoroughly first with distilled water and then with 1 x PBS buffer (pH 7.4) the roots were incubated with WGA Alexa Fluor 488 in PBS (1:200) over night. Root sections (50 µm longitudinal or cross sections) were collected in 1 x PBS, and stained directly without KOH treatment. The roots (or root sections) were washed carefully and mounted in glycerol for analysis using the epifluorescence microscope.

2.2.4.4 In situ hybridization

For the visualization of *in planta* expressed fungal transcripts, mycorrhizal roots were embedded in paraffin for subsequent sectioning and *in situ* hybridization. 0.5 mm root fragments were dehydrated in an ethanol series (20 %, 40%, 60 %, 80 %, 90 % and 100 % EtOH in DEPC-H₂O; 1 h at 4 °C each step). Ethanol was gradually replaced by xylene (100 % EtOH, 50 % xylene in EtOH, 100 % xylene; 1 h each step) and the sections in xylene were covered with a layer of liquid paraffin for 2 h at room temperature. The samples were heated to 58 °C and washed repeatedly with paraffin (2h each step). Finally, the samples in paraffin were poured into aluminium containers and let cool down. Blocks with root fragments were cut out after the paraffin solidified.

The paraffin-embedded root pieces were cut in 10 µm cross sections using the Rotary Microtome Leica RM2265. For each hybridized probe and its corresponding negative control (sense RNA probe), subsequent sections were used to ensure that the compared sections derived from the same cell layer.

After cutting; the root sections were deparaffinized (100% xylene, 50% xylene in ethanol, 100% EtOH, 50% ethanol in DEPC-H₂O, DEPC-H₂O; 5 min each step), deproteinated (proteinaseK 1 µg/ml in TE buffer, 10 min at 37 °C) and fixed in 4 % PFA (4 min at room temperature). Afterwards the sections were acetylated (tri-ethanol amine, conc. HCl, acetic anhydride) and dehydrated by an ethanol series (30%, 60%, 80%, 90%, 100% EtOH in DEPC-H₂O; 30 sec each step). The sections were dried at room temperature and subsequently hybridized in ENZO hybridization buffer (Roche) containing 0.025 pmol/µl of the respective DIG labelled RNA probe or sense control probe. After 5 min denaturation at 80 °C the slides were incubated over night at 35 °C (melting temperature $T_m - 10$ °C) in a humid chamber with 1 x SSC and 50 % formamide. The slides were then washed repeatedly in 2 x SSC (1 x 10 min, RT), 2 x SSC (2 x 15 min 35 °C), 1 x SSC (2 x 15 min 35 °C) and 0.1 x SSC (2 x 30 min 35 °C), and blocked with blocking sol. A (+ 1,5 % Blocking Reagent (Roche) and 2 % BSA, Albumin Fraction V) over night at 4 °C. Finally, the slides were washed, covered in 1:500 Anti-DIG AP in Blocking sol. A, and incubated at RT for 1.5 h. After washing off the antibody solution, the sections were stained with WG Alexa fluor 488 (1:500 in PBS) for 1 h, washed in TBS, and equilibrated in NBT/BCIP buffer for 10 min. NBT/BCIP stock solution (roche) was added to NCBT/BCIP buffer (20 µl/ml) and the slides were incubated in the staining solution in a coplin jar at room temperature until dark purple precipitates appeared (over night). The staining reaction was stopped by washing the slides in water. The samples were covered in glycerine:PBS (9:1), covered with a coverslip, and sealed before microscopy.

2.2.5 Microscopy

2.2.5.1 Cryosectioning and laser capture microdissection (LCM)

M. truncatula roots 4 wpi with *R. irregularis* were washed in iced water and embedded in TFM Tissue Freezing Medium. They were then cut longitudinally into 35 µm under constantly freezing temperatures (-22 °C) using the Leica CM1950 Cryostat. The slides were warmed briefly, causing the medium to melt very shortly and fix the cutting on the slide, and were frozen again immediately. The slides were washed in 70 % EtOH (3 min), DEPC- H₂O (25 - 30 min) and 100 % EtOH (3 min), dried at 37 °C for 30 min, and stored at -80 °C.

Via laser capture microdissection (PALM Microlaser Technologies) arbuscule-containing cells were selected and catapulted into the lid of a PALM tube. After approximately 10.000 cells were collected, 350 µl RLT Buffer (Qiagen) with 8.75 µl RNase Inhibitor (RNaseOUT, life technologies) and 3,5 µl β-Mercaptoethanol were added to the cells. The sample was vortexed thoroughly, centrifuged for 2 min at full speed and incubated at 56 °C for 5 min. The vortex and centrifugation steps were repeated once and the samples were stored at -80 °C.

2.2.5.2 Vibratome sectioning

For light microscopic analyses, roots were sectioned with the Leica Vibrating-Blade Microtome VT1000S. Short root pieces were embedded in 4 % agarose, cut out in small blocks, fixed in the sample holder with super glue, and sectioned either longitudinally or as cross sections (50 µm). The cuttings were collected in PBS, stained if required, and placed on glass slides in 10 % glycerine. The sections were analysed with the Microscope Olympus BX51.

2.2.5.3 Epifluorescence and confocal microscopy

WGA Alexa fluor 488 stained roots or root sections (GUS assays and *in situ* hybridization) were visually analysed with the epifluorescent microscope BX61 (Olympus) and the cellSens Dimension software or the BX51 with the cellP software. The GFP filter (excitation filter 470/40 nm, emission filter LP500>) and the DsRed filter (excitation filter 550/20 nm, emission filter 590>) were used for the detection of green and red fluorescence, respectively. Individual pictures were taken in each channel (fluorescent and/or bright-field) and overlays were produced using Adobe Photoshop CS5, if needed.

For the analyses of uncut roots or localization studies in tobacco leaves, the confocal microscope Leica TCS SP5 (2.3.1 build 5194) was used. For the detection of the different fluorescent signals, the manufacturer's settings were used (GFP excitation: 488nm, emission detection range: 500 - 600 nm; mCherry excitation: 561 nm, emission detection range: 570 - 700 nm). Gain and offset were kept equal for the detection of each flourophore in different samples. Overlays of the different channels were directly produced in the microscope software (LAS AF, Leica Application Suite Advanced Fluorescence).

2.2.6 Bioinformatic methods

2.2.6.1 Processing of metabolic profiling data

The ratios between the values normalized to the internal standard ($^{13}\text{C}_6$ -sorbitol) and fresh weight [g] of either mycorrhizal and non-mycorrhizal or *hxt1* and WT plants were calculated. The value of one biological replicate of one condition (myc or *hxt1*) was divided by the average of all replicates of the respective time-point (3, 5, or 7 wpi) and tissue (source leaves or roots) of the other condition (nonmyc or WT, respectively) to preserve the variation between biological replicates for statistical analysis. Averages were calculated from the ratios *hxt1*/WT and myc/nonmyc. These were Log_2 transformed and further analyses were based on the Log_2 -fold changes (LFCs).

Data visualizations were performed using the multi-experiment viewer software MeV, Version 4.6.2, <http://www.tm4.org/mev/> (Saeed *et al.*, 2003; Saeed *et al.*, 2006). Statistical assessments of the data were performed using Microsoft Excel 2007. Statistical testing (Student's t-test) was not performed on the Log_2 -transformed data, but on the raw data normalized to internal standard and fresh weight, to confirm the statistical relevance of their differential abundance (ratio).

Metabolites with significantly altered levels between either mycorrhizal and non-mycorrhizal conditions or between the two genotypes were selected if they had a LFC of >1 or <-1 with a p-value of at ≤ 0.05 .

For ICAs, The values were normalized to the average of the WT non-mycorrhizal condition of the respective tissue and time-point and log_2 -transformed. Independent components were calculated using MetaGeneAlyse (<http://metagenealyse.mpimp-golm.mpg.de/>) (Daub *et al.*, 2003) with 2 principal components, ICAs were then produced from these ICs in Microsoft Excel 2007.

2.2.6.2 Processing of Illumina SBS high-throughput sequencing data

The sequencing raw data obtained from Eurofins MWG Operon (Ebersberg) were computationally processed in cooperation with the in-house bioinformatics services (Dr. Sasmuel Arvidsson, Dr. Dirk Walther). RNA-Seq data of two samples were compared: LCM collected arbuscules, samples also containing intraradical hyphae, therefore referred to as arbuscules or *in planta* tissues in the following, and extraradical hyphae and germinating spores, referred to as ERM or extraradical tissues.

Initially, the raw data were mapped against the *M. truncatula* genome to identify and remove all *M. truncatula* reads from the dataset (figure 3). They were then filtered to remove all possible

contamination with *E. coli*, yeast, PhiX, adapter or vector sequences. Since no *R. irregularis* reference genome was available at the time the data were obtained, the unique reads of both libraries were combined to assemble contigs using Trinity, a program for the *de novo* assembly of RNA-Seq reads (<http://trinityrnaseq.sourceforge.net/>). These transcontigs were then used to perform a read-count based expression profiling: the raw reads of each library were separately mapped to the transcontigs using Bowtie (Langmead *et al.*, 2009). For the quantification of the transcripts, RSEM (RNA-Seq by Expectation Maximization) was used, a software which uses a bayesian approach to assign multi-mapping reads to the most probable transcript with which gene abundances can be calculated without a reference genome (Li and Dewey, 2011). The estimation of the transcript abundance has also been calculated using a second method, RPKM (Reads Per Kilobase and Million mapped reads) to corroborate the results of the RSEM estimation. Both methods largely resulted in similar trends, but due to the expected higher accuracy of the results of the RSEM estimation, these were used for further analyses.

The log₂ fold change (LFC) was calculated from the RSEM estimated expression values of each contig:

$$\text{Log}_2 \left(\frac{RSEM_{arb}}{RSEM_{erm}} \right)$$

For the first functional annotation of the transcontigs, they were aligned against known *Glomus* sequences (*Glomus* DB, <http://mycor.nancy.inra.fr/IMG/GlomusGenome/index3.html>) the NCBI nucleotide sequence collection (nt, <ftp://ftp.ncbi.nih.gov/blast/db/nt>) and non-redundant protein collection (nr, <ftp://ftp.ncbi.nih.gov/blast/db/nr>).

Additionally, as an indication of possible transporter protein coding genes, transmembrane domains (TMDs) of the transcontigs were predicted, since these are a common necessary feature of transporter proteins and can therefore be used as an indication of the potential function of the gene product. For this, the reading frame was predicted using TransDecoder (<http://transdecoder.sourceforge.net/>) and the peptides were checked for transmembrane helices (<http://www.cbs.dtu.dk/services/TMHMM/>).

The resulting candidate genes were selected from a combination of the results of both, the differential expression and the TMDs. Only transcontigs with two or more TMDs and a LFC of > 3 or < -3 were selected. A few *M. truncatula* sequences were found and removed from the resulting list of candidates. The remaining transcontigs were annotated by hand, using the predicted peptide sequences for blastp searches against all fungal sequences available at NCBI. All candidates that could be annotated as transporter genes were used as candidate genes.

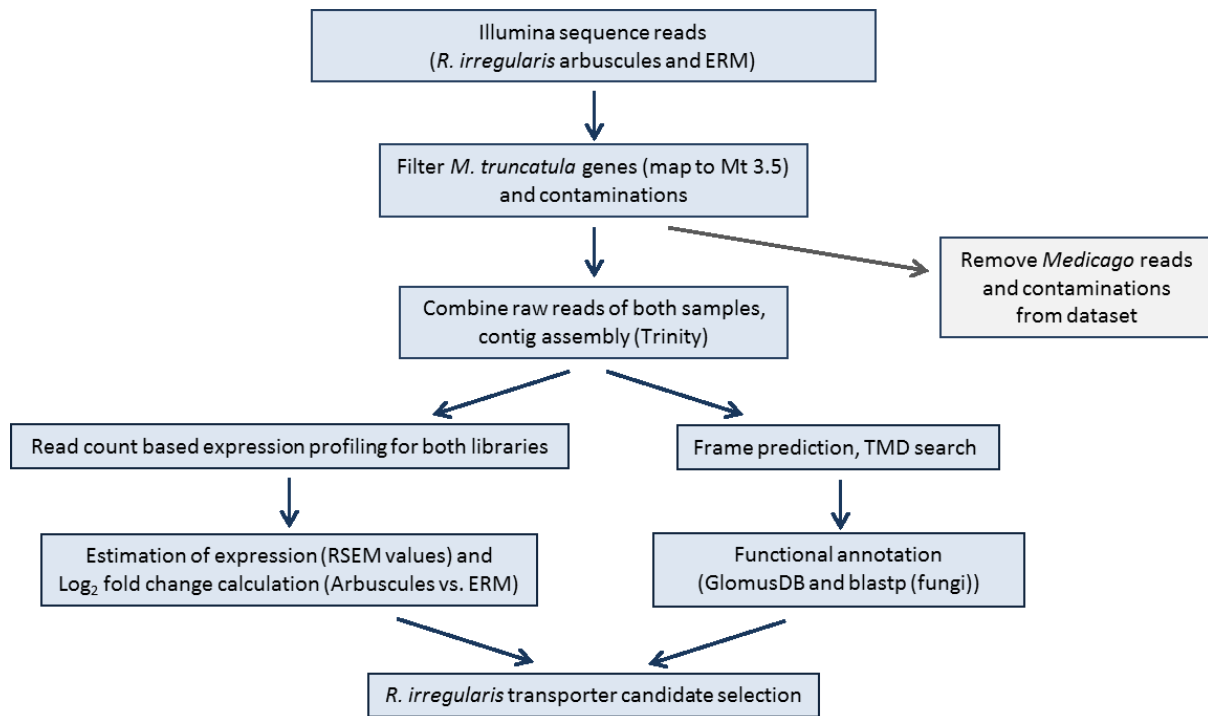


Figure 3: Schematic workflow of the analysis of the Illumina reads. Contig assembly, differential expression profiling, and annotation for the selection of *in planta* regulated *R. irregularis* candidate transporter genes.

Only after the candidate selection was completed, the first successfully assembled genome sequence derived from single nuclei of one *R. irregularis* spore was generated (Francis Martin, INRA, Nancy, personal communication). This was kindly made available to us by F. Martin. Since the candidates had already been selected before, the genome sequences were used to verify them. The contigs were blasted against the *R. irregularis* genome to confirm their assembled sequences and to obtain the full length genomic sequence if available.

The full coding sequences of the candidate genes were amplified with gene specific primers that were designed upon the availability of the genomic sequences. They were sequenced in order to check and, if necessary, revise the sequence information and the predicted exon/intron structure of the genes.

3 RESULTS

3.1 Characterization of cell type-specifically regulated *Medicago truncatula* genes involved in transport mechanisms

To get a deeper insight into AM-induced transcriptional changes on a cell type-specific level, laser capture microdissection (LCM) and microarray experiments have been combined (Gaude *et al.*, 2012). Via Affymetrix GeneChip hybridization of RNA isolated from arbuscule-containing cortex cells (ARB), non-arbusculated cortex cells of mycorrhizal roots (NAC) and cortex cells of non-mycorrhizal roots (COR), a large number of specifically regulated *M. truncatula* transcripts have been identified. Using the MapMan software (<http://mapman.gabipd.org/web/guest>) (Usadel *et al.*, 2009) these genes have been classified and predicted functions have been annotated (Gaude *et al.*, 2012). AM-regulated genes were found in defined functional classes, like lipid metabolism, transcription regulation, protein metabolism and processing, and defence/stress response (figure 4). Also, 15 genes of the 49 probe sets in the genome array that were identified as putative fungal genes were present in the set of differentially expressed transcripts.

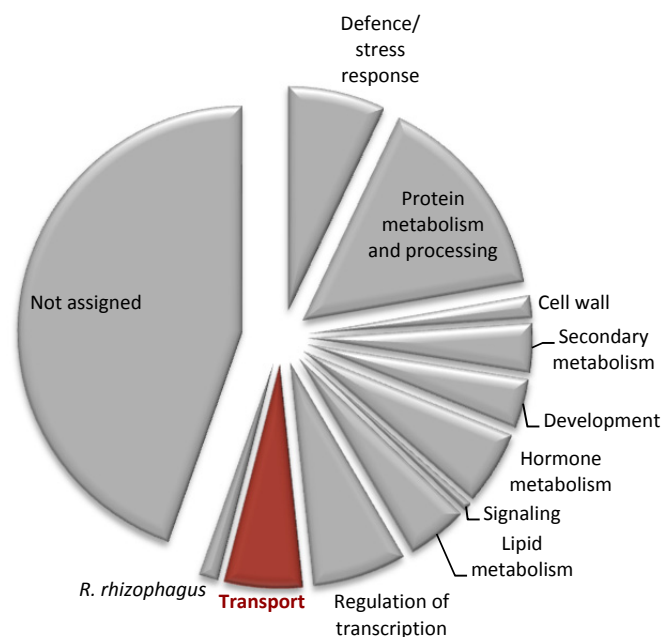


Figure 4: Distribution of cell-specifically regulated *M. truncatula* transcripts in response to mycorrhizal colonization across different functional classes (based on Gaude *et al.*, 2012).

3.1.1 Selection and confirmation of candidate genes

As expected, also a high number of genes involved in transport mechanisms are cell-specifically regulated in response to the colonization of the roots by the AM fungus (figure 4). The expression of 26 transporter genes is up-regulated in arbuscule-containing cells in comparison to cortical cells with a \log_2 -fold change ($LFC_{ARB/COR}$) of more than 2, 12 of these are up-regulated in NAC cells as well. One putative transporter gene is down-regulated in arbuscule-containing cells in comparison to cortical cells and 5 genes are specifically up-regulated in NAC cells (Gaude *et al.*, 2012) (figure 5).

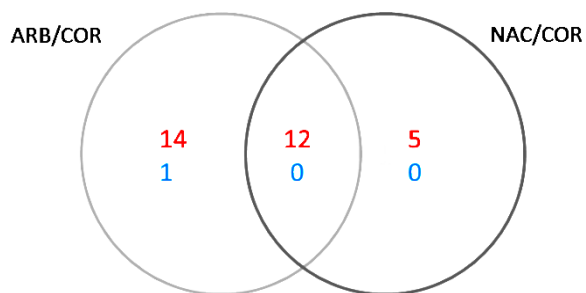


Figure 5 : Venn diagram of the cell-specifically regulated transporter genes. Red: up-regulated genes, blue: down-regulated genes, ABR: arbuscule-containing cells, NAC: non-arbusculated cortical cells, COR: cortical cells of uncolonized roots. $LFC > 2$ or < -2 (based on Gaude *et al.*, 2012).

The predicted transporter encoding genes regulated with a LFC of either > 2 or < -2 with a p -value of < 0.05 in arbuscule-containing cells vs. cortical cells of non-colonized roots have been selected for this study. Also, three potential transporter genes have been selected which were specifically up-regulated in non-arbusculated cells of mycorrhizal roots in comparison to cortex cells of non-colonized roots. Unless already described in *Medicago truncatula*, the genes were named after their closest *Arabidopsis thaliana* homolog. Well-known mycorrhiza induced genes like *MtPt4*, *MtHa1* and *MtStr2* were found in this approach, too, but they were omitted for the further analyses. The 16 final transporter gene candidates are listed in table 6. The Mt3.0 and Affymetrix GeneChip identifiers are listed in the Supplementary table S 2.1.

Table 6: AM-specifically regulated transporter candidate genes of *M. truncatula*. The annotation, the gene identifier as well as the transcriptional regulation are given (based on Gaude *et al.*, 2012).

Annotation	Affymetrix ID/ IMGAG ID Mt3.5	Log ₂ -fold change		
		ARB/NAC	NAC/COR	ARB/COR
Copper transporter <i>MtCot</i>	mtr.37110.1.s1_at	2.71	6.50	9.21*
Nitrate transporter <i>MtNrt1</i>	Medtr2g017750.1	3.94	4.66	8.60*
Mitochondrial phosphate transporter <i>MtMpt1</i>	Medtr7g083790.1	2.04	3.47	5.51*
Dicarboxylate transporter <i>MtDit2</i>	Medtr2g009220.1	1.99	1.10	3.06*
Amino acid transporter <i>MtAap1</i>	mtr.44555.1.s1_at	1.37	1.20	2.57*
Ammonium transporter <i>MtAmt2</i>	Medtr8g095040.1	1.95	-0.17	1.78*
Nucleobase-ascorbate transporter <i>MtNat2</i>	Medtr8g086520.1	-1.58	2.14	0.57
Sucrose/H ⁺ symporter <i>MtSut4-1</i>	Medtr5g067470.1	-2.33	2.61	0.28
Hexose/H ⁺ symporter <i>MtHxt1</i>	Medtr1g104780.1	-2.72	2.86	0.13
H ⁺ -dependent Oligopeptide transporter <i>MtPtr1</i>	Medtr8g087780.1	6.08	0.94	7.02*
H ⁺ -dependent Oligopeptide transporter <i>MtPtr3</i>	Medtr7g098040.1	2.69	2.00	4.68*
H ⁺ -dependent Oligopeptide transporter <i>MtPtr4</i>	Medtr8g087810.1	3.95	0.42	4.36*
ABC transporter/MDR <i>MtAbcb15</i>	Medtr8g022270.1	1.86	4.25	6.11*
ABC transporter/MDR <i>MtPgp18</i>	Medtr3g086430.1	0.42	0.64	1.06*
Major intrinsic protein <i>MtNip1</i>	Medtr8g087710.1	2.35	4.36	6.71*
Major intrinsic protein <i>MtNip4</i>	Medtr5g063930.1	1.60	0.91	2.51*

* Regulation confirmed by qRT-PCR

The already described putative copper transporter *MtCot* (mtr.37110.1.s1_at) (Frenzel *et al.*, 2005) has been found to be highly up-regulated in arbuscule-containing as well as neighbouring cells. This regulation has been confirmed via qRT-PCR (A. Reinert, Dissertation 2012).

A putative ammonium transporter, *MtAmt2* (Mt3.5: Medtr8g095040.1), is up-regulated in arbuscule-containing cells. Among the up-regulated candidates there are also several potential ATP-binding cassette transporters, two of them most likely to belong to the ABCB subfamily, *MtAbcb15* and *MtPgp15* (Medtr8g022270.1 and Medtr3g086430.1). The third of the ABC transporters (Medtr5g030910.1) is the *MtStr2* gene previously described by Zhang *et al.* (2010). There are also two putative major intrinsic proteins. *MtNip4* (Medtr5g063930.1) is specifically up-regulated in arbuscule-containing cells, *MtNip1* (Medtr8g087710.1) in both, arbuscule-containing and neighbouring cells. The potential transcripts of three putative oligopeptide transporters *MtPtr1*, *MtPtr3* and *MtPtr4* (Medtr8g087780.1; Medtr7g098040.1; Medtr8g087810.1) as well as a putative dicarboxylate transporter *MtDit2* (Medtr2g009220.1) and a putative amino acid transporter *MtAap1*

(mtr.44555.1.s1_at) were found to accumulate in arbuscule-containing cells. Moreover, one putative mitochondrial substrate carrier *MtMpt1* (Medtr7g083790.1) and a putative nitrate transporter *MtNrt1* (Medtr2g017750.1) have been found to be highly up-regulated in arbuscule-containing cells and, to a lesser extent, also in neighbouring cells.

Three further transporter candidates have been selected which are regulated in a different way than the ones described above. These genes are a potential nucleobase-ascorbate transporter *MtNat2* (Medtr8g086520.1), a potential hexose/H⁺ symporter *MtHxt1* (Medtr1g104780.1) and a sucrose/H⁺ symporter *MtSut4-1* (Medtr5g067470.1) that has been confirmed as a sucrose transporter (Doidy *et al.*, 2012). The transcripts of these three genes are only very slightly regulated in arbuscule-containing cells in comparison to cortical cells (ARB/COR). However, they were found to accumulate in neighbouring non-arbusculated cells in comparison to cortex cells (NAC/COR), and in comparison to arbuscule-containing cells (ARB/NAC).

3.1.1.1 Transcriptional regulation of the putative transporter genes in mycorrhizal roots

Quantitative reverse transcription PCR (qRT-PCR) was performed using cDNA of mycorrhizal and non-mycorrhizal *M. truncatula* whole roots (4 wpi) to confirm the transcriptional regulation of the transporter candidates. If genomic sequences of the candidates were available, predicted intron/exon regions were used to design gene-specific qRT-PCR primers.

The transcriptional regulation in *M. truncatula* roots was confirmed for all putative transporter gene candidates listed above that were found to be up-regulated in arbuscule-containing cells (figure 6). Except for the genes up-regulated in non-arbuscule containing neighbouring cells, all candidates for which the AM-responsive regulation could not be experimentally confirmed were removed from the list of candidates. A successfully established and functional AM-symbiosis was indicated by the strongly induced transcript levels of the phosphate transporter *MtPt4* which is specifically transcribed in arbuscule-containing cells (Harrison *et al.*, 2002), and the transcript of the *Rhizophagus irregularis* ribosomal gene *RirRNA* (figure 7).

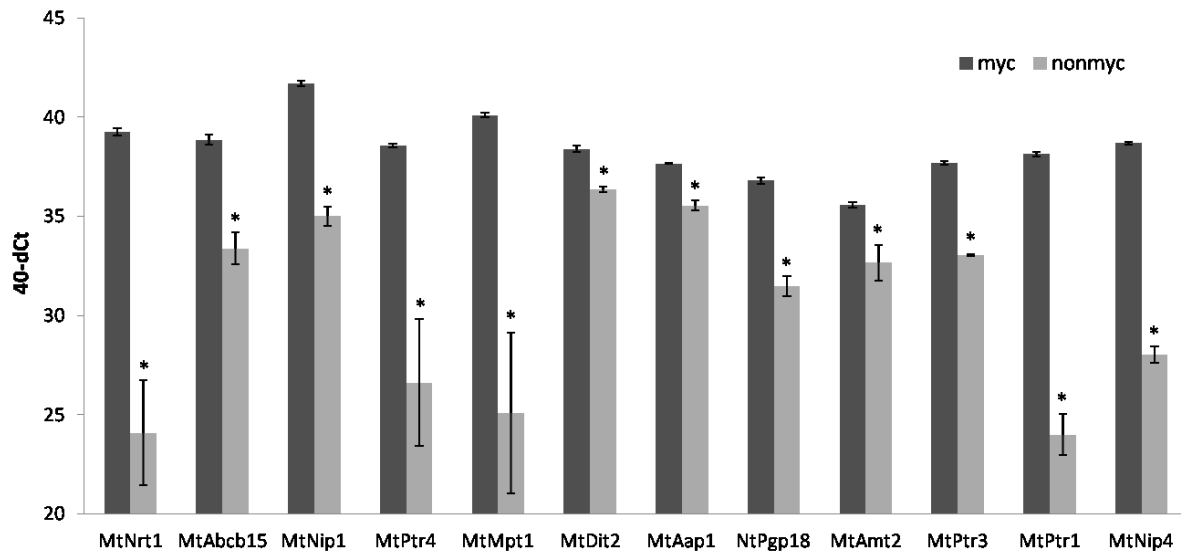


Figure 6: Relative expression levels (given as 40-dCt values) of the up-regulated putative transporter genes in *M. truncatula* roots determined by qRT-PCR. Wild-type roots were harvested 4 wpi with *R. irregularis* or as 4 weeks old non-inoculated roots. A reference gene index (*UbiExon*, *Pdf2* and *GapDH*) was used for normalization. Values shown are mean \pm standard deviation of three biological replicates with two technical replicates of each PCR reaction. *: p-value \leq 0.01.

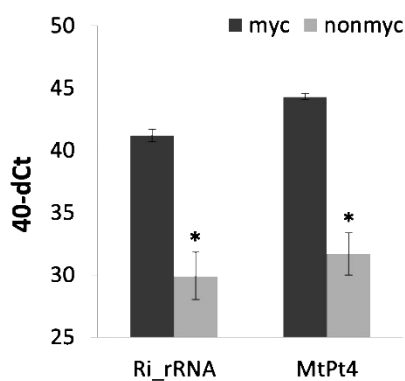


Figure 7: Relative expression levels (given as 40-dCt values) of the mycorrhizal marker gene *MtPt4* and the *RirRNA* in *M. truncatula* roots. Wild-type roots were harvested 4 wpi with *R. irregularis* or as 4 weeks old non-inoculated roots. A reference gene index (*UbiExon*, *Pdf2* and *GapDH*) was used for normalization. Values shown are mean \pm standard deviation of three biological replicates with two technical replicates of each PCR reaction. *: p-value \leq 0.01.

3.1.1.2 Cell-specific promoter activity of the transporter candidate genes

The potential promoter region of the transporter gene candidates (1 kb upstream of the ATG) was cloned via Gateway™ cloning in front of the *uidA* gene as a reporter for the promoter activity. The fragment was cloned into the vector pGWB433 for a β -glucuronidase (GUS) fusion (Nakagawa *et al.*, 2007) (figure 8).



Figure 8: Promoter-GUS fusions for the localization of the promoter activity in *M. truncatula* roots. RB, LB: right and left border of the T-DNA; *Tnos*: nopaline synthase terminator; *NptII*: kanamycin resistance for selection in plants, regulated by the *nos* promoter and terminator; promoter: ~1 kb fragment upstream of the ATG of the respective transporter gene; *uidA*: β -glucuronidase (GUS) gene.

M. truncatula seedlings were transformed via *A. rhizogenes*-mediated root transformation and after three weeks on selective medium the plants were potted into substrate containing *R. irregularis* inoculum. The roots were harvested and analysed 4 wpi and stained with X-Gluc (5-Bromo-4-chloro-1H-indol-3-yl β -D-glucopyranosiduronic acid). Blue parts representing GUS activity were selected, cut longitudinally into 50 μ m sections, and stained with WGA Alexa 488 fluor to visualize fungal structures. These fragments were then analysed by epifluorescence microscopy.

The promoter activity shown by the GUS staining and fungal structures visualized via WGA Alexa fluor co-localized in the expected pattern for nine of the candidate genes expected to be up-regulated in arbuscule-containing cells (figure 9).

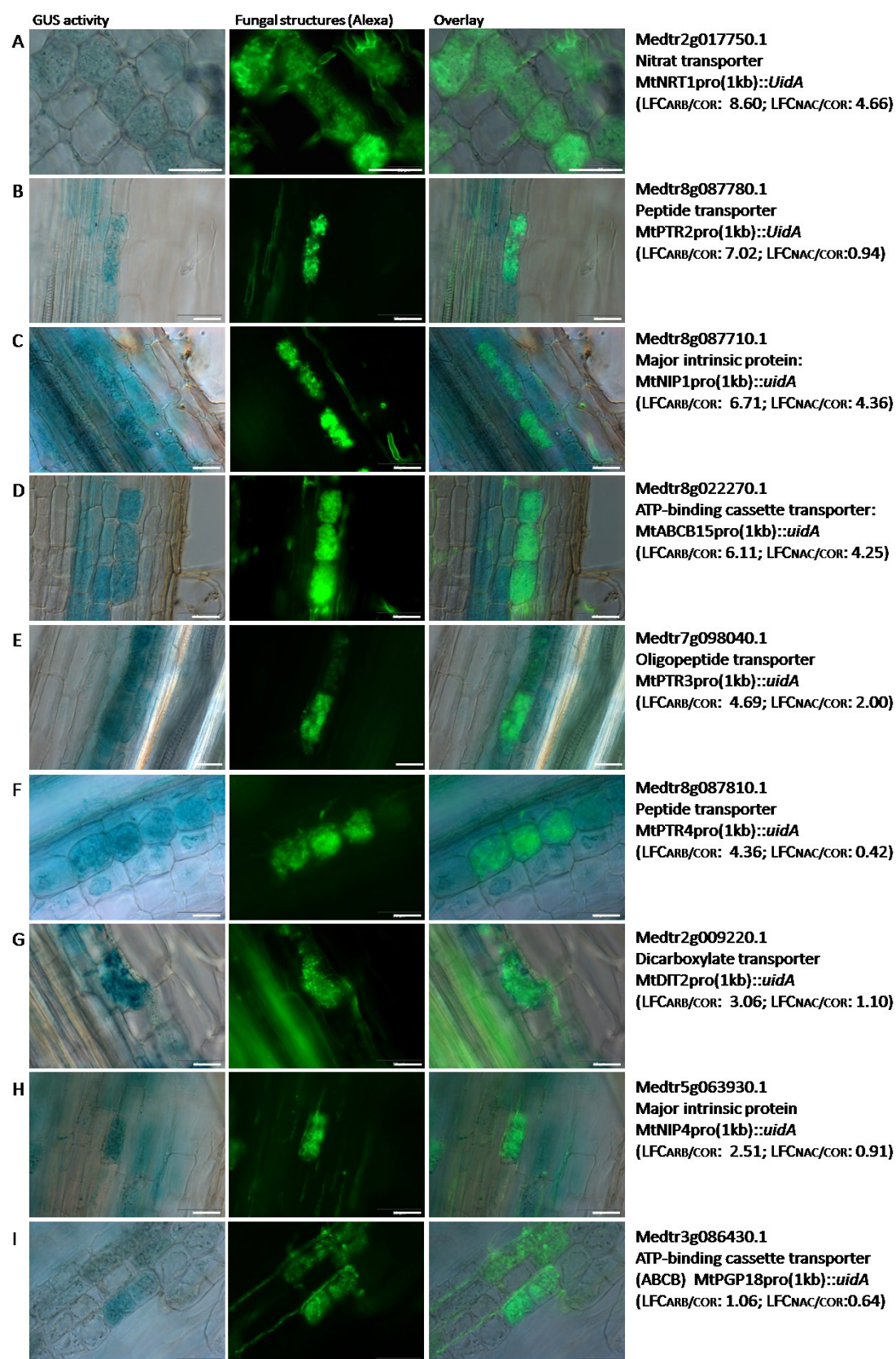


Figure 9: Localization of the promoter activity of selected genes transcriptionally regulated in ARB or NAC cells coding for putative transporter proteins in mycorrhizal *M. truncatula* roots (50 μ m). Promoter(\sim 1kb)::*uidA* fusions. Bright-field images show promoter-driven GUS activity, green fluorescence indicates fungal structures after staining with WGA Alexa 488 fluor. The putative gene functions as well as the Mt3.5 identifiers and the transcript regulation from Gaude *et al.* (2012) are given. Scale bar: 30 μ m.

In the Affymetrix GeneChip hybridization experiments, the gene coding for the nitrate transporter MtNRT1 (figure 9 A) was found to be strongly up-regulated in arbuscule-containing cells when compared to cortex cells whereas the up-regulation in non-arbusculated cells is less pronounced. This could be confirmed as the promoter study reported the strongest promoter activity in arbuscule-containing cells.

The promoter activities of the genes coding for the peptide transporters MtPTR1 (figure 9 B) and MtPTR4 (figure 9 F) were shown to be highly active very specifically in arbuscule containing cells. This is in line with the results of the GeneChip hybridization which revealed a high abundance of these transcripts in arbuscule-containing cells vs. cortical cells ($LFC_{ARB/COR}$ 7.0 and 4.4, respectively) whereas in neighbouring cells almost no induction of their expression could be detected in comparison to cortical cells of non-mycorrhizal roots ($LFC_{NAC/COR}$ 0.9 and 0.4, respectively). On the other hand, the putative oligopeptide transporter *MtPtr3* (figure 9 E) was shown to be up-regulated in neighbouring non-arbusculated cells as well as in arbuscule-containing cells, albeit to a lesser extent. The results for the promoter activity of this gene are in line with this finding.

The gene coding for the potential major intrinsic protein MtNIP1 (figure 9 C) was shown to be up-regulated in arbuscule-containing cells in comparison to cortex cells with a LFC of 6.7 and in adjacent cells to cortex cells with a LFC of 4.4. This was confirmed by the promoter-GUS fusion as uncolonized cells show a GUS signal as well, but weaker as compared to the arbuscule-containing cells. Also, the promoter of *MtNip4* (figure 9 H) was confirmed to be highly active very specifically in arbuscule-containing cells.

This also holds true for the potential ABC transporter MtABCB15 (figure 9 D). The promoter was highly active in arbuscule-containing cells but to a lower extent in non-arbusculated cells as well. The promoter fusion of the other potential ABC transporter, MtPGP18 (figure 9 I), confirmed the specific expression in arbuscule-containing cells.

The GUS fusion confirmed the strongest promoter activity of the putative dicarboxylate transporter gene *MtDit2* (figure 9 G) in arbuscule-containing cells. The accumulation of the transcript in neighbouring non-arbusculated cells was much lower ($LFC_{NAC/COR}$ 1.1), as was the GUS expression.

3.1.1.3 Potential transporter genes were confirmed to be cell-specifically regulated during AM symbiosis

A number of cell-specifically regulated potential transporter genes were found in a GeneChip hybridization experiment. The increased expression in mycorrhizal roots was confirmed via qRT-PCR (figure 6) for 12 of those that were found to be up-regulated in arbuscule-containing cells with a LFC ≥ 2 . The cell-specific promoter activity in arbuscule-containing cells of five of these genes and in arbuscule-containing and neighbouring cells of four of them was visualized via promoter-GUS fusions (figure 9).

3.1.2 Putative carbohydrate transporters with transcriptional regulation in mycorrhizal roots

3.1.2.1 Sugar transporters are cell-specifically regulated

In addition to the transporter genes that were found to be up-regulated in arbuscule-containing cells, two potential sugar transporters were found to be specifically up-regulated in NAC cells. These are a potential hexose transporter *MtHxt1* and a sucrose transporter *MtSut4-1*.

Cell-specific promoter activity

M. truncatula roots were transformed with a promoter-*uidA* fusion construct (figure 8) containing an approximately 1 kb promoter fragment of *MtSut4-1* and *MtHxt1*, respectively, harvested 4 wpi with or without *R. irregularis* inoculation, GUS-stained and cross sectioned. The localization of the promoter activity of the two sugar transporter genes confirmed the results of the GeneChip hybridization where they were found to be up-regulated in adjacent cells. The promoters of the sucrose transporter *MtSut4-1* and the potential hexose transporter *MtHxt1* were shown to be active in cells adjacent to fungal structures (figure 10).

The activity of the promoter of *MtSut4-1* co-localizes well with the root areas colonized by the fungus (figure 10 A-C). The GUS staining is clearly visible in those cortical cells that are located in the vicinity of intercellular hyphae growing in the apoplast or next to arbuscule-containing cells.

The GUS staining of the promoter fusion with the *MtHxt1* promoter region does co-localize with arbuscule-containing and neighbouring cells (figure 10 D-F). Some, but not all arbuscule-containing cells show a strong GUS staining, whereas cortex cells that are not colonized by the fungus but are located next to arbuscule-containing cells often do exhibit a GUS staining, too.

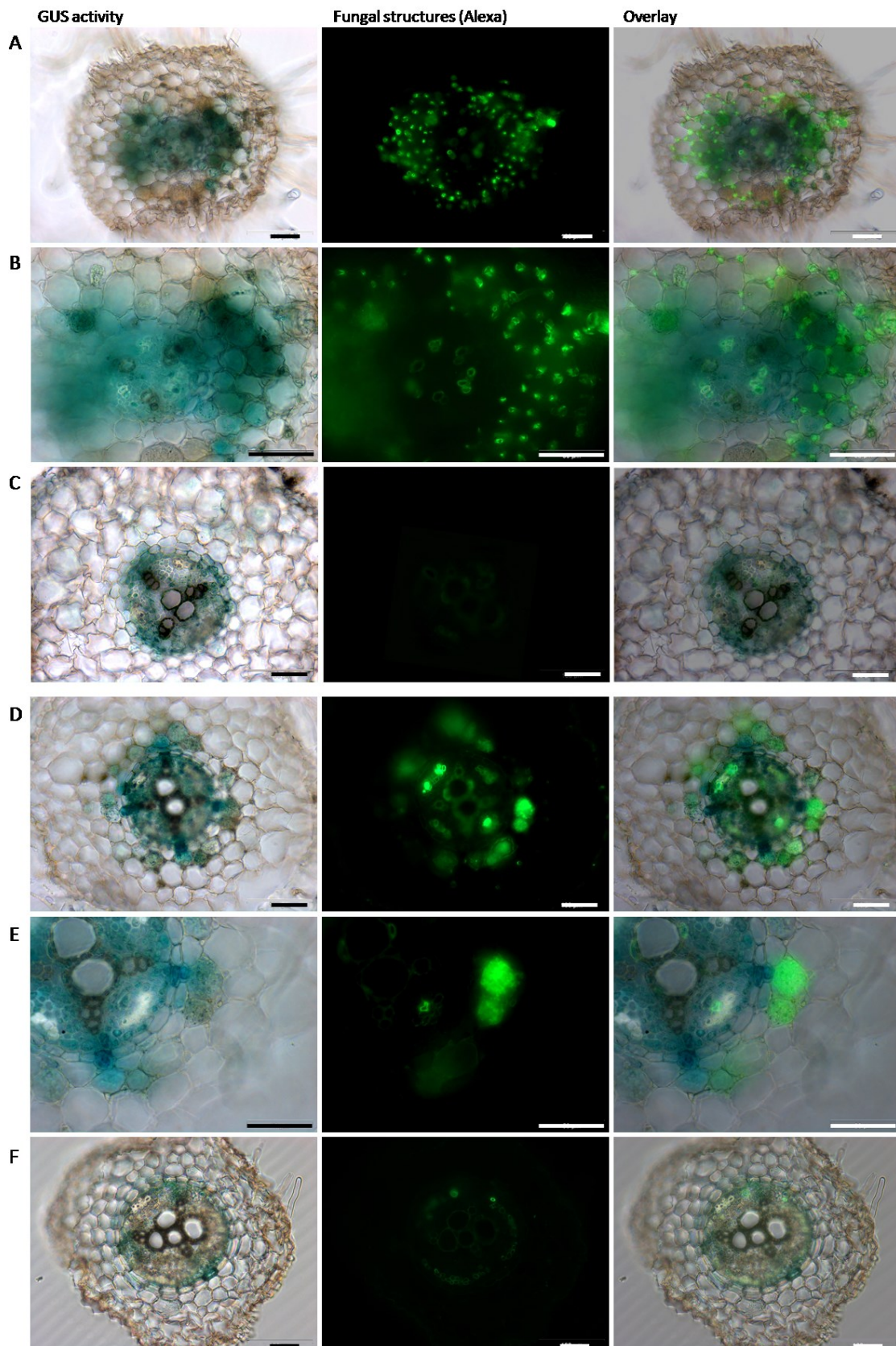


Figure 10: Localization of the promoter activity of selected genes transcriptionally regulated in ARB or NAC cells coding for putative sugar transporter proteins in mycorrhizal *M. truncatula* roots (50 μm cross sections). Promoter($\sim 1\text{kb}$):*uidA* fusions. Bright-field images showing promoter-driven GUS activity, green fluorescence indicating fungal structures after staining with WGA Alexa 488 fluor. A-C: *proMtSut4-1* (Medtr5g067470.1); D-F: *proMtHxt1* (Medtr1g104780.1). A, D: overview; B, E: detailed view; C, F: non-mycorrhizal roots. Scale bar: 50 μm .

Both promoter-*uidA* fusions did not lead to a staining in the cortex cells of non-colonized control roots (figure 10 C and F). But the cells of the endodermis surrounding the vascular stele and the central cylinder itself did show a GUS staining.

Transcriptional regulation of MtHxt1 and MtSut4-1 in response to nodulation

The *Medicago truncatula* Gene Expression Atlas (<http://mtgea.noble.org/v3/>) suggests an increased expression of both transporters in nodules. This was confirmed with the promoter-*uidA* fusion constructs described above (figure 8) in *M. truncatula* roots nodulated with *S. meliloti* (figure 11). The GUS staining indicated an activity of both promoters in the outer layers of the nodules, directly beneath the epidermis, and in the roots at the base of the nodule where it emerges from the root.

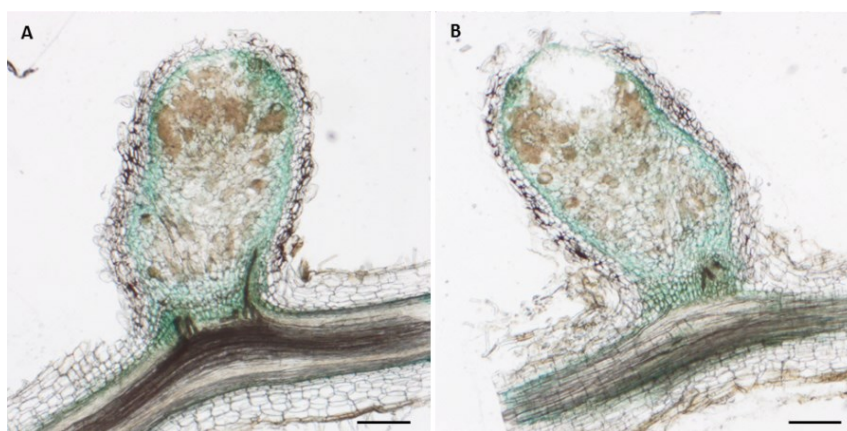


Figure 11: Localization of the promoter activity of selected genes transcriptionally regulated in ARB or NAC cells and coding for putative sugar transporter proteins in *S. meliloti* nodules of *M. truncatula* roots (50 μ m). Promoter(~1kb)::*uidA* fusions. A: proMtHxt1 (Medtr1g104780.1); B: proMtSut4-1 (Medtr5g067470.1). Scale bar: 200 μ m.

qRT-PCR was performed with cDNA of uninfected *M. truncatula* A17 roots (N fertilized), *S. meliloti* nodules of *M. truncatula* roots, and previously nodulated roots from which the nodules have been removed (denodulated roots). Transcript levels of the nodule-specific membrane protein N24 (Moreau *et al.*, 2011) were measured as a marker for nodule contamination of the denodulated and symbiosis-free roots (figure 12). As expected, it is highly expressed in nodules but almost undetectable in the root samples.

Both, *MtHxt1* and *MtSut4-1*, are strongly expressed in nodules. *MtHxt1* has a very low expression in roots and denodulated roots in comparison to nodules, while the expression of *MtSut4-1* in denodulated roots is lower than it is in nodules, but still higher than in roots that were not nodulated at all (figure 12).

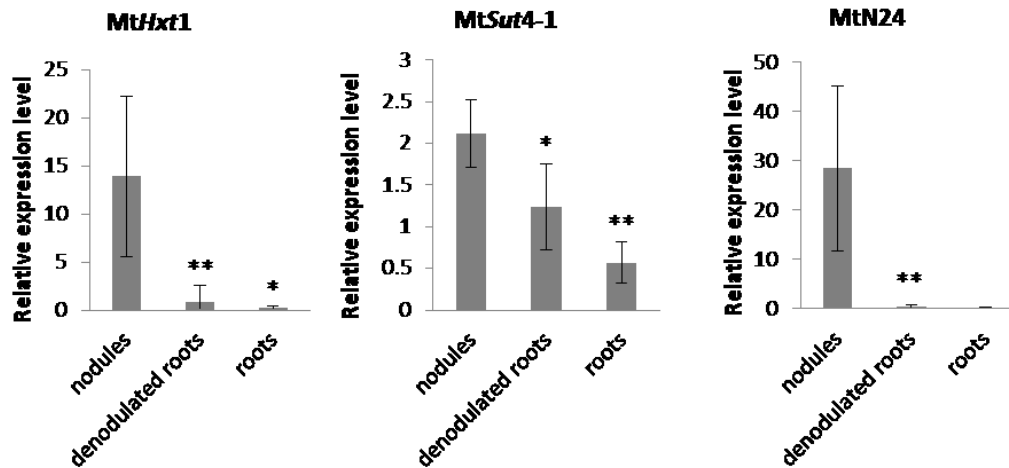


Figure 12: Relative expression levels (2^{-dCt} values) of the putative *M. truncatula* sugar transporters *MtHxt1* and *MtSut4-1*, and the nodule marker gene *MtN24* in nodulated and non-nodulated *M. truncatula* roots determined by qRT-PCR. Wild-type roots were harvested 5 wpi with *S. melloti* or after 5 weeks of growth without a symbiotic interaction. The nodules were removed and RNA was isolated separately from the nodules and the remaining denodulated roots. A reference gene index (*UbiExon*, *Pdf2* and *GapDH*) was used for normalization. Values shown are mean \pm standard deviation of two to six biological replicates with two technical replicates of each PCR reaction. *: p-value \leq 0.05; **: p-value \leq 0.01, compared to the expression in nodules.

Intracellular localization of MtHXT1 and MtSUT4-1

Comparative sequence analyses revealed that the sucrose transporter MtSUT4-1 shows highest similarity to the *Lotus japonicus* sucrose transporter LjSUT4 (81 % identity on amino acid level). This transporter is localized at the tonoplast, mediating a proton-coupled import of sucrose from the vacuole into the cytoplasm (Reinders *et al.*, 2008). The potential hexose transporter MtHXT1, on the other hand, shows highest similarities (77 % identity on amino acid level) to *AtSTP13*, an *Arabidopsis thaliana* hexose/H⁺ symporter which is localized in the plasma membrane and imports hexoses from the apoplast into the cytosol (Norholm *et al.*, 2006).

Due to these sequence similarities, MtSUT4-1 and MtHXT1 are expected to also be localized at the tonoplast and the plasma membrane, respectively. This was corroborated by protein fusions of both transporters to the Green Fluorescent Protein (GFP). C- and N-terminal fusions as well as a GFP fusion to both ends of the protein were assayed. For MtHXT1, the N-terminal fusion (in pK7WGF2) resulted in a strong fluorescence, clearly localized at the plasma membrane. For MtSUT4-1 only the GFP fusion to both ends (C- and N-terminal in pK7FWGF2) resulted in a satisfactory fluorescent signal, which could be detected at the tonoplast. A mCherry marker for the tonoplast was used to be able to distinguish between these two membranes. In this control vector, the tonoplast localization was achieved by fusing the coding region of the fluorescence protein mCherry to the C-terminus of c-TIP, an aquaporin of the vacuolar membrane (Nelson *et al.*, 2007). The co-localization experiments

were performed in *Nicotiana benthamiana* leaves. While the GFP signal fused to MtSUT4-1 co-localized with the red fluorescence of the tonoplast marker (figure 13 D - F), the GFP-MtHXT1 fluorescence (figure 13 A - C) is clearly localized at the plasma membrane, surrounding the outermost surface of the cells and is not overlapping with the red tonoplast fluorescence.

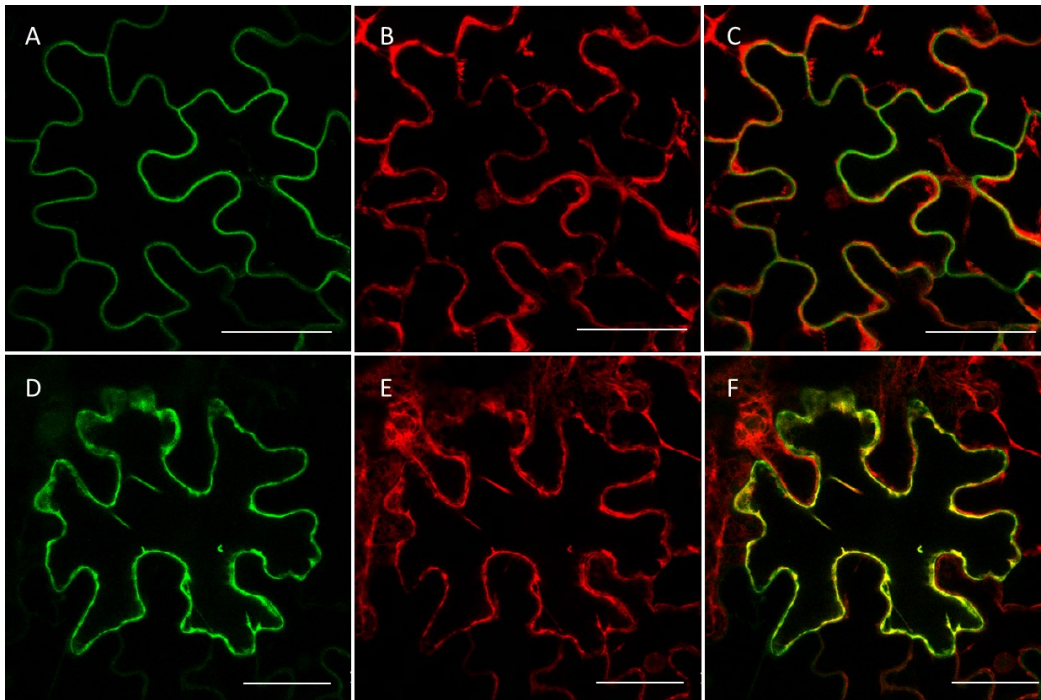


Figure 13: Intracellular localization of MtsUT4-1 and MtHXT1 in *N. benthamiana* leaves. A - C: MtHXT1 (N-terminal GFP fusion); D - E: MtsUT4-1 (C- and N-terminal GFP fusion); A, D: detection of GFP fusion proteins; B, E: mCherry tonoplast marker; C, F: overlay. Scale bar: 30 μ m.

3.1.2.2 Further genes involved in major carbohydrate metabolism with transcriptional regulation in mycorrhizal roots

The GeneChip hybridization experiment also showed that several further genes involved in major carbohydrate metabolism are differentially expressed in the different cell types of mycorrhizal and non-mycorrhizal *M. truncatula* roots (Gaude *et al.*, 2012). A putative amylase (Medtr3g099510.1) was found to be up-regulated in non-arbusculated cells of mycorrhizal roots ($LFC_{NAC/COR} = 2.30$, $LFC_{ARB/NAC} = -2.63$) as well as a putative cytoplasmic invertase (Medtr1g096110.1, $LFC_{NAC/COR} = 1.11$, $LFC_{ARB/NAC} = -1.12$). On the other hand, a putative vacuolar invertase (Medtr4g101630.1) was down-regulated in both neighbouring and arbuscule-containing cells in comparison to cortical cells of uncolonized roots ($LFC_{NAC/COR} = -1.49$, $LFC_{ARB/NAC} = -3.36$). In arbuscule-containing cells the putative sucrose synthase *MtSus6* was up-regulated ($LFC_{ARB/COR} = 2.49$) and in addition to the putative vacuolar invertase, a putative cytoplasmic invertase (Medtr1g096140.1) was down-regulated as well ($LFC_{ARB/COR} = -1.89$) (table 7).

Table 7: Cell type-specifically regulated genes involved in major carbohydrate metabolism. The annotation, the gene identifier as well as the transcriptional regulation are given (based on Gaude *et al.*, 2012).

Annotation	IMGAG ID Mt3.5	Log ₂ -fold change		
		ARB/NAC	NAC/COR	ARB/COR
Fructose-1,6-bisphosphatase	Medtr2g008030.1	-2.39	2.97	0.59
Glucose-1-phosphate adenylyltransferase	Medtr7g111020.1	-0.60	-1.97	-2.57
Isoamylase/glycogen debranching enzyme GlgX	Medtr3g099510.1	-2.69	2.53	-0.16
Neutral/alkaline invertase, putative	Medtr1g096140.1	-2.11	0.22	-1.89
Neutral/alkaline invertase, putative	Medtr1g096110.1	-1.12	1.11	0.00
Vacuolar acid invertase	Medtr4g101630.1	-1.87	-1.49	-3.36
Sucrose synthase, SUS6	Medtr6g081120.1	2.85	-0.36	2.49

The transcriptional changes of these genes in combination with the previously described putative sugar transporters MtHXT1 and MtSUT4-1 indicate substantial transcriptional modifications related to sugar metabolism and transport in response to mycorrhizal colonization of the roots.

To further understand the role of the cell type-specific regulated sugar transporters in the course of the interaction between *M. truncatula* and *R. irregularis*, the analysis of knock-out mutants was a promising approach. A collection of *M. truncatula Tnt1* mutants is available (Tadege *et al.*, 2008). Since no insertional mutant for *MtSut4-1* was available, only a *MtHxt1* insertion mutant will be analysed in the following.

3.2 The influence of the *MtHxt1* knock-out on the mycorrhizal interaction and primary metabolites in *M. truncatula*

3.2.1 Characterization of *MtHxt1* knock-out plants

A *Tnt1* insertion line for *MtHxt1* was available (Tadege *et al.*, 2008). All *M. truncatula* *Tnt1* insertion lines are plants of the genotype R108 (Tadege *et al.*, 2008). The insertion 22 of the line NF3151B is located in the 5th exon of the *MtHxt1* gene between the 1178th and the 1179th bp of the CDS (figure 14).

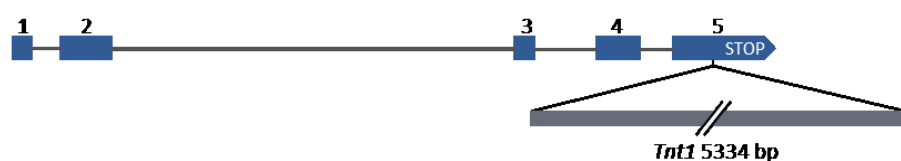


Figure 14: Schematic overview of the *Tnt1* insertion in the *MtHxt1* gene. Blue: exons one to five separated by introns (grey lines); dark grey: *Tnt1* insert in 5th exon of the gene.

Heterozygous seeds were obtained from the S.R. Noble foundation (<http://medicago-mutant.noble.org/mutant/>) and the plants were selfed to obtain homozygous plants for further analyses. In the following section, plants referred to as wild-type (WT) are plants (line NF3151B) that do not have a *Tnt1* insertion in the *MtHxt1* gene, while *hxt1* plants indicate plants that are homozygous for that insertion. This was determined via PCR analyses of genomic DNA of the respective plants (figure 15, table 8).

The primer combination 2 (P1 + P3) and 5 (P2 + P3) produced unspecific amplicons in all samples. Still, combination 2 only resulted in the expected 299 bp amplicon in the homozygous and heterozygous insertion plants and no amplicon for the WT plants. Combination 5 as well as combination 4 (P1 + P4) did not result in a specific amplification in any of the plants, demonstrating the orientation of the insertion. In heterozygous plants, the amplicons of the primer combinations 2 and 3 (P2 + P4) as well as the 495 bp WT amplicon of combination 1 (P1 + P2) were present, the WT band was quite weak. In the homozygous insertion plants, on the other hand, the 495 bp WT amplicon of the primer combination 1 is absent but the 5.8 kb amplicon including the insertion was present. The combinations 2 and 3 resulted in specific amplicons of the expected size for the insertion lines. The WT plants only showed the WT amplicon with combination 1 but no specific amplifications with any of the other primer combinations (figure 15).

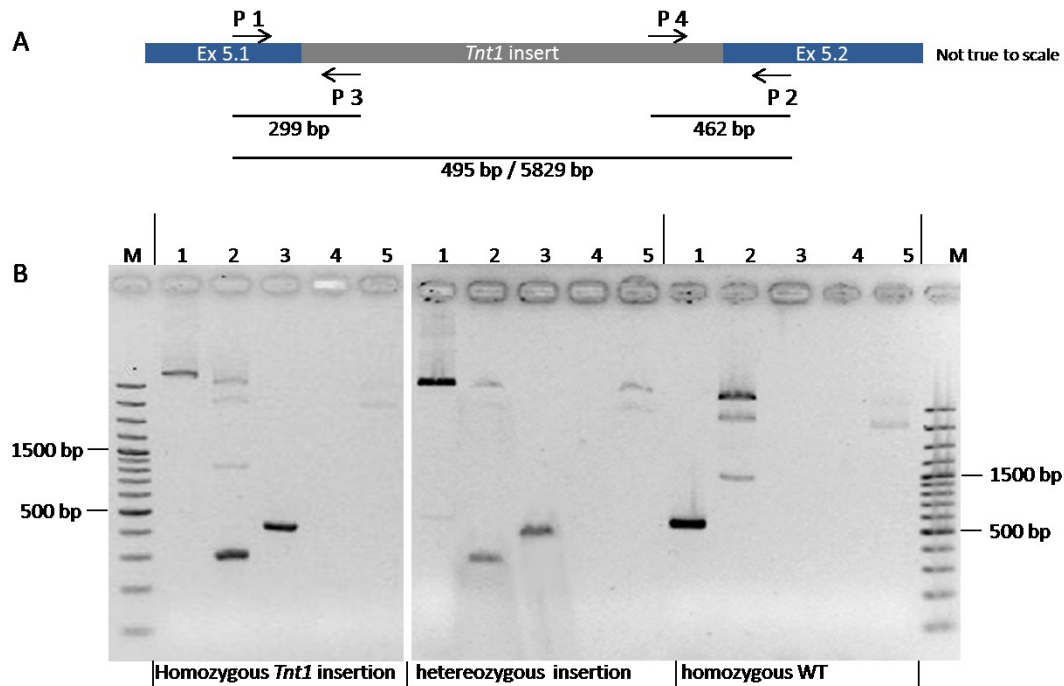


Figure 15: Screening of the first generation of *M. truncatula* *Tnt1* insertion plants. A: schematic overview of binding positions of the primers used for screening. Not true to scale. P1 and P2 bind in the *MtHxt1* CDS, directing towards the insert; P3 and P4 bind in the *Tnt1* insert, directing towards the ends of the insert. B: 1,5 % agarose gel electrophoresis of the PCR products of the *Tnt1* screen. 1-5: primer combinations given in table 7; M: GeneRuler 100 bp Plus DNA Ladder.

Table 8: Expected amplification sizes of the *Tnt1* insertion screening.

Number	Primer combination	Description	Expected size WT	Expected size insertion
1	P1 + P2	Wild-type amplicon	495 bp	5829 bp
2	P1 + P3	Insert sense orientation	-	299 bp
3	P2 + P4	Insert sense orientation	-	426 bp
4	P1 + P4	Insert antisense orientation	-	243 bp
5	P2 + P3	Insert antisense orientation	-	482 bp

Only homozygous *hxt1* and WT plants were selfed for seed production and their progeny was used for further analyses.

3.2.2 Influence of the *MtHxt1* knock-out on the mycorrhizal symbiosis

3.2.2.1 Phenotypic and molecular characterization of *hxt1* plants

Hxt1 plants showed a strong phenotype. Compared to WT plants, they grew longer before they started to flower, got very tall and produced an increased amount of biomass (Supplementary figure S1). Once they did develop flowers, most of these died before pods were produced (Supplementary figure S2) and the pods that were produced were smaller, lighter and contained significantly fewer seeds (Supplementary figure S3 and S4). This led to a low amount of seeds per plant. Plants that were heterozygous for the *Tnt1* insertion did not show a growth phenotype. They were not used in this study.

Despite the fact that the *hxt1* plants show such diverse phenotypes, the influence of the *MtHxt1* knock-out on the AM symbiosis was analysed. In a first experiment, *hxt1* and WT plants were grown under mycorrhizal and non-mycorrhizal conditions and harvested 4 wpi. The fresh weight of the roots and shoots was determined separately. While there was no significant difference in the root fresh weight in the different conditions, the shoot fresh weight was significantly higher in mycorrhizal WT plants as compared to non-mycorrhizal WT plants. This positive effect of the mycorrhizal colonization was absent in the *hxt1* plants.

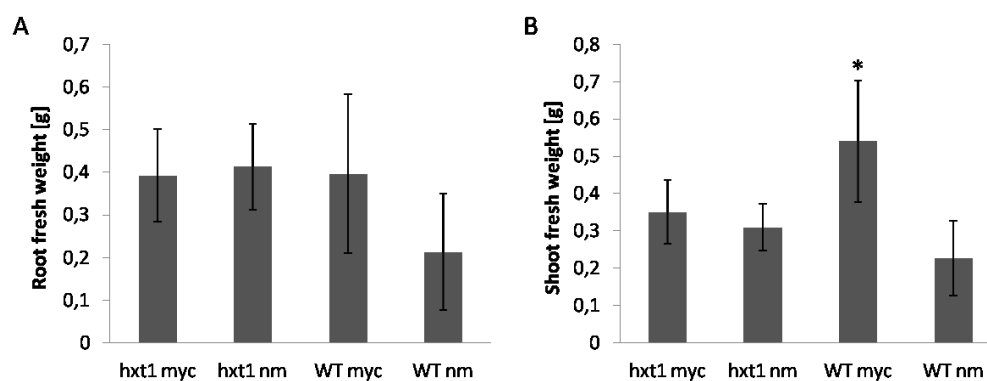


Figure 16: Root and shoot fresh weight of mycorrhizal and non-mycorrhizal *hxt1* and WT plants (4 wpi). A: root fresh weight; B: shoot fresh weight. Shown as average of three to four plants/condition. *: p-value ≤ 0.05, comparing mycorrhizal and non-mycorrhizal conditions within each genotype.

Quantitative RT-PCR was used to determine the expression of AM marker genes to evaluate the degree of fungal colonization and the development of the symbiosis (figure 17).

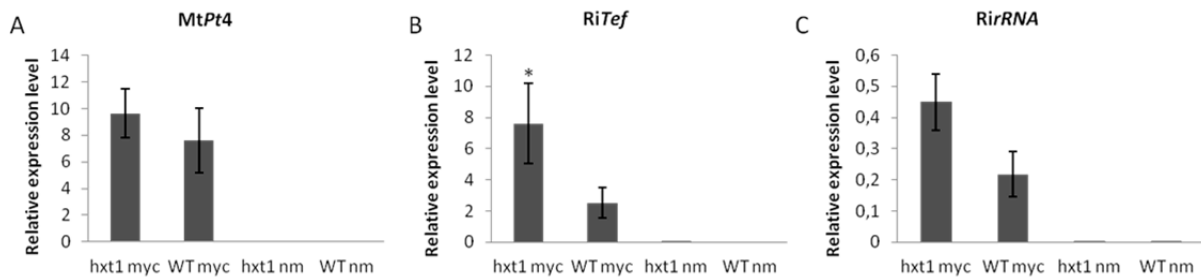


Figure 17: Relative expression levels ($2^{-\text{dCt}}$ values) of AM marker genes in *M. truncatula hxt1* and WT roots determined by qRT-PCR. Roots were harvested 4 wpi with *R. irregularis* (myc) or 4 weeks old non-inoculated roots (nm). A reference gene index (*UbiExon*, *Pdf2* and *EF1 α*) was used for normalization. Values shown are mean \pm standard deviation of three to four biological replicates with two technical replicates of each PCR reaction. *: p-value \leq 0.05, **: p-value \leq 0.01, comparison between *hxt1* and WT within the same mycorrhizal condition.

The amplification of *MtHxt1* transcripts with gene specific primers on either side of the *Tnt1* insertion confirmed the PCR screening results of the parent plants (figure 15). Due to the 5334 bp *Tnt1* insert, the transcript could not be amplified from *hxt1* cDNA and was therefore not measured in these samples, while its expression was shown in all WT samples (figure 18).

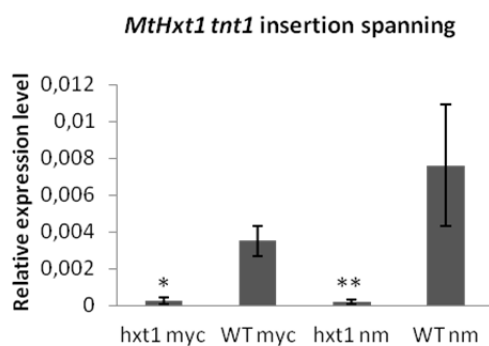


Figure 18 Relative expression levels ($2^{-\text{dCt}}$ values) *MtHxt1* in *M. truncatula hxt1* and WT roots determined by qRT-PCR. Roots were harvested 4 wpi with *R. irregularis* (myc) or 4 weeks old non-inoculated roots (nm). A reference gene index (*UbiExon*, *Pdf2* and *EF1 α*) was used for normalization. Values shown are mean \pm standard deviation of three to four biological replicates with two technical replicates of each PCR reaction. *: p-value \leq 0.05, **: p-value \leq 0.01, comparison between *hxt1* and WT within the same mycorrhizal condition.

RiTef and *RirRNA* are fungal genes which can be used to quantify the fungal mass in a root sample (Isayenkov *et al.*, 2004; Helber *et al.*, 2011). The significantly higher expression levels of *RiTef* in *hxt1* roots (figure 17 C) and the trend to a higher, albeit not significantly increased expression level of *RirRNA* in the *hxt1* samples (figure 17 D) indicated a higher amount of fungal mass in colonized roots of the *MtHxt1* knock-out plants. In contrast, *MtPt4*, a marker for fully developed arbuscules and thereby for a fully functional symbiosis, was expressed at the same levels in both the WT and the *hxt1* genotype (figure 17 A).

To determine the amount of arbuscules in relation to the overall fungal mass colonizing the roots, the expression level of *MtPt4* was normalized to the fungal reference genes *RiTef* and *RirRNA*. This showed that the *MtPt4* expression level is higher relative to the fungal mass in WT roots than it is in *hxt1* roots although due to high variations this is not statistically significant (figure 19).

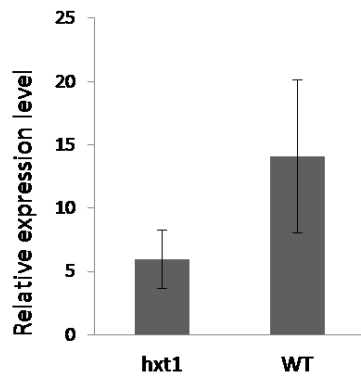


Figure 19: Relative expression levels ($2^{-\text{dct}}$ values) of *MtPt4* normalized to fungal reference genes in mycorrhizal *M. truncatula hxt1* and WT roots determined by qRT-PCR. Roots were harvested 4 wpi with *R. irregularis*. A fungal reference gene index (*RiTef*, *RirRNA*) was used for normalization. Values shown are mean \pm standard deviation of four biological replicates with two technical replicates of each PCR reaction.

In addition to the molecular phenotype, the AM phenotype was assessed visually. Roots were harvested 4 wpi and stained with WGA Alexa fluor 488, fungal structures were quantified microscopically and AM parameters were calculated (Trouvelot *et al.* 1986) (figure 20).

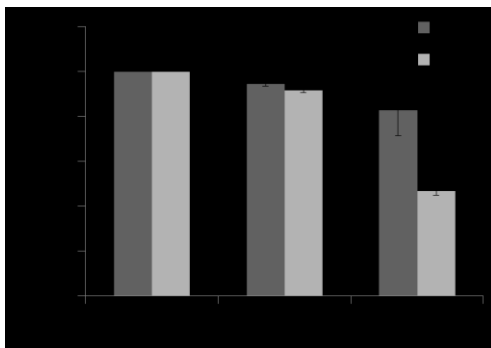


Figure 20: Mycorrhiza parameters in WGA Alexa fluor stained root fragments of *hxt1* and WT plants. Mycorrhizal WT and *hxt1* plants were harvested 4 wpi. Mycorrhiza parameters were calculated according to Trouvelot *et al.* (1986).

While the overall frequency (F%) and intensity (M%) of mycorrhizal colonization did not differ between WT and *hxt1* plants, the arbuscule abundance in the root system (A%) was considerably higher in WT plants (approx. 80 %) than it was in the *hxt1* plants (approx. 40 %). Since the roots were very small at the point of harvest, and the majority of the material was used for RNA extraction, only a small amount of root material of each biological replicate was available for the phenotypic characterization. Due to the low amounts of material for the quantification the significance of these results needs to be treated cautiously, but they confirm the results of the molecular characterization.

3.2.2.2 Primary metabolite changes in *hxt1* plants

Hxt1 plants were used to investigate the impact of the MtHXT1 function on the primary metabolism of mycorrhizal and non-mycorrhizal plants. The primary metabolites of *hxt1* and WT plants in mycorrhizal and non-mycorrhizal conditions were measured by GC-EI/TOF-MS. For all four conditions, source leaves and roots of five plants of each condition were harvested at 3, 5 and 7 wpi.

The mycorrhizal marker genes shown in 3.2.2.1 were also measured by qRT-PCR for the first two time-points to ensure the consistency of the results above. The variations are higher than in the 4 wpi samples, but the tendencies are the same (supplementary figure S 3).

The data obtained showed high variations and therefore high standard deviations. General trends between mycorrhizal and non-mycorrhizal plants, but not between the genotypes, could be seen. When plotting the results of the different time-points and tissues separately, the mycorrhizal and non-mycorrhizal conditions could be separated by independent component analysis (ICA) in roots but not in leaves (figure 21). The different genotypes did not show a clear separation in either tissue. Values were normalized to the mean of the WT non-mycorrhizal condition of the respective tissue and time-point, and \log_2 transformed. Two principal components were used for the ICA.

In the roots of both genotypes (figure 21 A, C, E), mycorrhizal and non-mycorrhizal conditions could be separated in all time-points analyzed here except for one outlier in the 5 wpi time-point (figure 21 C). In the leaves, neither the mycorrhizal conditions nor the genotypes were separated (figure 21 B, D, F). The ICAs shown here represent between 58.02 % and 71.21 % of the variance of the respective datasets.

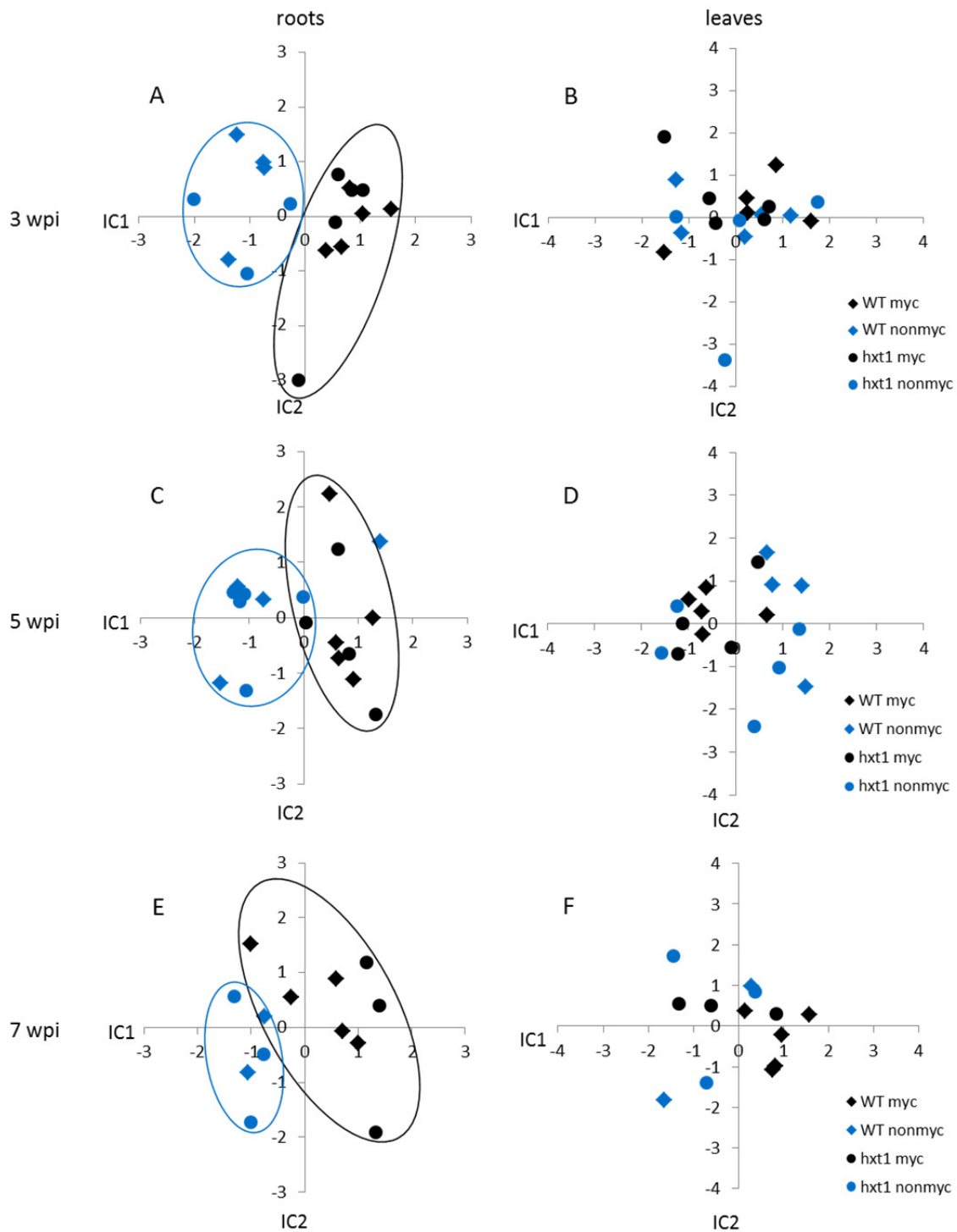


Figure 21: ICAs of the metabolite profiles of mycorrhizal and non-mycorrhizal WT and *hxt1* roots and leaves harvested at 3, 5 and 7 wpi. Values were normalized to WT non-mycorrhizal conditions of each tissue and time-point, and \log_2 transformed prior to ICA. 2 PCs were used for the analyses. A: roots, 3 wpi, 71.21 % of variance; B: leaves, 3 wpi, 69.39 % of variance; C: roots, 5 wpi, 58.02 % of variance; D: leaves, 5 wpi, 64.92 % of variance; E: roots, 7 wpi, 65.99 % of variance; F: leaves, 7 wpi, 60.07 % of variance.

AM -dependent changes in metabolite levels

In the roots of both genotypes several metabolites were found to be exclusively present in mycorrhizal conditions. These metabolites had a common pattern: they were not measured in a single replicate in non-mycorrhizal conditions in at least two time-points because their level was below the detection level, while they were present in all, or all but one, replicates in mycorrhizal conditions (table 9). When comparing the leaf samples of the two genotypes or the two genotypes to each other, no metabolites with this pattern were found; i.e. no metabolites exclusively present in the leaves of mycorrhizal plants or either of the genotypes were found. This represents a merely qualitative description, purely present/absent call, no quantitative assessment can be made from this observation.

Table 9: Metabolites present in mycorrhizal roots and absent in non-mycorrhizal conditions.

Metabolite	WT roots		
	3 wpi	5 wpi	7 wpi
Quinic acid	myc	myc	myc
Glutamic acid		myc	myc
Adenine	myc	myc	myc
Dehydroascorbic acid		myc	myc
Dehydroascorbic acid dimer		myc	myc
Trehalose, alpha,alpha'-	myc	myc	myc
<i>hxt1</i> roots			
	3 wpi	5 wpi	7 wpi
Quinic acid	myc	myc	myc
Alanine, 3-cyano-	myc		
Adenine	myc	myc	
Dehydroascorbic acid dimer		myc	myc
Trehalose, alpha,alpha'-	myc	myc	myc

myc: metabolite is specific for mycorrhizal roots.

As expected, trehalose is only present in mycorrhizal roots in both genotypes while it is absent in non-mycorrhizal conditions. Quinic acid shows the same behavior and adenine the same trend, it can only be detected in non-mycorrhizal *hxt1* roots 7 wpi.

For the all other measured metabolites, a more detailed, quantitative comparison was possible since they were detectable in at least two samples of every condition. Averages of the ratios myc/nonmyc were calculated and Log₂-transformed for either the roots (table 10) or the leaves (table 11). Metabolites were regarded to be differentially accumulating in response to mycorrhizal colonization if they had a LFC of ≥ 1 or ≤ -1 with a p-value of ≤ 0.05 . Empty cells in the tables are due to missing values in all biological samples in either of the conditions because the metabolite level was below the

detection limit. Therefore, no LFC could be calculated for the respective comparison. If only one replicate resulted in a measurable concentration, no statistics could be performed. Mass spectral tags of metabolites or metabolite derivatives (MSTs) of unknown metabolites are not displayed here.

Table 10: Significantly altered metabolite levels in mycorrhizal vs. non-mycorrhizal roots. Empty cells are due to missing values in either of the conditions for the respective metabolite.

Time-point	Class	Metabolite	Log ₂ fold change myc/nonmyc	
			WT	<i>hxt1</i>
3 wpi				
	Amino Acids	Asparagine	2.51*	2.17
	Amino Acids	Pyroglutamic acid	2.37**	2.84*
	Polyhydroxy Acids	Dehydroascorbic acid dimer	1.09	1.89*
	N- Compounds	Carbodiimide	-2.62*	0.44
5 wpi				
	Acids	Citric acid	-0.54	-1.11*
	Acids	Vanillic acid	-1.18	-1.45*
	N- Compounds	Putrescine	1.20*	-0.22
	Phosphates	Phosphoric acid	1.70	1.16*
	Polyols	Ononitol	1.13*	0.45
	Polyols	Pinitol	1.95*	1.09
	Sugars	Fructose	-0.62	-1.29*
7 wpi				
	Acids	Benzoic acid,	-1.52*	-1.12
	Acids	Butanoic acid, 4-amino-3-hydroxy-	0.72	2.37**
	Acids	Glutaric acid	-1.33*	
	Acids	Malic acid	0.69	2.36**
	Acids	Malonic acid	-0.22	1.59*
	Amino Acids	Aspartic acid	0.65	1.94*
	Amino Acids	Glutamic acid	undetected in WT myc	3.22*
	Amino Acids	Leucine	-1.28*	-1.45
	Phosphates	Phosphoric acid	0.99	1.62*
	Polyhydroxy Acids	Galactaric acid	2.46**	2.44*
	Polyhydroxy Acids	Galactonic acid	0.93*	1.81**
	Polyhydroxy Acids	Saccharic acid	1.38**	1.50*
	Polyhydroxy Acids	Ribonic acid	1.36	1.33*
	Polyols	Pinitol	1.32*	-0.23

p < 0.05: *; p < 0.01: **. Red: LFC ≥ 1; blue: LFC ≤ -1, darker colouring indicates a higher difference between the mycorrhizal conditions.

In the roots, phosphoric acid levels increased upon mycorrhizal colonization in both genotypes (table 10). At 5 and 7 wpi they were higher in mycorrhizal roots than in non-mycorrhizal roots of both genotypes, but this change is only significant in the *hxt1* plants. Moreover, glutamic acid levels were

significantly higher in mycorrhizal than in non-mycorrhizal *hxt1* roots at 7 wpi, which is in line with the presence of glutamic acid in later stages only in mycorrhizal and not in non-mycorrhizal WT roots (table 9). Fructose levels were lower in mycorrhizal than in non-mycorrhizal roots of both genotypes at 5 wpi, the difference was more pronounced and only significant in *hxt1* plants. At later stages, carboxylic acid levels, like malic and malonic acid, increased in mycorrhizal in comparison to non-mycorrhizal *hxt1* roots, while their levels did not differ notably or are even lower in mycorrhizal than in non-mycorrhizal WT roots.

Table 11: Significantly altered metabolite levels in the leaves of mycorrhizal vs. non-mycorrhizal plants.

Time-point	Class	Metabolite	Log ₂ fold change myc/nonmyc	
			WT	<i>hxt1</i>
3 wpi				
5wpi				
	Amino Acids	Aspartic acid	1.66**	0.27
	Amino Acids	Glutamic acid	1.62*	0.23
	Amino Acids	Lysine	2.40*	-0.09
	Acids	Butanoic acid, 4-amino-3-hydroxy-	-0.75	-1.72*
	Polyhydroxy Acids	Glyceric acid	1.23*	0.76
	Polyhydroxy Acids	Threonic acid	-0.13	-1.54*
	Polyols	Inositol, myo-	-1.50	-1.36*
	Polyols	Ononitol	1.21	-0.71*
	Sugars	Glucose	2.53*	-0.14
	Sugars	Fructose	2.63*	-0.21
	Sugars	Mannose	1.25*	-0.19
7 wpi				
	Acids	Butanoic acid, 4-amino-3-hydroxy-	-1.28**	-0.59
	Acids	Malic acid	-1.45**	-0.49
	Acids	Fumaric acid, 2-methyl-	-1.90	1.65*
	Acids	Fumaric acid	-1.44*	-0.07
	Acids	Glutaric acid, 2-oxo-	-1.17**	-0.30
	Polyols	Pinitol	-1.59*	-0.44
	Polyols	Ononitol	-1.27**	-1.45
	Sugars	Glucopyranoside, 1-O-methyl-, beta-	-1.27*	-1.22
	Sugars	Glucose	-1.43*	-0.16

p < 0.05: *; p < 0,01: **. Red: LFC ≥ 1; blue: LFC ≤ -1, darker colouring indicates a higher difference between the mycorrhizal conditions.

In leaves, the levels of most of the significantly altered metabolites were decreased in mycorrhizal in comparison to non-mycorrhizal conditions in the WT at 7 wpi. At 5 wpi the majority of significantly altered metabolites were more abundant in mycorrhizal WT plants and less abundant in *hxt1* plants

(table 11). Glucose, fructose, and mannose, for instance, were more abundant in leaves of mycorrhizal WT plants than of non-mycorrhizal WT plant, while their levels were similar in the leaves of mycorrhizal and non-mycorrhizal *hxt1* plants. At 7 wpi, however, this could not be observed any more. Also several amino acids were more abundant in the leaves of mycorrhizal WT plants, while their levels are basically the same in the leaves of mycorrhizal and non-mycorrhizal *hxt1* plants at 5 wpi. In WT plants, polyol and carboxylic acid levels were lower in mycorrhizal than in non-mycorrhizal leaves. In the *hxt1* leaves, no significant differences in their levels could be detected.

Genotype-dependent changes in metabolite levels

Averages were also calculated from the ratios *hxt1*/WT and again the LFCs were calculated. Metabolites were regarded to be differentially accumulating in the two genotypes if they had a LFC of ≥ 1 or ≤ -1 with a p-value of ≤ 0.05 . The selected metabolites from the leaf samples are listed in table 12. Table 13 shows the selected metabolites for the root samples.

Table 12: Significantly altered metabolite levels in *hxt1* vs. WT roots. Empty cells are due to missing values in either of the conditions for the respective metabolite.

Time-point	Class	Metabolite	Log ₂ fold change <i>hxt1</i> /WT	
			myc	nonmyc
3 wpi				
	Acids	Malonic acid	-1.39*	-0.31
	N- Compounds	Carbodiimide	1.82*	-1.25
	Sugars	Fructose	-1.10*	-0.64
	Sugars	Glucopyranoside	-1.31*	
	Sugars	Glucose	-1.22*	-0.73
5 wpi				
	N- Compounds	Putrescine	-0.26	1.16*
	Sugars	Raffinose	1.09*	-0.15
7 wpi				
	Acids	Glutaric acid, 2-oxo-	1.26**	0.72
	Acids	Malic acid	0.61**	-1.02*
	Acids	Malonic acid	1.42**	-0.40
	Acids	2-Piperidinecarboxylic acid	1.32*	1.44
	Amino Acids	Valine	1.65**	-0.30
	Sugars	Xylose	0.18	-1.46*

p < 0.05: *; p < 0,01: **. Red: LFC ≥ 1 ; blue: LFC ≤ -1 , darker colouring indicates a higher difference between the genotypes.

When comparing the two genotypes, fewer differentially abundant metabolites were detected than in the comparison of the mycorrhizal conditions (table 12). Sugar levels in the roots varied the most at 3 wpi: fructose, glucopyranoside, and glucose levels were significantly lower in mycorrhizal *hxt1* roots than they were in mycorrhizal WT roots. The changes in non-mycorrhizal conditions were more subtle and not significant. At later stages, several carboxylic acids were higher in mycorrhizal *hxt1* root than in WT roots. In non-mycorrhizal roots, however, their levels were similar or even lower in *hxt1* than in WT roots.

Table 13: Significantly altered the levels of metabolite levels in the leaves *hxt1* vs. WT plants.

Time-point	Class	Metabolite	Log ₂ fold change <i>hxt1</i> /WT	
			myc	nonmyc
3 wpi				
5 wpi				
	Acids	Butanoic acid	1.10*	2.08*
	Acids	Malic acid	1.09*	2.06
	Acids	Malic acid, 2-methyl-	0.30	1.84**
	Polyhydroxy Acids	Threonic acid	0.38	1.79*
	Polyols	Inositol, myo-	-0.31	1.53*
	Polyols	Ononitol	-0.72	1.19**
	Polyols	Ribitol	0.12	1.22*
7 wpi				
	Polyols	Inositol, myo-	2.03**	1.36
	Sugars	Glucose	3.47*	1.88
	Sugars	Fructose	3.82*	2.94
	Sugars	Mannose	2.18*	1.90*

p < 0.05: *; p < 0,01: **. Red: LFC ≥ 1; blue: LFC ≤ -1, darker colouring indicates a higher difference between the genotypes. MSTs: mass spectral tags of metabolites or metabolite derivatives.

In leaves, differentially abundant metabolites were only detected in the later stages (table 13). At 5 wpi, several polyols were more abundant in *hxt1* than in WT leaves in non-mycorrhizal conditions, but unaltered in mycorrhizal plants. Again, carboxylic acid levels were affected by the genotype: in mycorrhizal conditions, butanoic and malic acid levels were higher in *hxt1* than in WT leaves. At 7 wpi, all the significantly altered metabolites were more abundant in *hxt1* than in WT in both mycorrhizal and non-mycorrhizal conditions. The levels of three sugars, fructose, glucose, and mannose, were elevated in *hxt1* leaves as compared to WT leaves at 7 wpi. The differences in the sugar levels between the genotypes was more pronounced in mycorrhizal than in non-mycorrhizal plants.

3.3 Identification of *in planta* expressed *Rhizophagus irregularis* transporter genes

So far, only very little is known about fungal proteins involved in transport processes in arbuscule-containing cells and the mechanisms of the nutrient exchange on the fungal side of the interaction. This is mainly due to the obligate biotrophy of AM fungi, the insufficient amount of biological material and, until recently, the lack of a sequenced genome as a reference for transcriptome profiling approaches. However, using laser capture microdissection (LCM)-mediated harvesting of arbuscules and SBS (sequencing by synthesis) sequencing, fungal transporter genes that are induced *in planta* were identified in order to get more insight into the fungal transport processes involved in the symbiotic interaction.

3.3.1 *Rhizophagus irregularis* transcriptome sequencing

3.3.1.1 Isolation of *Rhizophagus irregularis* RNA

R. irregularis-colonized *M. truncatula* roots were cryo-sectioned longitudinally into 35 μm fragments. Arbuscules were isolated from these sections using LCM (figure 22).

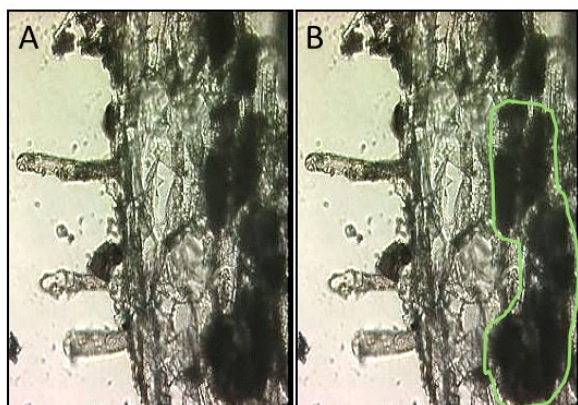


Figure 22: Isolation of arbuscule-containing cells from *M. truncatula* roots using laser capture microdissection. A: mycorrhizal root section with arbuscule containing cortex cells; B: selected arbuscules (green circle).

Arbuscule RNA was isolated from the LCM-collected cells. Several isolations were performed with approx. 10.000 cells each and pooled to obtain 100 ng of total arbuscule RNA. As a reference, hyphae and spores were grown and harvested in a two compartment petridish and RNA was isolated. Additionally, spores were isolated from mycorrhizal *M. truncatula* ROCs, germinated in water, and RNA was isolated. The hyphae and spore RNA was pooled as one extraradical mycelium (ERM) sample.

The RNA quality and quantity were determined with the Bioanalyzer PicoChip (Agilent) (figure 23). Only samples with highest RNA contents and an RNA integrity number (RIN) above six were used for sequencing. All these high quality LCM collected arbuscule samples as well as the high quality samples of both ERM populations were pooled into one arbuscule and one ERM sample before sequencing to obtain a minimum amount of 100 ng of RNA for each sample.

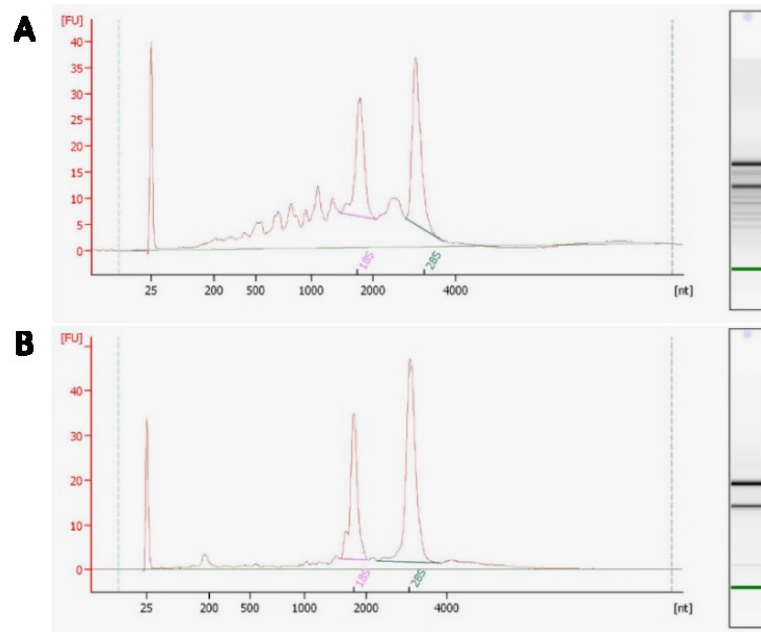


Figure 23: Quality control of the RNA samples. Bioanalyzer measurement performed at Eurofins MWG Operon. A: electropherogram and artificial gel of the arbuscule RNA; B: electropherogram and artificial gel of the best ERM RNA.

3.3.1.2 Identification of differentially expressed genes

Both *R. irregularis* RNA populations were sequenced using the Illumina technology (Eurofins MWG Operon). This resulted in more than 25 Mio reads from the arbuscule RNA and over 42 Mio reads from the ERM tissues.

The initial bioinformatic processing of the data was performed by Dr. Samuel Arvidsson (AG Walther, MPIMP). He did the filtering, the contig assembly and the calculation of the estimated expression (RSEM values) of the contigs in both samples, as well as the frame prediction and the transmembrane (TMD) domain search.

Almost half of the reads from the arbuscule library were derived from *M. truncatula* (blast search in the Medicago genome Mt3.5). This was expected due to the fact that the arbuscules were isolated directly out of the root tissue and therefore contain plant and fungal material to an approximately equal amount. As expected, no significant amounts of reads matching to *M. truncatula* sequences

were found in the library derived from hyphae and spores. The approx. 55.6 Mio remaining raw reads from both libraries were then taken together for the contig assembly resulting in 5089 transcontigs of more than 500 bp length. For a first annotation, these transcontigs were subjected to homology searches in public databases (NCBI blastn and blastx) and in the GlomusDB. Subsequently, the raw reads of each library were mapped to the contigs. The transcript abundances of the genes (represented by the transcontigs) in both libraries were estimated using two different quantification methods, RPKM (Reads per kilobase per million mapped Reads) and RSEM (RNA-Seq by Expectation-Maximization). The trend was similar in both calculation methods: A contig that was found to be up-regulated *in planta* in comparison to the ERM in one calculation method was also, albeit possibly to a considerably higher or lower extent, found to be up-regulated *in planta* according to the other calculation method. Since RSEM is specially designed to not require a full reference genome these values were used for further analyses. The calculation of the RSEM values attempts to normalize the read counts with respect to the read amount of each library, as well as the length of the contigs and reads, and the read distribution. With these estimated expression values, the Log_2 fold change between the two samples could be calculated for each gene. The contigs of 1087 genes had a LFC of ≥ 2 or ≤ -2 . In parallel, frame predictions were performed and transmembrane domains were predicted for the peptides. The peptides of 78 contigs of the 1087 candidates that were strongly regulated contained one TMD, 34 of these contained two or more TMDs. Via homology searches against fungal sequences (blastp, NCBI) and detailed searches in the GlomusDB, the potential functions were assigned to the genes that are represented by the contigs. Seven genes that were found to be potential transporter genes were selected as candidates for further analyses (figure 24) (table 14).

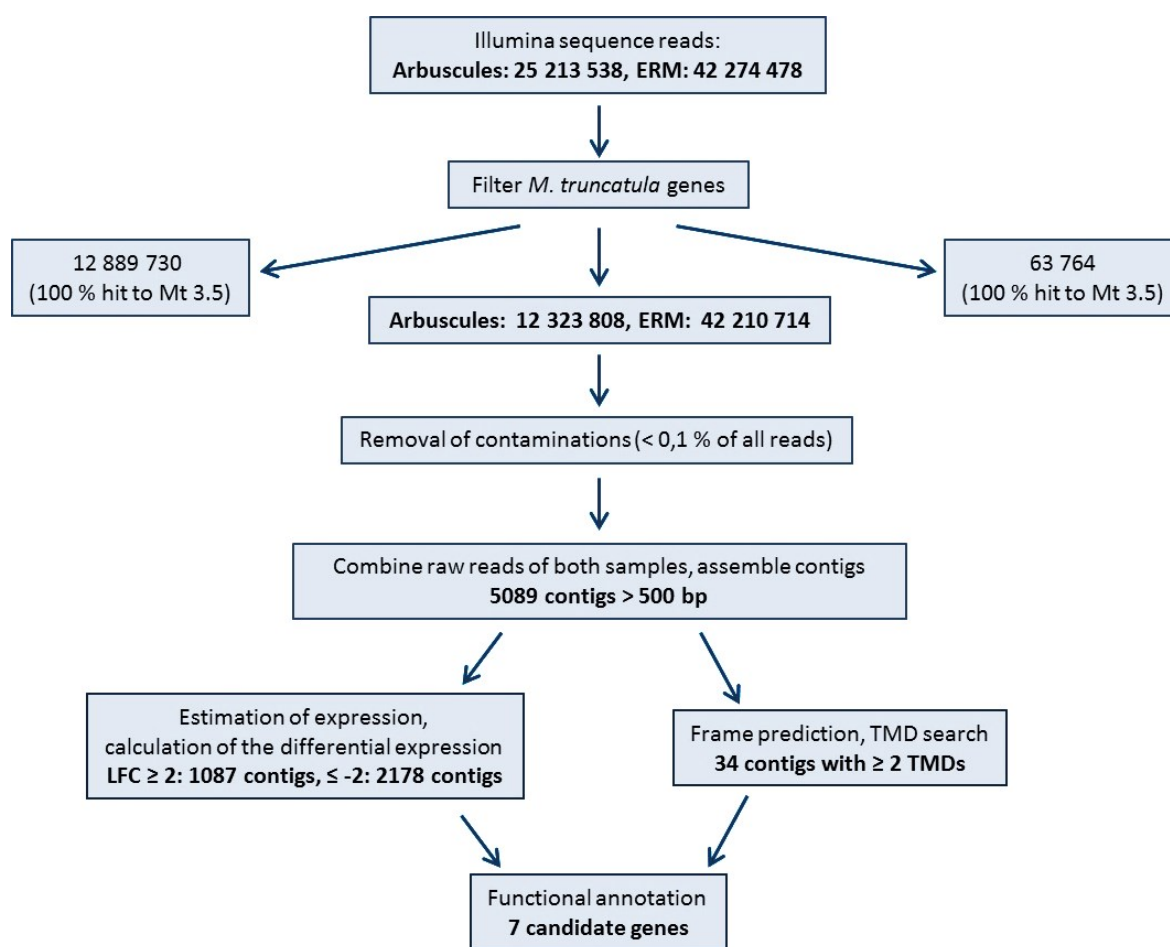


Figure 24: Schematic overview of the results of the bioinformatic analysis of the *R. irregularis* Illumina sequencing data.

3.3.1.3 Identification and annotation of potential transporter gene candidates

Seven differentially regulated potential fungal transporter genes have been found (table 14). Two of these are up-regulated in the ERM, five are induced *in planta* compared to extraradical tissues.

One of the contigs (comp_29_seq1) is a 100 % match to the coding sequence of the phosphate transporter *GiPt* (Maldonado-Mendoza *et al.*, 2001), although it does not cover the full length of the transcript. Since *G. intraradices* has been renamed to *R. irregularis*, this gene will be referred to as *RiPt* in the following work. In the read-count based expression profiling more reads for this contig were found in the ERM. Since *RiPt* has already been described to be up-regulated in the ERM, this can be seen as a proof of concept for the used calculations. *RiPt* is therefore used as a positive control in the following analyses. Only several months after the selection of the candidates, access to the first successfully assembled *R. irregularis* genome was granted (Francis Martin, INRA, Nancy). Except for two candidates, comp2866_c0 and comp19601_c0, the full genomic sequences could be obtained there, and the annotation given is taken from there.

Table 14: Differentially regulated *R. irregularis* transporter gene candidates.

Contig ID	Genome ID/ AccessionNo	Annotation (<i>R. irregularis</i> genome DB if available)	LFC (arb/ERM)	TMD
comp29_c0	AY037894	RiPt, Phosphate transporter	-7.51	3
comp8571_c0	e_gw1.2824.2.1	Major facilitator superfamily transporter (RiMFS1)	-3.53	2
comp2270_c0	gm1.366_g	Major facilitator superfamily transporter (RiMFS2)	3.61	2
comp4884_c0	gm1.2614_g	Major facilitator superfamily transporter (RiMFS3)	7.40	3
comp11677_c0	gm1.11960_g	Sugar transporter/MFS (RiSut1)	4.49	3
comp2866_c0	-- *	High-affinity glucose transporter [<i>Magnaporthe oryzae</i>] (RiGlct1)	10.26	2
comp19601_c0	-- *	Potassium ion channel Yvc1 [<i>Trichophyton rubum</i>] (RiYvc1)	9.75	2

*: No blast hits in the *R. irregularis* genome.

Three putative major facilitator superfamily (MFS) transporters were found (table 14). MFS transporters are single-polypeptide carriers transporting small solutes along chemiosmotic gradients. One candidate of this group, comp8571_c0 (RiMFS1), is induced in extraradical tissues in comparison to arbuscules. comp2270_c0 (RiMFS2) and comp4884_c0 (RiMFS3) are both induced in arbuscules. comp11677_c0 (RiSut1) is induced in arbuscules as well. Due to sequence homologies it can be annotated as an MFS transporter but also as a sugar transporter, making it a very interesting candidate. The other two candidates are comp2866_c0 (RiGlct1) and comp19601_c0 (RiYvc1). Blasting the contigs did not result in any hits in the *R. irregularis* genome. They are both very strongly induced in arbuscules in comparison to the ERM, both with a LFC around 10. Sequence similarities with other fungi suggest the annotation as a potential high affinity glucose transporter and a potassium ion channel, respectively. In the following, the names given in table 14 will be used to refer to the genes.

Also, the raw reads of the two samples, arbuscules and ERM, were mapped to the sequences of known *R. irregularis* genes. The raw reads were normalized to the total amount of reads in each sample and the Log₂-fold changes (arbuscules/ERM) were calculated from the normalized reads mapping to each gene. All of these genes are listed in the supplementary table S 3.1, the most interesting transport-related ones are listed in table 15. Since the LFCs given here are calculated from the reads mapping to each gene and not from the calculated expression values of the contigs as above, the LFC for GiPT differs slightly from the value in table 14.

Table 15: Published differentially expressed *R. irregularis* genes. LFCs of the reads normalized to the total amount of reads in each sample from the SBS sequencing for previously described *R. irregularis* genes are given.

GenBank accession	Description	LFC or normalized reads (arb/ERM) ^x	Reference
FJ861239.1	Aquaporin 1 (AQP1)	(0/21) ^x	Aroca <i>et al.</i> (2009)
AJ880327.1	Ammonium transporter 1 (AMT1)	-7.88	Lopez-Pedrosa <i>et al.</i> (2006)
FM993985.2/ FR744743.1	Ammonium transporter 2 (AMT2)	-3.98*	Perez-Tienda <i>et al.</i> (2011)
GQ249346.1	ATP-binding cassette transporter 1 (ABC1)	-7.55	Gonzalez-Guerrero <i>et al.</i> (2010)
GU111909.1	Glutamine synthetase 1 (GS1)	-4.06	Tian <i>et al.</i> (2010)
GU111910.1	Glutamine synthetase 2 (GS2)	-3.43	Tian <i>et al.</i> (2010)
GU111911.1	Argininosuccinate synthase (ASS)	-6.15	Tian <i>et al.</i> (2010)
GU111912.1	Ornithine aminotransferase (OAT1)	-4.21	Tian <i>et al.</i> (2010)
GU111913.1	Arginase (CAR1)	1.62	Tian <i>et al.</i> (2010)
GU111919.1	Nitrate transporter (NT)	-2.61	Tian <i>et al.</i> (2010)
AF359112.1/ AY037894.1	Phosphate transporter (PT)	-8.26*	Maldonado-Mendoza <i>et al.</i> (2001)
HQ896039.1	Phosphate transporter <i>G. intraradices</i> strain BEG158	-11.40	Schwer <i>et al.</i> (2011)
HM143864.1	Sugar transporter (MST2)	-0.06	Helber <i>et al.</i> (2011)
HQ848965.1	Sugar transporter (MST4)	-5.30	Helber <i>et al.</i> (2011)
HQ848966.1	Sugar transporter (SUC1)	-6.38	Helber <i>et al.</i> (2011)

^x: Log₂-fold changes could not be calculated if 0 reads were found in either of the libraries. If that was the case, the normalized raw reads are given.

*: reads were mapped to the full gene and mRNA sequences. The LFC is the mean of results from both.

3.3.2 Characterization of AM-specifically expressed *Rhizophagus irregularis* transporter genes

3.3.2.1 Confirmation of transcriptional regulation during root colonization

The regulation of the candidate genes *in planta* that was found in the read count-based expression profiling of the Illumina-sequenced libraries was verified using qRT-PCR. The transcript abundance was normalized against the fungal reference genes *RiTef1* and *RirRNA*. cDNA from mycorrhizal *M. truncatula* roots (4 wpi) was used as *in planta* samples, for the ERM sample hyphae and spores from root organ cultures (ROCs) were used. Prior to the qRT-PCR measurements, the specificity of the primers to fungal sequences was assessed, using a standard PCR with mycorrhizal and non-mycorrhizal *M. truncatula* root cDNA as a template (figure 25).

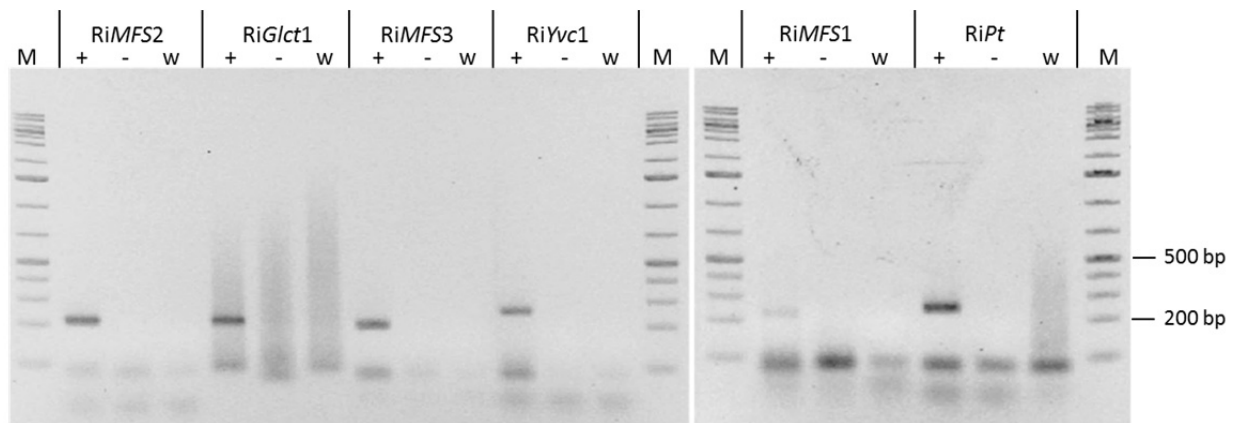


Figure 25: Primer specificity to fungal transcripts. 2 % agarose gel electrophoresis of PCR products with *R. irregularis* transporter candidate qRT-PCR primers. M: 1 kb plus DNA Ladder; +: mycorrhizal *M. truncatula* root cDNA as template. -: non-mycorrhizal *M. truncatula* root cDNA as template; w: H₂O control.

Since none of the qRT-PCR primers tested for the potential sugar transporter comp11677_c0 resulted in a fungus-specific amplification (data not shown), no qRT-PCR experiments could be performed for this gene. For the other candidates, qRT-PCR was performed with cDNA of mycorrhizal roots (4 wpi) as an *in planta* sample and germinated spores as an ERM sample. For all the selected candidates, the up-regulation *in planta* or in the ERM, respectively, was confirmed (figure 26).

As expected, the *RiPt* expression is significantly higher in extraradical tissues than *in planta*. Also, the expression pattern that was calculated from the read count-based expression profiling of the Illumina reads for the candidate genes could be confirmed: *RiMFS1* was found to be up-regulated in the ERM. This is confirmed by the qRT-PCR results with a significantly higher expression level in the ERM compared to mycorrhizal roots. Likewise, the four potential transporters that were found to be up-regulated in arbuscules showed the same transcriptional regulation when measured by qRT-PCR. While this up-regulation was highly significant for three of them, *RiMFS2*, *RiGlct1*, and *RiYvc1*, the p-value for the *RiMFS3* was > 0,05 due to high variance between the biological samples. Still, the trend shows an up-regulation of the expression of this gene *in planta* (figure 26).

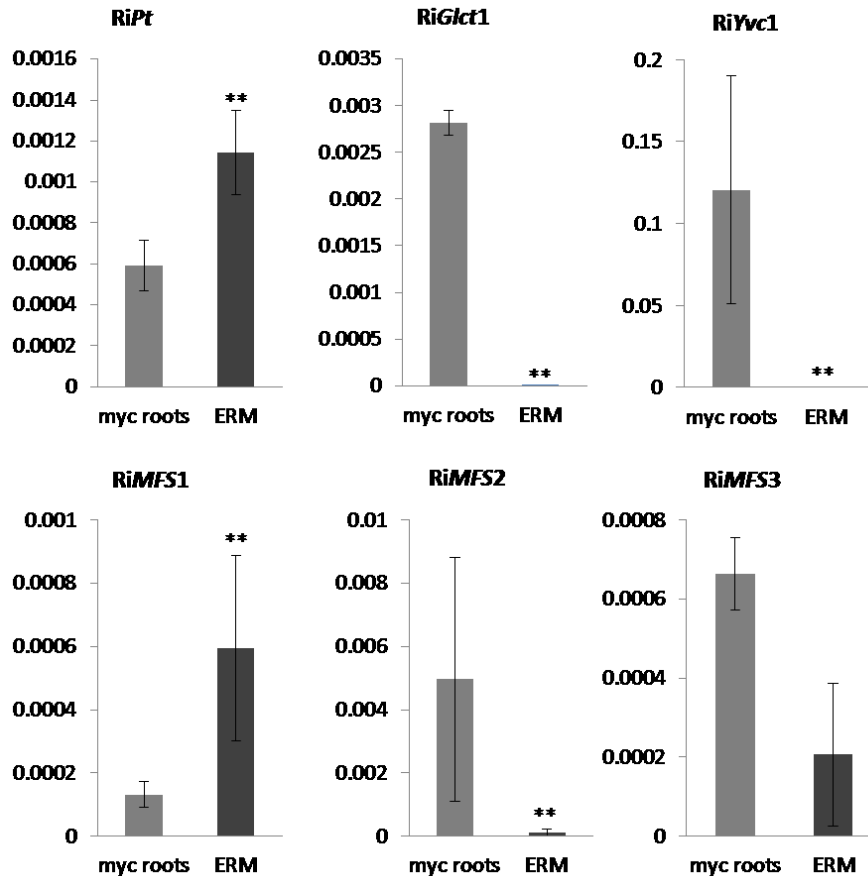


Figure 26: Relative expression levels (2^{-dct} values) of the differentially regulated potential *R. irregularis* transporter genes determined by qRT-PCR. Wild-type roots were harvested 4 wpi with *R. irregularis*, the ERM sample are spores, isolated from ROCs and germinated for 3 days. A reference gene index of fungal genes (*GirRNA* and *GiTef*) was used for normalization. Values shown are mean \pm standard deviation of four biological replicates with two technical replicates of each PCR reaction. *: p value < 0.05, **: p value < 0.01.

3.3.2.2 Identification of full length transcript sequences of transporter candidate genes

Only recently, access to the first successfully assembled *R. irregularis* genome was granted by F. Martin (INRA, Nancy). The contigs were blasted against the genome database. For four of the contigs of the candidate genes, genome hits were available. Only the contig comp19601_c0 could not be found, and comp2866_c0 only got hits in the EST libraries, but no assembled genomic sequence could be matched to this contig. The corresponding genome database hits are listed in table 14.

With the genomic sequences available, gene specific primers to amplify the complete coding sequences were designed. They were then amplified from mycorrhizal roots or ERM cDNA, respectively. The PCR products were TA-cloned and sequenced. The final CDS sequences of the candidate genes are listed in the supplemental data (section 3.1).

For *RiMFS1* (comp8571_c0) the resulting cDNA sequence showed that the automatic exon/intron prediction of the corresponding genome sequence e_gw1.2824.2.1 is inaccurate. There is no intron between the predicted exons 2 and 3, the predicted intron region is part of the coding sequence. This was shown in 2 individually amplified and cloned fragments. Therefore, this gene has 6 instead of the predicted 7 exons and the coding sequences is 1762 bp long. Otherwise, the contig from the Illumina reads, the genomic sequence, and the sequencing results of the CDS amplified from *R. irregularis* cDNA match perfectly with not a single mismatch.

For *RiMFS2* (comp2270_c0) the sequence of the CDS amplified from fungal cDNA revealed a total of 41 single base substitutions and 5 double replacements compared to the genomic sequence gm1.366_g. These were confirmed by two individually cloned and sequenced PCR products amplified from different mycorrhizal root cDNAs. The nucleotide replacements lead to the alteration of 13 amino acids in the translated sequence. Since no nucleotides were added or deleted, the length of the CDS, 1485 bp, is not altered from the original genomic sequence.

For *RiSut1* (comp11677_c0) the sequencing results of the cloned CDS also revealed a few contradictions with the genomic sequence gm1.11960_g. 19 nucleotides were not in agreement with the genomic sequence. Again, two separately amplified and cloned fragments were sequenced. Interestingly, it was with the corrected sequence that the contig from the Illumina reads matched 100 %. Since there were no deletions but only base replacements the CDS remains to be 1445 bp of length.

RiMFS3 (comp4884_c0) could not be cloned. Therefore, the sequence from the genome database could not be verified. Since the contigs of the potential high-affinity glucose transporter *RiGlc1* (comp2866_c0) and potassium ion channel *RiYvc1* (comp19601_c0) did not result in any blast hits in the *R. irregularis* genome, there was no full length sequence information available.

3.3.2.3 *In situ* localization of candidate transcripts

To investigate where exactly the *R. irregularis* transporter candidate genes are expressed, *in situ* hybridization experiments were performed. These were aimed to visualize whether the transcripts accumulate in the arbuscules, the intracellular hyphae, or both.

So far, an *in situ* hybridization was performed for one candidate, the *RiMFS2*. For this purpose, a 5'DIG labelled RNA oligo (20mer) from Aparas Bioscience was used. As a negative control a sense 5'DIG-labelled RNA oligo for the same region was used. Mycorrhizal *M. truncatula* roots were harvested 4 wpi, embedded in paraffin, fixed in xylol, cut in 10 µm cross sections and used for the hybridization. NBT/BCIP was used for visualization and the sections were stained with WGA Alexa fluor 488 to visualize fungal structures.

The results for the localization of the *RiMFS2* transcripts will have to be treated cautiously, as the *in situ* localization results are derived from sections of only two root pieces. Still, the dark purple staining produced by the conversion of the NBT/BCIP to diformazan by the alkaline phosphatase which is bound to the DIG antibody can clearly be seen with the *RiMFS2* probe while it is absent in the sense control. The staining can be seen in arbuscules as well as intracellular hyphae growing in the root apoplast. In the overview (figure 27) sections that were counterstained with WGA Alexa fluor to visualize fungal tissues are shown. The purple staining indicates an accumulation of the transcripts is visible in the arbuscules and, even more pronounced, in the intraradical hyphae, visualized by the green fluorescence of the stained fungal cell wall in the apoplastic space between the root cells (figure 27 A). Only a very weak background signal is present in the section hybridized with the sense control (figure 27 B). The higher magnification (figure 28) shows a section that was not WGA Alexa-stained. In the negative control (figure 28 B), the arbuscules are visible as dense structures within the root cells. In the section hybridized with the *RiMFS2* probe (figure 28 A), the purple coloring can be seen in the arbuscules. Also, quite a strong purple signal has appeared in the apoplastic space, where an intraradical hypha is likely to be present, but since the fungal structures were not stained here its presence cannot be seen.

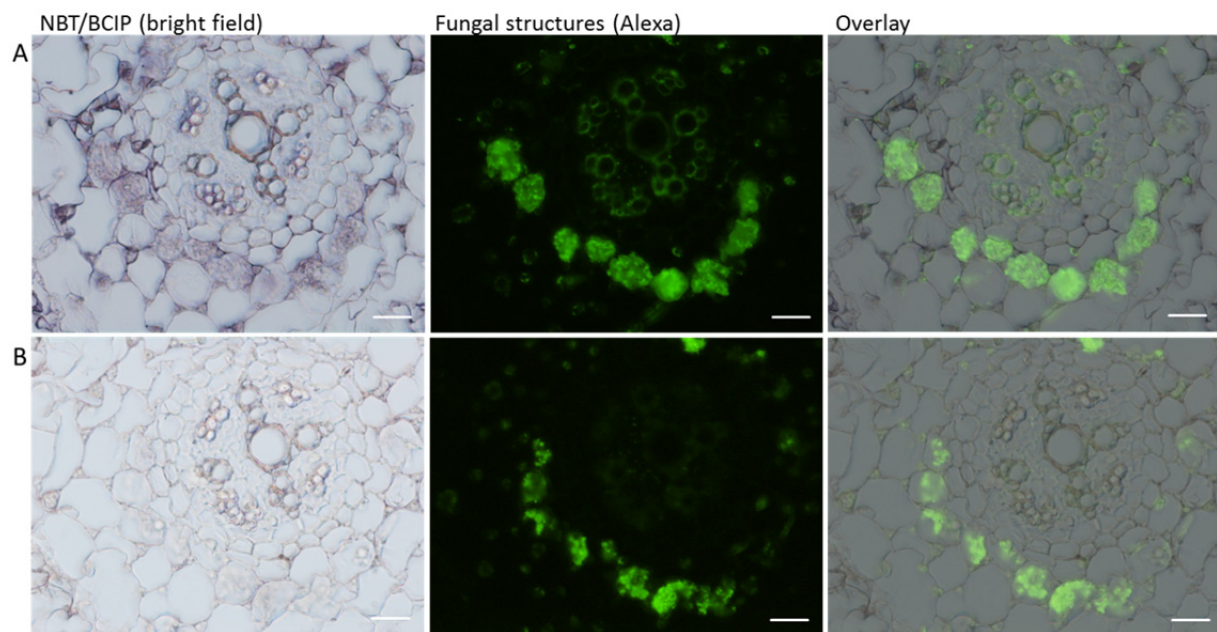


Figure 27: Localization of *RiMFS2* transcript accumulation in *R. irregularis* hyphae and arbuscules in mycorrhizal *M. truncatula* roots and arbuscule-containing cells. Root cross sections hybridized using 5'DIG labelled RNA oligos. Signals caused by *RiMFS2* transcript accumulation were visualized by NBT/BCIP staining and subsequent microscopy, fungal structures stained with WGA Alexa fluor. A: hybridization with the *RiMFS2* probe; B: hybridization with a sense control probe (negative control). Scale bar 20 μ m.

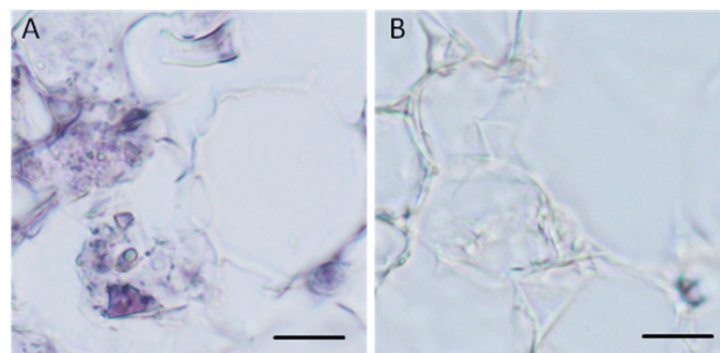


Figure 28: Localization of *RiMFS2* transcript accumulation in *R. irregularis* hyphae and arbuscules in mycorrhizal *M. truncatula* roots and arbuscule-containing cells. Root cross sections hybridized using 5'DIG labelled RNA oligos. Signals caused by *RiMFS2* transcript accumulation were visualized by NBT/BCIP staining and subsequent microscopy. A: hybridization with the *RiMFS2* probe; B: hybridization with a sense control probe (negative control). Scale bar 10 μ m.

3.3.2.4 Potential *Rhizophagus irregularis* transporter encoding genes are specifically regulated in planta

So far, very little is known about the mechanisms of the nutrient transfer on the fungal side of the AM symbiosis. Here, *R. irregularis* transcriptome analyses were performed on a tissue-specific level. SBS sequencing of RNA isolated from LCM-collected *R. irregularis* arbuscules compared to the ERM resulted in the identification of 3265 differentially regulated genes. The identification of TMDs and successive annotation based on sequence similarities to fungal proteins showed that six of these differentially regulated genes very likely code for transporter proteins. The AM-specific regulation of these potential transporter genes was confirmed, and for one transcript, *RiMFS2*, its accumulation in arbuscules and even stronger in intraradical hyphae was confirmed via *in situ* hybridization.

4 DISCUSSION

4.1 AM-specifically regulated genes involved in transport processes and carbohydrate metabolism give new insight into transport processes during the symbiosis

4.1.1 Several transporter genes are AM-specifically regulated

The bi-directional nutrient exchange between the plant and the fungal partner is the key-element of the arbuscular mycorrhizal symbiosis. Therefore unsurprisingly, GeneChip hybridization experiments revealed a high amount of *M. truncatula* genes involved in transport mechanisms that are up-regulated cell-specifically upon mycorrhizal colonization of the roots (Gaude *et al.*, 2012), encouraging the statement that an extensive reprogramming takes place. The up-regulation of 12 of these genes in arbuscule-containing cells was confirmed via quantitative RT-PCR (figure 6), and their promoters were confirmed to be active either exclusively in arbuscule-containing cells (ARB) or in ARB cells and non-arbusculated cells adjacent to fungal structures (NAC) (figure 9).

Some, but not all the genes described in this study have already been found in other studies. *MtNrt1*, *MtPtr1*, *MtPtr3*, *MtAbcb15*, *MtNip1*, and *MtHxt1* have already been reported to be regulated in response to the AM symbiosis by either Benedito *et al.* (2010) or Hoge Kamp *et al.* (2011) or in both of these studies. Also, well-known mycorrhiza-specifically regulated genes like *MtPt4*, *MtHa1* and *MtStr2* as well as the already described potential copper transporter *MtCot* (Frenzel *et al.*, 2005; Reinert, 2012) have been found to be highly up-regulated in arbuscule-containing or in non-colonized neighbouring cells.

It has been reported previously that the AM symbiosis has a considerable impact on the plant's nitrogen nutrition (Govindarajulu *et al.*, 2005; Tian *et al.*, 2010; Casieri *et al.*, 2013). The genes presented in these studies indicate the presence of specific plant transporters facilitating the uptake of nitrogen compounds. Nitrogen is considered to be taken up by the plant in the form of ammonium (NH_4^+) (Kobae *et al.*, 2010) or nitrate (NO_3^-) (Guether *et al.*, 2009) from the periarbuscular space (PAS). In line with that, here an ammonium transporter, *MtAmt2* (Medtr8g095040.1), is up-regulated as well as a nitrate transporter *MtNrt1* (Medtr2g017750.1). The fact that both a nitrate and an ammonium transporter have been found here supports this idea and increases the evidence for the impact of the fungal partner on the nitrogen nutrition of the host plant. While the induction of the transcription of *MtAmt2* is very specifically restricted to arbuscule-containing cells ($\text{LFC}_{\text{ARB/COR}} = 1.78$), *MtNrt1* is increasingly expressed in both cell-types of mycorrhizal roots ($\text{LFC}_{\text{ARB/COR}} = 8.60$,

LFC_{NAC/COR} = 4.66) that were analysed. For *MtNrt2* this expression pattern has also been confirmed by promoter-GUS analyses (figure 9). This regulation supports the assumption that cortex cells prepare for the colonization by an arbuscule in advance when they get in close contact to fungal structures and therefore transcriptional re-programming occurs even before a cell is colonized. This was also suggested for *Sorghum bicolor* (Koegel *et al.*, 2013). Two ammonium transporters, SbAMT3;1 and SbAMT4, have been found to be expressed in neighbouring cells and were therefore considered to play a role in the preparations for an upcoming colonization by an arbuscule. SbAMT3;1 is also present in arbuscules and might play a role in the nitrogen transfer from the fungus to the plant.

Of the three ATP-binding cassette transporters that were found here, one is the already described *MtStr2* gene. STR2 forms a heterodimer with STR1 and is proposed to export an essential signal or nutrient from the plant cell into the PAS, the interface with the fungus (Zhang *et al.*, 2010). The other two ABC transporter candidates most likely belong to the ABCB/multidrug resistance (MDR) subfamily, the closest *A. thaliana* homologs are AtABCB15 and AtPGP18 (supplementary table S2.1). The promoter-GUS analyses confirmed their regulation patterns: *MtAbcb15* is transcribed in arbuscule-containing cells but to a lower extent also in non-arbusculated cells, while *MtPgp18* is specifically expressed in arbuscule-containing cells (figure 9). While MtSTR1 and 2 have been shown to be essential for the AM symbiosis, their knock-out leading to a stunted arbuscule phenotype, the effect of the two newly identified AM-specifically expressed ABC transporters is as yet unknown. ABCB transporters are often involved in auxin transport, AtABCB15 was associated with auxin transport previously (Cho and Cho, 2012). But other activities have been demonstrated for ABCBs as well (Rea, 2007), so to understand the function of these particular candidates, they need to be functionally characterized.

Two major intrinsic proteins (MIPs) (Medtr8g087710.1; Medtr5g063930.1) were identified. Most MIPs are known to function as water channels and facilitate the passive transport of small polar molecules across membranes in plants (Johanson and Gustavsson, 2002). Three oligopeptide transporters (Medtr8g087780.1; Medtr7g098040.1; Medtr8g087810.1) were found. Two of them, *MtPtr1* and *MtPtr4*, very specifically induced in arbuscule-containing cells while *MtPtr3* is also up-regulated in NAC cells compared to uncolonized cortical cells. These results were confirmed in the promoter-GUS assay.

All in all, the cell-specific expression patterns of the AM-induced transporter genes corroborate the concept that transporter genes are induced not only upon colonization of a cell by an arbuscule, but well in advance. Cells have to be able to sense the oncoming colonization by an arbuscule and the

vicinity of fungal structures in the roots. The specific set of transporters that is up-regulated exclusively in arbuscule-containing cells is likely to be localized in the periarbuscular membrane (Parniske, 2008; Pumplin and Harrison, 2009). The PAM's exact composition is unknown, but it has been hypothesized previously that AM-specific transporters are localized there to facilitate the nutrient exchange between the symbiotic partners.

4.1.2 Carbohydrates are mobilized and symplastically provided to the arbuscule-containing cells

Three further transporter candidates have been selected which are only very slightly regulated in arbuscule-containing cells in comparison to cortical cells (ARB/COR). However, they are up-regulated in neighbouring non-arbusculated cells in comparison to cortex cells (NAC/COR) and in comparison to arbuscule-containing cells (ARB/NAC) (Gaude *et al.*, 2012). These genes are a potential nucleobase-ascorbate transporter (Medtr8g086520.1), a hexose/H⁺ symporter (Medtr1g104780.1) and a sucrose/H⁺ symporter (Medtr5g067470.1).

The sucrose/H⁺ symporter has been renamed *MtSut4-1* (Doidy *et al.*, 2012) since it belongs to the clade 4 of the sucrose transporter family. It has also been shown to be a functional sucrose/H⁺ importer, effectively complementing deficient yeast strains, and is considered to represent a low-affinity/high-capacity transporter (Doidy *et al.*, 2012). The assumed localization in the tonoplast could be corroborated here in *N. benthamiana* leaves (figure 13). The localization pattern looks slightly ambivalent and might be hard to clearly separate from the cytoplasm, but given the good co-localization with the tonoplast control (Nelson *et al.*, 2007) it gives a good indication that MtSUT4-1 is indeed very likely localized at the tonoplast. *MtHxt1*, on the other hand, was expected to be localized in the plasma membrane due to sequence similarities to *AtStp13*. Its localization was confirmed in Tobacco leaves as well. Despite the lack of a cytoplasm control, which could not be shown due to technical reasons, the clear localization pattern of the GFP-labelled MtHXT1 corroborates the predicted localization.

Upon mycorrhizal colonization, the photosynthesis rate of the host plant and the sink strength of the roots is increased (Wright *et al.*, 1998). Sucrose is delivered to the roots from the source organs and can be unloaded from the phloem into the apoplast. Here it can either be split into glucose and fructose by apoplasmic invertases or be directly taken up by the plant cells as sucrose. *R. irregularis* is known to only be able to take up carbohydrates in the form of hexoses (Baier *et al.*, 2010). It has been shown that intraradical structures of AM fungi are unable to take up and utilize sucrose

(Shachar-Hill *et al.*, 1995) and no sucrose cleaving activities have been identified in AM fungi so far (Schubert *et al.*, 2003). Whether hexoses are taken up at the arbuscule, the intraradical hyphae, or both is currently unknown. While the interaction between plant and fungus is mutual, it is still unlikely that the plant provides carbohydrates to the fungus uncontrolled. Rather, it seems likely that the plant has a way of holding back carbohydrates as desired, or at least up to a certain point. It has been shown *in vitro* that roots can distinguish between the quality of the fungal partner, i.e. the amount of phosphate they receive from it, and adjust or modulate the carbon release to the fungus accordingly (Kiers *et al.*, 2011). This indicates that plants would have the means to hold back carbohydrates if needed.

However, there is also experimental evidence that the exchange of phosphate and photoassimilates is not strictly coupled (Walder *et al.*, 2012). One might assume that the plant has an excess of photoassimilates and therefore carbon is not a limiting factor. In fact, up to 20 % of the net photosynthetically fixed carbon is calculated to be exuded into the rhizosphere through root exudates (Marschner, 1995; Walker *et al.*, 2003). This clearly represents a significant carbon loss for the plant. However, the exact function of root exudations is not entirely understood, yet. One possible function is the solubilisation of phosphorus by acidification. The exudation of carboxylates is, next to the mycorrhizal interaction, one of the major strategies of plant phosphorus acquisition (Ryan *et al.*, 2012). It was shown in *Kennedia* species, a close relative to *Medicago*, belonging to the same subfamily, the Faboideae, that upon mycorrhizal colonization, the amount of root exudates released into the rhizosphere can be significantly reduced (Ryan *et al.*, 2012). Therefore, since one cause of carbon loss, the root exudation into the surrounding soil, is reduced upon mycorrhizal colonization, while an additional carbon sink, the AM fungus, is added, the total carbon loss of the plant might not increase markedly in mycorrhizal conditions. In fact, if light and water availability are optimal, as it is the case in standard experimental greenhouse conditions, carbon might not be a limiting factor for plant growth. Further evidence that there might be no strict correlation of photoassimilate and phosphate exchange comes from the analysis of nutrient and carbon distributions in common mycorrhizal networks with different plant species being connected by an AM fungal mycelium (Walder *et al.*, 2012). In these networks, a strong asymmetry in the carbon and phosphorus transfer has been revealed. While *S. bicolor* received very little phosphate, it still provided a high amount of carbon to the fungus.

The high transcript levels of the putative hexose/H⁺ symporter *MtHxt1* as well as the sucrose/H⁺ symporter *MtSut4-1* in the cells adjacent to fungal structures of mycorrhizal roots point to a mechanism to restrict the carbon flow to the fungal partner as indicated above. Promoter-GUS

fusions confirm their expression specifically in mycorrhizal roots, preferentially in cells adjacent to fungal structures and surrounding the central cylinder (figure 10). The plant might compete with the fungus for the sugar that is present in the roots, increasing the sugar uptake from the apoplastic space where it would be available to the fungus to retain as much of it as possible.

4.1.3 AM-specifically regulated genes involved in carbohydrate metabolism and transport provide new insight into carbohydrate allocation in mycorrhizal roots

Upon the mycorrhizal colonization, not only arbuscule-containing cells but also cells that are adjacent to arbuscule-containing cells or in the vicinity of the spreading fungal hyphae undergo drastic transcriptional changes. Among many others, several genes involved in major carbohydrate metabolism are specifically up- or down-regulated in one or both of these cell-types (table 7) (Gaude *et al.*, 2012). These findings, in combination with the expression of the two sugar transporters MtHXT1 and MtSUT4-1, lead to a model of how carbohydrates might be allocated in mycorrhizal roots (figure 29). It suggests that carbohydrates, especially hexoses, are removed from the apoplast where they could be reached by the fungal hyphae or the arbuscules, since the (PAS) is continuous with the rest of the apoplast. Still, a high amount of carbon is needed in the arbuscule-containing cells to build up the large new membrane, the periarbuscular membrane (PAM) surrounding the arbuscule. Since no increased expression of sugar uptake transporters could be detected in arbuscule-containing cells, symplastic rather than apoplastic import of carbon must be suggested. Plasmodesmata reportedly connect arbuscule-containing cells to their surrounding cells, indicating a means to an easier symplastic transport of carbon compounds (Blee and Anderson, 1998). Also, it has been shown that in *M. truncatula* symplastic rather than apoplastic transport is mediating the carbon exchange in the root nodule symbiosis which also represents a strong carbon sink (Complainville *et al.*, 2003). Therefore, sugar is hypothesized to be mobilized in the NAC cells. Sucrose is moved to the cytoplasm and split into hexoses, and starch is broken down. Carbohydrates may then be moved into the arbuscule-containing cells symplastically. Like this, the ARB cells will be provided with a sufficient amount of carbohydrates for the synthesis of the PAM, while at the same time, carbohydrates are being kept away from the fungus as efficiently as possible.

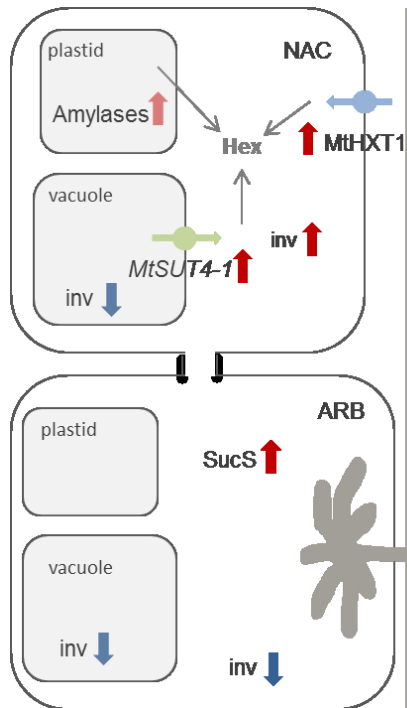


Figure 29: Working model of the carbon allocation in mycorrhizal roots.

Graphic representation of AM-regulated genes related to major carbohydrate metabolism and carbohydrate transport identified by transcriptome analysis of LCM-isolated arbuscule-containing cells of mycorrhizal roots (ARB) and non-arbuscule-containing cells of mycorrhizal roots (NAC) as compared to cortical cells of non-mycorrhizal roots. Transcriptional changes point to a mobilization and import of hexoses (Hex) into the cytoplasm of NAC cells. Here, transcript levels of an amylase, a cytosolic invertase (Medtr1g096110.1) (*inv*), a putative vacuolar sucrose transporter (MtSUT4-1), and a hexose transporter of the plasma membrane (MthXT1) are induced. Carbon is removed from the apoplast and mobilized within the NAC cells in order to be provided to the ARB cells to build up the PAM. Here, decreased transcript levels of a cytosolic invertase (Medtr1g096140) and increased transcript levels of a sucrose synthase (SucS) were observed. A putative vacuolar invertase is down-regulated in both cell-types of mycorrhizal roots. Modified from Gaude *et al.* (2012).

4.1.4 Outlook: AM specifically regulated transporter genes in *Medicago truncatula*

While this work has provided a broad overview of genes involved in the nutrient exchange in the AM symbiosis in general, and the carbon allocation in particular, a more detailed analysis of the roles of the single genes remains to be performed.

For particularly interesting candidates, like the nitrate- and ammonium transporters, RNA_i approaches to determine the effect of the loss of their functions could reveal a lot about their roles in the interaction with the fungal partner. Also, their predicted transporter activities remain to be confirmed experimentally.

For the sugar transporters, a functional characterization of *MtHxt1* to confirm its predicted function as a hexose transporter is necessary. Due to sequence similarities it has been annotated as a hexose transporter here as well as in the annotation of the genome sequence (XM_003592372), but it has not been experimentally confirmed, yet. Since only one *Tnt1* insertion line is available for this gene, an RNA_i approach to confirm the results would be feasible. Also for *MtSut4-1*, an RNA_i approach will help to better understand the function of this particular gene in the course of the symbiosis. Given that the *Lotus japonicus* vacuolar transporter LjSUT4 is considered to play a role in the release of sucrose toward nodules during the rhizobial symbiosis (Doidy *et al.*, 2012), MtSUT4-1 might also be involved in the allocation of vacuolar sucrose towards colonized root areas during the AM symbiosis.

4.2 *MtHxt1* influences the mycorrhizal interaction and primary metabolism of *Medicago truncatula*

Since *MtHxt1* is assumed to be involved in the carbon distribution in mycorrhizal roots, the metabolic changes in mycorrhizal and non-mycorrhizal *hxt1* and WT *M. truncatula* plants were analysed. Phenotypic and molecular characterizations showed that in relation to the fungal mass colonizing the roots, the amount of arbuscules is reduced by about half in *hxt1* roots in comparison to WT roots, while the overall frequency and intensity of mycorrhizal colonization remains unchanged (figure 19, figure 20).

High variances in the metabolite levels between different samples even in the same condition hindered the interpretation of the results. High variations are a common problem when analysing mycorrhizal plants. Still, the data provide a good general overview of the metabolic changes in mycorrhizal vs. non-mycorrhizal *M. truncatula* plants in general and give a first hint as to what influences the hexose/H⁺ symporter MthXT1 might have in the course of the interaction. So far, metabolite profiling analyses focusing on the AM symbiosis have been performed by Schliemann *et al.* (2008) in *M. truncatula* roots. They were able to show that the levels of certain amino acids and fatty acids are increased upon mycorrhizal colonization. Also, fungus-specific acids, palmitvaccenic and vaccenic acid, were shown to accumulate. The authors suggest that they might be used as markers for fungal root colonization, but they were not found in this study. In contrast to Schliemann *et al.* (2008), here also the effect of the mycorrhizal colonization on the metabolite profile in source leaves is analysed. The influence of the knock-out of an AM-induced hexose transporter, *MtHxt1*, on the metabolite composition of both, roots and source leaves of mycorrhizal plants, is examined to enhance the knowledge of its influence on the sugar distribution in mycorrhizal plants.

4.2.1 Mycorrhizal colonization leads to metabolic changes in *hxt1* and WT *Medicago truncatula* plants

When comparing mycorrhizal and non-mycorrhizal plants of both genotypes, a few metabolites were present only in mycorrhizal roots while their levels were under the detection limit in non-mycorrhizal conditions (table 9). These metabolites can be considered either highly symbiosis-specific, or, very likely, of fungal origin. As expected, alpha,alpha-trehalose is among them. Trehalose, a disaccharide formed from two α -glucose units, is the main form of carbon within the

fungus (figure 2) (Bécard *et al.*, 1991; Schubert *et al.*, 1992). It is synthesized in the intraradical mycelium (IRM) where sugar is taken up by the arbuscule or the fungal hyphae and moved to the extraradical mycelium (ERM). The fact that it was exclusively detected in mycorrhizal roots is in line with previous studies (Schliemann *et al.*, 2008) and increases the confidence in the accuracy of the measurement. Moreover, quinic acid shows the same pattern of presence in mycorrhizal and absence in non-mycorrhizal roots (table 9). Quinic acid is an alternative intermediate of the shikimic pathway and is known to occur freely in plants but is actively metabolized during growth (Seigler, 1995). Why it is only present in mycorrhizal conditions will yet have to be determined. Adenine levels are also under the detection level in non-mycorrhizal roots and only present in mycorrhizal roots in WT plants, and in 3 and 7 wpi in *hxt1* plants, but again, the reason for this remains elusive.

As expected, phosphate levels were affected by the mycorrhizal colonization. Phosphoric acid (H_3PO_4) levels were slightly increased upon mycorrhizal colonization in the roots of both genotypes at 5 and 7 wpi (table 10). Given that it is well established that phosphate is transferred from the fungus to the plant (Smith and Smith, 2012), an increase in soluble phosphate is to be expected. In leaves, however, phosphoric acid concentrations do not differ notably between mycorrhizal and non-mycorrhizal conditions. This might be due to the fact that mycorrhizal plants are bigger, resulting in a similar final concentration of phosphate in the tissue. It may also result from fast metabolic incorporation, since only soluble phosphate, which makes up a very small fraction of the total phosphate in the plant, is measured here. The findings here are in line with previous findings (Branscheid, 2012) where soluble phosphate of *M. truncatula* roots and shoots was measured directly over a time-course from 1 to 8 wpi, and no significant changes in the phosphate content between mycorrhizal and non-mycorrhizal conditions could be determined in the shoots.

Also unsurprisingly, the levels of several amino acids altered significantly between mycorrhizal and non-mycorrhizal conditions in both, source leaves and roots of both genotypes (table 10 and table 11). In roots, glutamic and aspartic acid levels are higher in mycorrhizal than in non-mycorrhizal roots in *hxt1* plants in later stages of the colonization (7 wpi). This is even more pronounced in the WT, as glutamic acid is present in mycorrhizal roots but below the detection limit in non-mycorrhizal roots at later stages of the colonization (5 and 7 wpi) (table 9). At early stages, asparagine and pyroglutamic acid (a derivatization artifact of glutamic acid) accumulate in roots upon mycorrhizal colonization in both genotypes. The AM-specific accumulation of glutamic, pyroglutamic, and aspartic acid as well as asparagine was shown by Schliemann *et al.* (2008). They found that under mycorrhizal conditions most amino acids, including these four, peaked at 6 wpi. Here, on the other hand, the changes in asparagine and pyroglutamic acids were observed in roots at early stages of the

colonization while the differences in the glutamic and aspartic acid levels were most pronounced at late stages. Aspartic and glutamic acid and asparagine are, together with glutamine, the dominant components of the total free amino acid pool in most legumes and crop plants (Lam *et al.*, 1996). Also together with glutamine, they are considered to be the major form of nitrogen transport (Lam *et al.*, 1995; Delrot *et al.*, 2001). Because of its relative stability and high nitrogen to carbon ratio, asparagine is also considered important for the storage of nitrogen resources (Lam *et al.*, 1996). A higher level of these amino acids in mycorrhizal roots might therefore indicate a better nitrogen supply to the plants due to the mycorrhizal symbiosis, supporting previous findings that the AM symbiosis improved the plants' nitrogen nutrition (Govindarajulu *et al.*, 2005). In source leaves, the difference between the two genotypes can be detected (table 11). Aspartic and glutamic acid and lysine were found to be more abundant in mycorrhizal than in non-mycorrhizal WT plants, while their levels are basically equal in the leaves of mycorrhizal and non-mycorrhizal *hxt1* plants at 5 wpi. That the improved nitrogen status of the mycorrhizal plants is less pronounced in *hxt1* plants, i.e. the levels of these amino acids did not alter significantly between the mycorrhizal conditions in leaves of *hxt1* plants, may be a result of the ineffective AM symbiosis. The lower amount of arbuscules in the *hxt1* plants is likely to lead to a reduced nitrogen transfer towards the plant. This can be seen most clearly in the most active stage of the mycorrhizal symbiosis (Schliemann *et al.*, 2008), at approx. 5 wpi, and seems to particularly affect the level of nitrogen compounds in the shoot.

The changes in the carboxylic acid levels between both genotypes are most striking in mycorrhizal roots (table 10 and table 11). The levels of malic and malonic acid, for instance, are much higher in mycorrhizal than in non-mycorrhizal *hxt1* roots, but unaltered in the WT (table 10) in later stages of the interaction. Their higher concentration is also apparent in the direct comparison of the two genotypes. In mycorrhizal roots, their levels are increased in *hxt1* in comparison to WT plants, while they are similar in non-mycorrhizal conditions. The secretion of carboxylates into the rhizosphere is a way for the plants to facilitate the uptake of phosphate (Walker *et al.*, 2003; Ryan *et al.*, 2012). The increased production of these compounds might be the reason why the myc to nonmyc ratio of the phosphate levels in the roots of mycorrhizal *hxt1* plants is comparable to WT plants, even though the transfer through the mycorrhiza might be impaired.

Of course, plant carbon metabolism and partitioning was expected to be particularly strongly influenced by the *MtHxt1* knock-out. In roots, the sugar levels vary the most at 3 wpi: fructose, glucopyranoside, glucose, and xylose levels are significantly lower in mycorrhizal *hxt1* roots than they are in mycorrhizal WT roots (table 12). This is in line with the findings in leaves, but here changes in the ratio of the levels of different sugars occurred in the intermediate stages of

mycorrhizal interaction (5 wpi). The hexoses glucose, fructose, and mannose are more abundant in the leaves of mycorrhizal plants than of non-mycorrhizal plants at 5 wpi in the WT, while their ratios are unchanged in the *hxt1* plants for all three sugars (table 11). Both of these findings might point to a higher loss of sugars in the *hxt1* plants, caused by the impaired removal of hexoses from the root apoplast and therefore increasing loss of sugars to the fungus. At 7 wpi, the latest stage analysed here, however, this trend cannot be observed any more. When comparing the leaf metabolites of *hxt1* and WT plants at 7 wpi (table 13), the levels of glucose, fructose, and mannose are higher in *hxt1* plants than in WT plants in both, mycorrhizal and non-mycorrhizal conditions. Surprisingly, this effect is even more pronounced in mycorrhizal conditions. It has to be admitted, though, that the variations in the sugar levels, as in the levels of all other metabolites, were particularly high in the 7 wpi samples.

Taken together, these data showed that the mycorrhizal interaction has a stronger impact on the metabolite profiles of both, roots and leaves of the plants, than the *MtHxt1* knock-out has, at least in the experimental conditions applied here.

4.2.2 Mycorrhizal colonization of *hxt1* and WT *Medicago truncatula* plants leads to changes in the primary metabolite profile in roots and source leaves

MtHxt1 knock-out plants show a severe phenotype in biomass production and flower and seed development. Mycorrhizal *hxt1* root also contain significantly fewer arbuscules in relation to the overall fungal mass than WT roots. Since *MtHxt1* is considered to be involved in the carbon allocation in mycorrhizal roots, metabolic profiling of *hxt1* and WT roots and leaves was performed in mycorrhizal and non-mycorrhizal plants. AM-responsive changes in metabolite levels were found in roots as well as in leaves. Fungus derived trehalose was found in mycorrhizal roots exclusively. Elevated phosphate levels were detected in the roots of mycorrhizal plants, demonstrating the improved phosphate status of the plants due to the mycorrhizal interaction. The *MtHxt1* knock-out influenced the levels of different sugars in the roots at early and intermediate time-points of mycorrhizal colonization and in the leaves at later time-points. The levels of fructose, glucopyranoside, glucose and xylose were lower in mycorrhizal *hxt1* roots than in WT roots in early stages of mycorrhizal colonization, indicating a higher carbon loss in the *hxt1* plants than in the WT. In leaves, the levels of glucose, fructose and mannose were significantly higher in mycorrhizal than in non-mycorrhizal plants of both genotypes. Also, the improved nitrogen-supply to the plants by the mycorrhizal interaction, reflected by elevated levels of certain amino acids in the leaves upon AM

colonization, is reduced by the *MtHxt1* knock-out. Finally, it seems likely that the efficiency of the nutrient transfer through the AM symbiosis is reduced in *hxt1* plants since apparently alternative uptake mechanisms, like an increased production of carboxylates, are being employed.

4.2.3 Outlook: *hxt1* metabolite profiling

As mentioned earlier, a functional characterization of *MtHxt1* to confirm its predicted function as a hexose transporter is necessary. In addition to the analysis of the one available *Tnt1* line, an RNA_i approach might be needed to confirm the results presented here. The metabolite data obtained in this experiment give a broad first overview of the metabolic changes upon mycorrhizal colonization and the possible effects the *MtHxt1* knock-out might have. Still, results will need to be repeated with technical procedures optimized to minimize the variations in the measurements. The extraction and derivatization need to be optimized for *M. truncatula* and probably using different time-points, including a 4 wpi measurement, would be feasible.

4.3 *Rhizophagus irregularis* transcriptome analyses reveal previously unknown fungal transporter genes involved in the AM symbiosis

Despite the fact that *Rhizophagus irregularis* (DAOM 197198) is widely used as a model organism for the analysis of AM symbioses, only incomplete genomic information was available until recently. Transcriptome analyses have therefore been impeded by the lack of a reference genome, and so far only a small number of symbiosis-related transcriptomic changes were published (Tisserant *et al.*, 2012) and very few transcripts that are directly involved in this interaction are known (Maldonado-Mendoza *et al.*, 2001; Lopez-Pedrosa *et al.*, 2006; Helber *et al.*, 2011; Perez-Tienda *et al.*, 2011).

To get a more detailed insight into the molecular basis of the fungal side of the symbiosis, the transcriptome of LCM-collected arbuscules was compared to extraradical tissues. This approach led to the identification of symbiosis-related transcriptional changes *R. irregularis*.

4.3.1 Potential fungal transporter genes are specifically regulated *in planta*

The NGS sequencing results were first analysed without a reference genome. The reads were used for contig assembly and a read-count based expression profiling. Since this work is focused on transport processes, potential transporter genes were identified by finding transmembrane domains and annotation based on sequence homologies to known fungal genes (table 14).

Three major facilitator superfamily (MFS) transporters were identified. One of them, *RiMFS1* (comp8571_c0), was found to be induced in extraradical tissues in comparison to arbuscules. Blastx in all fungal sequences results in mainly MFS and sugar transporters, giving a first indication what might be transported by *RiMFS1*. For the second MFS transporter, *RiMFS2* (comp2270_c0), blastx of the full CDS results in only hypothetical proteins, giving no further indication as to the potential substrate that might be transported. Also for *RiMFS3* (comp4884_c0) no further indication as to what is transported can be gained by sequence similarities, as blastx only results in MFS transporters without further information on what they transport.

RiSut1 (comp11677_c0) is annotated as a sugar transporter in the *R. irregularis* genome database. This is in line with blastx results against other fungal genes. The majority of the blast results are sequences annotated as sugar transporters. Given the focus of this work, this makes *RiSut1* a very interesting candidate. Localizing the transcripts *in planta* by *in situ* hybridization would give a further indication as to where exactly sugar is taken up into the fungus.

This is also true for *RiGlct1* (comp2866_c0). The short contig that was available after the assembly of the Illumina reads indicates a function as a glucose transporter. Since hexoses are considered to be taken up by AM fungi, this candidate is likely to be relevant for the carbon exchange in the AM symbiosis, since it is very highly up-regulated in planta in comparison to the ERM, with the highest LFC (10.26) of all candidates (table 14). It might therefore be involved in the uptake of hexoses, presumably glucose, from the root apoplast.

Also very highly up-regulated is *RiYvc1* (comp19601_c0). But, just as for *RiGlct1*, the complete CDS is not available in the genome database. It is a well-established assumption that carbohydrates may be taken up by AM fungi in the form of glucose, providing a straight forward hypothesis for the function of *RiGlct1* in the interaction with the plant. Potassium, on the other hand, is considered to be one of the minerals made more easily available to the plant by the fungus (Smith and Read, 2008). Hints for both, direct and indirect effects of the fungus on the K⁺ supply were found, but no mechanism of the transfer was shown so far (Smith and Read, 2008). Being highly up-regulated *in planta*, *RiYvc1* might be facilitating the movement of K⁺ from the fungus into the apoplast towards the plant.

The qRT-PCR results confirmed the tissue-specific expression pattern revealed by the sequencing (figure 26). Still, due to technical reasons, the *in planta* sample, LCM-collected arbuscules, cannot be considered to exclusively contain arbuscules. Intraradical hyphae will have been harvested as well, so the sample was a mixture of RNA from both of these tissues. Therefore, localizing the transcripts *in planta* by *in situ* hybridization will be giving additional interesting insight.

In addition to the newly found transcripts, a high amount of previously described genes were found in this approach. The most interesting ones are listed in table 15. For the majority, the described expression pattern could also be shown here. The sugar transporter genes *RiMst4*, and *RiSuc1* were found to be increasingly expressed *in planta* in comparison to the ERM, confirming previous results (Helber *et al.*, 2011). Only *RiMst3* did not have any matching reads here. *RiMst2*, on the other hand, only had a LFC_{ARB/ERM} of 0.06, therefore was found not to be differentially expressed in extraradical and intraradical tissues. This was in line with qRT-PCR analyses conducted in this study (data not shown), but does contradict the results of Helber *et al.* (2011). Why their results could not be confirmed here remains to be investigated further and might be due to different growth conditions used. *RiPt* (Maldonado-Mendoza *et al.*, 2001) was mentioned before and was used as a positive control in this study. The results presented here are in line with its regulation pattern reported earlier. It was shown to be expressed in the ERM and regulated in response to external phosphate concentrations. Here, the plants were grown under low phosphate conditions (20 mM in the fertilizing solution). Therefore, as expected, *RiPt* is highly expressed in the ERM. Several genes found

by Tian *et al.* (2010) were found here as well, and only for one of them, *RiOat1*, the reported regulation pattern disagreed with the findings presented here. Here, *RiOat1* was found to be higher expressed in the ERM than *in planta*, while Tian *et al.* (2010) showed the opposite regulation pattern. The transcript levels of *RiGs1* and *RiNt* were only slightly altered between both tissues, their level was only slightly higher in the ERM than in the IRM (Tian *et al.*, 2010) while the results presented in this study indicate that they are up-regulated in the ERM. *RiAbc1* was described not to be differentially expressed between ERM and *in planta* samples (Gonzalez-Guerrero *et al.*, 2010) and *RiAmt2* was described to be up-regulated *in planta* (Perez-Tienda *et al.*, 2011). Both of these genes were shown to be higher expressed in the ERM than in arbuscules in this study. The up-regulation of *RiAmt1* in the ERM (Lopez-Pedrosa *et al.*, 2006), on the other hand, was confirmed.

The fact that transcripts which could not be shown to be differentially expressed in previous studies were found here, and that the difference between the transcript levels in the different tissues was higher in this study, is very likely due to the higher resolution of the approach used here. Using LCM-collected fungal tissues instead of mycorrhizal roots as *in planta*, IRM or arbuscule samples decreases the dilution effects, enhances the sensitivity and efficiently reduces the contamination of the *in planta* samples with extraradical hyphae that grow from mycorrhizal roots.

Localization of in planta expressed R. irregularis transcripts

The transcripts of *RiMFS2* were shown to accumulate in arbuscules but also, to an even higher amount, in intraradical hyphae. *RiMFS2* is a highly up-regulated *in planta*, therefore probably involved in the interaction with the plant root, i.e. involved in the transport of nutrients over the fungal membrane. MFS transporters move small solutes along chemiosmotic ion gradients. What is transported by *RiMFS2* is not known, yet. Many MFS transporters are known to transport sugars, but other substrates like amino acids, phosphate compounds and a variety of organic and inorganic anions and cations can function as substrates, too. The fact that *RiMFS2* transcripts are not only present in arbuscules, but also in the hyphae growing in the root apoplast, indicates that the amount of fungal transport processes is increasing not only in the arbuscules, as expected, but also in the intraradical hyphae. This is in line with the hypothesized carbon allocation from the plant to the fungus described in 4.1.3 (figure 29).

4.3.2 SBS RNA sequencing of LCM-collected arbuscules identifies specifically regulated *Rhizophagus irregularis* transporter genes

Six potential *R. irregularis* transporter genes were identified by Illumina sequencing of *in planta* and ERM tissues. Three new potential MFS transporters, one of them up-regulated in the ERM, two *in planta*, and a potential sugar transporter, a potential high-affinity glucose transporter, and a potential potassium ion channel up-regulated *in planta* were found. These AM-responsively expressed transporters are likely to play a role in the nutrient exchange between the plant and the fungus in the course of this interaction.

4.3.3 Outlook: *in planta* transcriptome of *Rhizophagus irregularis*

The transcriptome sequencing approach resulted in a broad overview of *R. irregularis* genes differentially regulated between arbuscules and the ERM. The list of candidates concentrated on here is focused on those involved in transport processes, but obviously, much more information can be gained from the dataset. For example, genes involved in the signalling between the symbiotic partners will very likely be differentially regulated, and identifying those will give important new insight into the signalling of the fungus and its communication with the plant. Especially now that a reference genome is available (Francis Martin, INRA, Nancy, personal communication), the identification of AM-responsively regulated genes in this and other functional groups will be facilitated. By mapping the reads of both libraries analysed here, new genes that are specifically induced *in planta* can be identified and will be giving new insight into the AM-specific transcriptional reprogramming of the fungal partner.

As to the transporter candidates selected in this study, firstly 5'RACE analyses will need to be performed for the potential high affinity glucose transporter *RiGlt1* and the potential potassium ion channel *RiYvc1* to obtain their full length cDNA sequences. They are the two most highly up-regulated candidates, and especially *RiGlt1* is a very interesting candidate given the focus of this work. With the full sequence at hand, further analyses will be possible as they are for the other candidates.

Obviously, a functional characterization of all the candidates needs to be performed to confirm their assigned transporter functions. For *RiSut1*, for instance, determining which sugars can be transported will give one more piece of information to unravel the mechanisms of the carbon

allocation in the AM-symbiosis. But also for the other candidates, confirming their predicted transporter functions or, in case of the MFS transporters, identifying their substrates, will be necessary for further interpretation of their roles during the interaction with the plant. Expressing the MFS proteins in *Xenopus* oocytes or yeast mutants is a suitable approach to identify their transporter function.

To determine the exact localization of the transporters, *in situ* hybridizations are the method of choice. They will need to be performed for genes up-regulated *in planta* to check whether the transcripts are most abundant in arbuscules, intraradical hyphae, or both. This will provide important information for the determination of the exact location of the nutrient exchange. While in general the arbuscules are considered to be the main site of the nutrient exchange, the results presented in 3.1 and 3.2 suggest that carbohydrates, for instance, may also be taken up from the root apoplast by the intraradical hyphae. This theory could be corroborated by placing the transcripts of *RiGlc1* or, for example, *RiSut1* or the MFS transporters in the intraradical hyphae.

The *in situ* localization of *RiMFS2* transcripts gave a good indication that its transcripts are localized mainly in the intraradical hyphae but also in the arbuscules. Nevertheless, these analyses will have to be verified by repeating the hybridization with different root sections.

Finally, a knock-out approach for promising AM-induced genes would of course supply very valuable insights into their function during the interaction with the plant and to whether or not they are essential for the symbiosis. Unfortunately, to date transforming *R. irregularis*, or any other AM fungus, proves to be challenging. Helber *et al.* (2011) reported a successful knock-out of MST2 in *R. irregularis* via host induced gene silencing (HIGS) (Nowara *et al.*, 2010), but to date this approach has not been successful in our hands.

5 TABLE OF FIGURES

Figure 1: The arbuscule.....	2
Figure 2: Schematic overview over the nutrient flow in the AM symbiosis.	5
Figure 3: Schematic workflow of the analysis of the Illumina reads.	34
Figure 4: Distribution of cell-specifically regulated <i>M. truncatula</i> transcripts in response to mycorrhizal colonization across different functional classes	35
Figure 5 : Venn diagram of the cell-specifically regulated transporter genes.....	36
Figure 6: Relative expression levels (given as 40-dCt values) of the up-regulated putative transporter genes in <i>M. truncatula</i> roots determined by qRT-PCR.	39
Figure 7: Relative expression levels (given as 40-dCt values) of the mycorrhizal marker gene <i>MtPt4</i> and the <i>RirRNA</i> in <i>M. truncatula</i> roots.	39
Figure 8: Promoter-GUS fusions for the localization of the promoter activity in <i>M. truncatula</i> roots.....	40
Figure 9: Localization of the promoter activity of selected genes transcriptionally regulated in ARB or NAC cells coding for putative transporter proteins in mycorrhizal <i>M. truncatula</i> roots.....	41
Figure 10: Localization of the promoter activity of selected genes transcriptionally regulated in ARB or NAC cells coding for putative sugar transporter proteins in mycorrhizal <i>M. truncatula</i> roots.....	44
Figure 11: Localization of the promoter activity of selected genes transcriptionally regulated in ARB or NAC cells and coding for putative sugar transporter proteins in <i>S. meliloti</i> nodules of <i>M. truncatula</i> roots	45
Figure 12: Relative expression levels (2^{-dCt} values) of the putative <i>M. truncatula</i> sugar transporters <i>MtHxt1</i> and <i>MtSut4-1</i> , and the nodule marker gene <i>MtN24</i> in nodulated and non-nodulated <i>M. truncatula</i> roots determined by qRT-PCR.....	46
Figure 13: Intracellular localization of MtSUT4-1 and MtHXT1 in <i>N. benthamiana</i> leaves.	47
Figure 14: Schematic overview of the <i>Tnt1</i> insertion in the MtHxt1 gene.....	49
Figure 15: Screening of the first generation of <i>M. truncatula</i> <i>Tnt1</i> insertion plants.....	50
Figure 16: Root and shoot fresh weight of mycorrhizal and non-mycorrhizal <i>hxt1</i> and WT plants (4 wpi).	51
Figure 17: Relative expression levels (2^{-dCt} values) of AM marker genes in <i>M. truncatula</i> <i>hxt1</i> and WT roots determined by qRT-PCR.....	52
Figure 18 Relative expression levels (2^{-dCt} values) <i>MtHxt1</i> in <i>M. truncatula</i> <i>hxt1</i> and WT roots determined by qRT-PCR.....	52

Figure 19: Relative expression levels ($2^{-\text{dCt}}$ values) of <i>MtPt4</i> normalized to fungal reference genes in mycorrhizal <i>M. truncatula hxt1</i> and WT roots determined by qRT-PCR.	53
Figure 20: Mycorrhiza parameters in WGA Alexa fluor stained root fragments of <i>hxt1</i> and WT plants.	53
Figure 21: ICAs of the metabolite profiles of mycorrhizal and non-mycorrhizal WT and <i>hxt1</i> roots and leaves harvested at 3, 5 and 7 wpi.....	55
Figure 22: Isolation of arbuscule-containing cells from <i>M. truncatula</i> roots using laser capture microdissection.....	61
Figure 23: Quality control of the RNA samples.....	62
Figure 24: Schematic overview of the results of the bioinformatic analysis of the <i>R. irregularis</i> Illumina sequencing data.....	64
Figure 25: Primer specificity to fungal transcripts.....	67
Figure 26: Relative expression levels ($2^{-\text{dCt}}$ values) of the differentially regulated potential <i>R. irregularis</i> transporter genes determined by qRT-PCR.....	68
Figure 27: Localization of <i>RiMFS2</i> transcript accumulation in <i>R. irregularis</i> hyphae and arbuscules in mycorrhizal <i>M. truncatula</i> roots and arbuscule-containing cells.....	71
Figure 28: Localization of <i>RiMFS2</i> transcript accumulation in <i>R. irregularis</i> hyphae and arbuscules in mycorrhizal <i>M. truncatula</i> roots and arbuscule-containing cells.....	71
Figure 29: Working model of the carbon allocation in mycorrhizal roots.....	78

6 LITERATURE

- Allwood JW, Erban A, de Koning S, Dunn WB, Luedemann A, Lommen A, Kay L, Loscher R, Kopka J, Goodacre R** (2009) Inter-laboratory reproducibility of fast gas chromatography-electron impact-time of flight mass spectrometry (GC-EI-TOF/MS) based plant metabolomics. *Metabolomics* **5**: 479-496
- Aroca R, Bago A, Sutka M, Paz JA, Cano C, Amodeo G, Ruiz-Lozano JM** (2009) Expression analysis of the first arbuscular mycorrhizal fungi aquaporin described reveals concerted gene expression between salt-stressed and nonstressed mycelium. *Mol Plant Microbe Interact* **22**: 1169-1178
- Bago B, Pfeffer PE, Abubaker J, Jun J, Allen JW, Brouillette J, Douds DD, Lammers PJ, Shachar-Hill Y** (2003) Carbon export from arbuscular mycorrhizal roots involves the translocation of carbohydrate as well as lipid. *Plant Physiol* **131**: 1496-1507
- Bago B, Pfeffer PE, Shachar-Hill Y** (2000) Carbon metabolism and transport in arbuscular mycorrhizas. *Plant Physiol* **124**: 949-958
- Baier MC, Keck M, Godde V, Niehaus K, Kuster H, Hohnjec N** (2010) Knockdown of the symbiotic sucrose synthase MtSucS1 affects arbuscule maturation and maintenance in mycorrhizal roots of *Medicago truncatula*. *Plant Physiol* **152**: 1000-1014
- Bapaume L, Reinhardt D** (2012) How membranes shape plant symbioses: signaling and transport in nodulation and arbuscular mycorrhiza. *Front Plant Sci* **3**: 223
- Barker DG, Pfaff T, Moreau D, Groves E, Ruffel S, Lepetit M, Whitehand S, Maillet F, Nair RM, Journet E-P** (2006) Growing *M. truncatula*: choice of substrates and growth conditions. *Medicago truncatula* handbook version November 2006
- Bécard G, Doner LW, Rolin DB, Douds DD, Pfeffer PE** (1991) Identification and quantification of trehalose in vesicular-arbuscular mycorrhizal fungi by *in vivo* C-13 Nmr and Hplc analyses. *New Phytologist* **118**: 547-552
- Bécard G, Fortin JA** (1988) Early events of vesicular-arbuscular mycorrhiza formation on Ri T-DNA transformed roots. *New Phytol* **108**: 211-218
- Benedetto A, Magurno F, Bonfante P, Lanfranco L** (2005) Expression profiles of a phosphate transporter gene (GmosPT) from the endomycorrhizal fungus *Glomus mosseae*. *Mycorrhiza* **15**: 620-627
- Benedito VA, Li H, Dai X, Wandrey M, He J, Kaundal R, Torres-Jerez I, Gomez SK, Harrison MJ, Tang Y, Zhao PX, Udvardi MK** (2010) Genomic inventory and transcriptional analysis of *Medicago truncatula* transporters. *Plant Physiol* **152**: 1716-1730
- Blee KA, Anderson AJ** (1998) Regulation of arbuscule formation by carbon in the plant. *Plant J* **16**: 523-530
- Boisson-Dernier A, Chabaud M, Garcia F, Becard G, Rosenberg C, Barker DG** (2001) *Agrobacterium rhizogenes*-transformed roots of *Medicago truncatula* for the study of nitrogen-fixing and endomycorrhizal symbiotic associations. *Mol Plant Microbe Interact* **14**: 695-700.
- Boldt K, Pörs Y, Haupt B, Bitterlich M, Kühn C, Grimm B, Franken P** (2011) Photochemical processes, carbon assimilation and RNA accumulation of sucrose transporter genes in tomato arbuscular mycorrhiza. *J Plant Physiol* **168**: 1256-1263
- Bonfante P, Genre A** (2010) Mechanisms underlying beneficial plant-fungus interactions in mycorrhizal symbiosis. *Nat Commun* **1**: 48

- Branscheid A** (2012) Phosphate homeostasis and posttranscriptional gene regulation during arbuscular mycorrhizal symbiosis in *Medicago truncatula*. Dissertation, University of Potsdam
- Casieri L, Ait Lahmidi N, Doidy J, Veneault-Fourrey C, Migeon A, Bonneau L, Courty PE, Garcia K, Charbonnier M, Delteil A, Brun A, Zimmermann S, Plassard C, Wipf D** (2013) Biotrophic transportome in mutualistic plant-fungal interactions. *Mycorrhiza*
- Casieri L, Gallardo K, Wipf D** (2012) Transcriptional response of *Medicago truncatula* sulphate transporters to arbuscular mycorrhizal symbiosis with and without sulphur stress. *Planta* **235**: 1431-1447
- Cho M, Cho HT** (2012) The function of ABCB transporters in auxin transport. *Plant Signal Behav* **8**
- Complainville A, Brocard L, Roberts I, Dax E, Sever N, Sauer N, Kondorosi A, Wolf S, Oparka K, Crespi M** (2003) Nodule initiation involves the creation of a new symplasmic field in specific root cells of medicago species. *Plant Cell* **15**: 2778-2791
- Corradi N, Bonfante P** (2012) The arbuscular mycorrhizal symbiosis: origin and evolution of a beneficial plant infection. *PLoS Pathog* **8**: e1002600
- Daub CO, Kloska S, Selbig J** (2003) MetaGeneAlyse: analysis of integrated transcriptional and metabolite data. *Bioinformatics* **19**: 2332-2333
- Deblaere R, Bytebier B, De Greve H, Deboeck F, Schell J, Van Montagu M, Leemans J** (1985) Efficient octopine Ti plasmid-derived vectors for *Agrobacterium*-mediated gene transfer to plants. *Nucleic Acids Res* **13**: 4777-4788
- Declerck S, Strullu D-G, Fortin JA, (Eds.)** (2005) *In vitro* culture of mycorrhizas. Springer, Heidelberg
- Delano-Frier JP, Tejeda-Sartorius M** (2008) Unraveling the network: Novel developments in the understanding of signaling and nutrient exchange mechanisms in the arbuscular mycorrhizal symbiosis. *Plant Signal Behav* **3**: 936-944
- Delrot S, Rochat C, Tegeder M, Frommer W** (2001) Amino acid transport. In PJ Lea, J-F Morot-Gaudry, eds, *Plant nitrogen*. Springer Berlin Heidelberg, Paris, pp 213-235
- Doidy J, Grace E, Kuhn C, Simon-Plas F, Casieri L, Wipf D** (2012) Sugar transporters in plants and in their interactions with fungi. *Trends Plant Sci* **17**: 413-422
- Doidy J, van Tuinen D, Lamotte O, Corneillat M, Alcaraz G, Wipf D** (2012) The *Medicago truncatula* sucrose transporter family: characterization and implication of key members in carbon partitioning towards arbuscular mycorrhizal fungi. *Mol Plant* **5**: 1346-1358
- Erbani A, Schauer N, Fernie AR, Kopka J** (2007) Nonsupervised construction and application of mass spectral and retention time index libraries from time-of-flight gas chromatography-mass spectrometry metabolite profiles. *Methods Mol Biol* **358**: 19-38
- Frenzel A, Manthey K, Perlick AM, Meyer F, Puhler A, Kuster H, Krajinski F** (2005) Combined transcriptome profiling reveals a novel family of arbuscular mycorrhizal-specific *Medicago truncatula* lectin genes. *Mol Plant Microbe Interact* **18**: 771-782
- Gaude N, Bortfeld S, Duensing N, Lohse M, Krajinski F** (2012) Arbuscule-containing and non-colonized cortical cells of mycorrhizal roots undergo extensive and specific reprogramming during arbuscular mycorrhizal development. *Plant J* **69**: 510-528
- Gaude N, Schulze WX, Franken P, Krajinski F** (2012) Cell type-specific protein and transcription profiles implicate periarbuscular membrane synthesis as an important carbon sink in the mycorrhizal symbiosis. *Plant Signal Behav* **7**: 461-464

- Gaur A, Adholeya A** (2004) Prospects of arbuscular mycorrhizal fungi in phytoremediation of heavy metal contaminated soils. *Current Science* **86**: 528-534
- Gianinazzi-Pearson V** (1996) Plant cell response to arbuscular mycorrhizal fungi: getting to the roots of the symbiosis. *The Plant Cell* **8**: 1871-1883
- Gianinazzi S, Gollotte A, Binet MN, van Tuinen D, Redecker D, Wipf D** (2010) Agroecology: the key role of arbuscular mycorrhizas in ecosystem services. *Mycorrhiza* **20**: 519-530
- Gilbert N** (2009) Environment: The disappearing nutrient. *Nature* **461**: 716-718
- Gomez SK, Javot H, Deewatthanawong P, Torres-Jerez I, Tang Y, Blancaflor EB, Udvardi MK, Harrison MJ** (2009) *Medicago truncatula* and *Glomus intraradices* gene expression in cortical cells harboring arbuscules in the arbuscular mycorrhizal symbiosis. *BMC Plant Biol* **9**: 10
- Gonzalez-Guerrero M, Benabdellah K, Valderas A, Azcon-Aguilar C, Ferrol N** (2010) GintABC1 encodes a putative ABC transporter of the MRP subfamily induced by Cu, Cd, and oxidative stress in *Glomus intraradices*. *Mycorrhiza* **20**: 137-146
- Govindarajulu M, Pfeffer PE, Jin H, Abubaker J, Douds DD, Allen JW, Bucking H, Lammers PJ, Shachar-Hill Y** (2005) Nitrogen transfer in the arbuscular mycorrhizal symbiosis. *Nature* **435**: 819-823
- Graham JHE**, ed (2000) Assessing costs of arbuscular mycorrhizal symbiosis in agroecosystems. AP, St. Paul, Minnesota, USA
- Guether M, Neuhauser B, Balestrini R, Dynowski M, Ludewig U, Bonfante P** (2009) A mycorrhizal-specific ammonium transporter from *Lotus japonicus* acquires nitrogen released by arbuscular mycorrhizal fungi. *Plant Physiol* **150**: 73-83
- Guttenberger M** (2000) Arbuscules of vesicular-arbuscular mycorrhizal fungi inhabit an acidic compartment within plant roots. *Planta* **211**: 299-304
- Harrison MJ, Dewbre GR, Liu J** (2002) A phosphate transporter from *Medicago truncatula* involved in the acquisition of phosphate released by arbuscular mycorrhizal fungi. *Plant Cell* **14**: 2413-2429.
- Harrison MJ, van Buuren ML** (1995) A phosphate transporter from the mycorrhizal fungus *Glomus versiforme*. *Nature* **378**: 626-629
- Hause B, Fester T** (2005) Molecular and cell biology of arbuscular mycorrhizal symbiosis. *Planta* **221**: 184-196
- Helber N, Wipfel K, Sauer N, Schaarschmidt S, Hause B, Requena N** (2011) A versatile monosaccharide transporter that operates in the arbuscular mycorrhizal fungus *Glomus* sp is crucial for the symbiotic relationship with plants. *Plant Cell* **23**: 3812-3823
- Hoagland DR, Arnon DI** (1950) The water-culture method for growing plants without soil. California Agricultural Experiment Station Circular **347**: 1-32
- Hogekamp C, Arndt D, Pereira PA, Becker JD, Hohnjec N, Kuster H** (2011) Laser microdissection unravels cell-type-specific transcription in arbuscular mycorrhizal roots, including CAAT-box transcription factor gene expression correlating with fungal contact and spread. *Plant Physiol* **157**: 2023-2043
- Hohnjec N, Perlick AM, Puhler A, Kuster H** (2003) The *Medicago truncatula* sucrose synthase gene MtSucS1 is activated both in the infected region of root nodules and in the cortex of roots colonized by arbuscular mycorrhizal fungi. *Mol Plant Microbe Interact* **16**: 903-915
- Hummel J, Strehmel N, Selbig J, Walther D, Kopka J** (2010) Decision tree supported substructure prediction of metabolites from GC-MS profiles. *Metabolomics* **6**: 322-333

- Isayenkov S, Fester T, Hause B** (2004) Rapid determination of fungal colonization and arbuscule formation in roots of *Medicago truncatula* using real-time (RT) PCR. *J Plant Physiol* **161**: 1379-1383
- Jakobsen I** (1995) Transport of phosphorus and carbon in VA mycorrhizas. *In* A Varma, B Hock, eds, *Mycorrhiza*. Springer Berlin Heidelberg, pp 297-324
- Johanson U, Gustavsson S** (2002) A new subfamily of major intrinsic proteins in plants. *Mol Biol Evol* **19**: 456-461
- Kakar K, Wandrey M, Czechowski T, Gaertner T, Scheible WR, Stitt M, Torres-Jerez I, Xiao Y, Redman JC, Wu HC, Cheung F, Town CD, Udvardi MK** (2008) A community resource for high-throughput quantitative RT-PCR analysis of transcription factor gene expression in *Medicago truncatula*. *Plant Methods* **4**: 18
- Karimi M, Inze D, Depicker A** (2002) GATEWAY vectors for Agrobacterium-mediated plant transformation. *Trends Plant Sci* **7**: 193-195
- Kiers ET, Duhamel M, Beesetty Y, Mensah JA, Franken O, Verbruggen E, Fellbaum CR, Kowalchuk GA, Hart MM, Bago A, Palmer TM, West SA, Vandenkoornhuysen P, Jansa J, Bucking H** (2011) Reciprocal rewards stabilize cooperation in the mycorrhizal symbiosis. *Science* **333**: 880-882
- Kobae Y, Tamura Y, Takai S, Banba M, Hata S** (2010) Localized expression of arbuscular mycorrhiza-inducible ammonium transporters in soybean. *Plant Cell Physiol* **51**: 1411-1415
- Koegel S, Ait Lahmidi N, Arnould C, Chatagnier O, Walder F, Ineichen K, Boller T, Wipf D, Wiemken A, Courty PE** (2013) The family of ammonium transporters (AMT) in *Sorghum bicolor*: two AMT members are induced locally, but not systemically in roots colonized by arbuscular mycorrhizal fungi. *New Phytol* **198**: 853-865
- Kopka J, Schauer N, Krueger S, Birkemeyer C, Usadel B, Bergmuller E, Dormann P, Weckwerth W, Gibon Y, Stitt M, Willmitzer L, Fernie AR, Steinhauser D** (2005) GMD@CSB.DB: the Golm Metabolome Database. *Bioinformatics* **21**: 1635-1638
- Krüger M, Krüger C, Walker C, Stockinger H, Schussler A** (2012) Phylogenetic reference data for systematics and phylotaxonomy of arbuscular mycorrhizal fungi from phylum to species level. *New Phytol* **193**: 970-984
- Lam HM, Coschigano K, Schultz C, Melo-Oliveira R, Tjaden G, Oliveira I, Ngai N, Hsieh MH, Coruzzi G** (1995) Use of Arabidopsis mutants and genes to study amide amino acid biosynthesis. *Plant Cell* **7**: 887-898
- Lam HM, Coschigano KT, Oliveira IC, Melo-Oliveira R, Coruzzi GM** (1996) The molecular-genetics of nitrogen assimilation into amino acids in higher plants. *Annu Rev Plant Physiol Plant Mol Biol* **47**: 569-593
- Langmead B, Trapnell C, Pop M, Salzberg SL** (2009) Ultrafast and memory-efficient alignment of short DNA sequences to the human genome. *Genome Biol* **10**: R25
- Li B, Dewey CN** (2011) RSEM: accurate transcript quantification from RNA-Seq data with or without a reference genome. *BMC Bioinformatics* **12**: 323
- Li T, Hu YJ, Hao ZP, Li H, Wang YS, Chen BD** (2013) First cloning and characterization of two functional aquaporin genes from an arbuscular mycorrhizal fungus *Glomus intraradices*. *New Phytol* **197**: 617-630

- Lopez-Pedrosa A, Gonzalez-Guerrero M, Valderas A, Azcon-Aguilar C, Ferrol N** (2006) GintAMT1 encodes a functional high-affinity ammonium transporter that is expressed in the extraradical mycelium of *Glomus intraradices*. *Fungal Genet Biol* **43**: 102-110
- Luedemann A, Strassburg K, Erban A, Kopka J** (2008) TagFinder for the quantitative analysis of gas chromatography--mass spectrometry (GC-MS)-based metabolite profiling experiments. *Bioinformatics* **24**: 732-737
- Maldonado-Mendoza IE, Dewbre GR, Harrison MJ** (2001) A phosphate transporter gene from the extra-radical mycelium of an arbuscular mycorrhizal fungus *Glomus intraradices* is regulated in response to phosphate in the environment. *Mol Plant Microbe Interact* **14**: 1140-1148
- Marleau J, Dalpe Y, St-Arnaud M, Hijri M** (2011) Spore development and nuclear inheritance in arbuscular mycorrhizal fungi. *BMC Evol Biol* **11**: 51
- Marschner H** (1995) Mineral nutrition of higher plants, Ed 2. Academic Press, London
- Marschner H, Dell B** (1994) Nutrient uptake in mycorrhizal symbiosis. *Plant and Soil* **159**: 89-102
- Martin F, Gianinazzi-Pearson V, Hijri M, Lammers P, Requena N, Sanders IR, Shachar-Hill Y, Shapiro H, Tuskan GA, Young JP** (2008) The long hard road to a completed *Glomus intraradices* genome. *New Phytol* **180**: 747-750
- Moreau S, Verdenaud M, Ott T, Letort S, de Billy F, Niebel A, Gouzy J, de Carvalho-Niebel F, Gamas P** (2011) Transcription reprogramming during root nodule development in *Medicago truncatula*. *PLoS One* **6**: e16463
- Nakagawa T, Suzuki T, Murata S, Nakamura S, Hino T, Maeo K, Tabata R, Kawai T, Tanaka K, Niwa Y, Watanabe Y, Nakamura K, Kimura T, Ishiguro S** (2007) Improved Gateway binary vectors: high-performance vectors for creation of fusion constructs in transgenic analysis of plants. *Biosci Biotechnol Biochem* **71**: 2095-2100
- Nelson BK, Cai X, Nebenfuhr A** (2007) A multicolored set of in vivo organelle markers for co-localization studies in Arabidopsis and other plants. *Plant J* **51**: 1126-1136
- Norholm MH, Nour-Eldin HH, Brodersen P, Mundy J, Halkier BA** (2006) Expression of the Arabidopsis high-affinity hexose transporter STP13 correlates with programmed cell death. *FEBS Lett* **580**: 2381-2387
- Nowara D, Gay A, Lacomme C, Shaw J, Ridout C, Douchkov D, Hensel G, Kumlehn J, Schweizer P** (2010) HIGS: host-induced gene silencing in the obligate biotrophic fungal pathogen *Blumeria graminis*. *Plant Cell* **22**: 3130-3141
- Oehl F, Sieverding E, Ineichen K, Mader P, Boller T, Wiemken A** (2003) Impact of land use intensity on the species diversity of arbuscular mycorrhizal fungi in agroecosystems of Central Europe. *Appl Environ Microbiol* **69**: 2816-2824
- Parniske M** (2008) Arbuscular mycorrhiza: the mother of plant root endosymbioses. *Nat Rev Microbiol* **6**: 763-775
- Perez-Tienda J, Testillano PS, Balestrini R, Fiorilli V, Azcon-Aguilar C, Ferrol N** (2011) GintAMT2, a new member of the ammonium transporter family in the arbuscular mycorrhizal fungus *Glomus intraradices*. *Fungal Genet Biol* **48**: 1044-1055
- Phillips JM, Hayman DS** (1970) Improved procedures for clearing roots and staining parasitic and vesicular-arbuscular mycorrhizal fungi for rapid assessment of infection. *Transactions of the British Mycological Society* **55**: 157-160

- Pumplin N, Harrison MJ** (2009) Live-cell imaging reveals periarbuscular membrane domains and organelle location in *Medicago truncatula* roots during arbuscular mycorrhizal symbiosis. *Plant Physiol* **151**: 809-819
- Quandt HJ, Puehler A, I. B** (1993) Transgenic root nodules of *Vicia hirsuta*: A fast and efficient system for the study of gene expression in indeterminate-type nodules. *Molecular Plant-Microbe interactions* **6**: 699-706
- Rea PA** (2007) Plant ATP-binding cassette transporters. *Annu Rev Plant Biol* **58**: 347-375
- Reinders A, Sivitz AB, Starker CG, Gantt JS, Ward JM** (2008) Functional analysis of LjSUT4, a vacuolar sucrose transporter from *Lotus japonicus*. *Plant Mol Biol* **68**: 289-299
- Reinert A** (2012) Identifizierung und funktionelle Charakterisierung von für die arbuskuläre Mykorrhizasymbiose spezifischen Genen in *Medicago truncatula*. Dissertation, University of Potsdam
- Ryan MH, Tibbett M, Edmonds-Tibbett T, Suriyagoda LD, Lambers H, Cawthray GR, Pang J** (2012) Carbon trading for phosphorus gain: the balance between rhizosphere carboxylates and arbuscular mycorrhizal symbiosis in plant phosphorus acquisition. *Plant Cell Environ* **35**: 2170-2180
- Saeed AI, Bhagabati NK, Braisted JC, Liang W, Sharov V, Howe EA, Li J, Thiagarajan M, White JA, Quackenbush J** (2006) TM4 microarray software suite. *Methods Enzymol* **411**: 134-193
- Saeed AI, Sharov V, White J, Li J, Liang W, Bhagabati N, Braisted J, Klapa M, Currier T, Thiagarajan M, Sturn A, Snuffin M, Rezantsev A, Popov D, Ryltsov A, Kostukovich E, Borisovsky I, Liu Z, Vinsavich A, Trush V, Quackenbush J** (2003) TM4: a free, open-source system for microarray data management and analysis. *Biotechniques* **34**: 374-378
- Sanchez DH, Schwabe F, Erban A, Udvardi MK, Kopka J** (2012) Comparative metabolomics of drought acclimation in model and forage legumes. *Plant Cell Environ* **35**: 136-149
- Schaarschmidt S, Roitsch T, Hause B** (2006) Arbuscular mycorrhiza induces gene expression of the apoplastic invertase LIN6 in tomato (*Lycopersicon esculentum*) roots. *J Exp Bot* **57**: 4015-4023
- Schauer N, Steinhauser D, Strelkov S, Schomburg D, Allison G, Moritz T, Lundgren K, Roessner-Tunali U, Forbes MG, Willmitzer L, Fernie AR, Kopka J** (2005) GC-MS libraries for the rapid identification of metabolites in complex biological samples. *FEBS Lett* **579**: 1332-1337
- Schliemann W, Ammer C, Strack D** (2008) Metabolite profiling of mycorrhizal roots of *Medicago truncatula*. *Phytochemistry* **69**: 112-146
- Schubert A, Allara P, Morte A** (2003) Cleavage of sucrose in roots of soybean (*Glycine max*) colonized by an arbuscular mycorrhizal fungus. *New Phytologist* **161**: 495-501
- Schubert A, Wyss P, Wiemken A** (1992) Occurrence of trehalose in vesicular-arbuscular mycorrhizal fungi and in mycorrhizal roots. *Journal of Plant Physiology* **140**: 41-45
- Schüßler A, Schwarzott D, Walker C** (2001) A new fungal phylum, the Glomeromycota: phylogeny and evolution. *Mycol Res* **105**: 1413-1421
- Schwer CS, Frossard E, Jansa J** (2011) Phosphate transporters as functional markers of mycorrhizal P uptake? unpublished
- Seigler DS** (1995) Shicimic acid pathway. *In* Plant secondary metabolism. Kluwer Academic Publishers, USA, pp 94-105

- Shachar-Hill Y, Pfeffer PE, Douds D, Osman SF, Doner LW, Ratcliffe RG** (1995) Partitioning of Intermediary Carbon Metabolism in Vesicular-Arbuscular Mycorrhizal Leek. *Plant Physiol* **108**: 7-15
- Sieh D, Watanabe M, Devers EA, Brueckner F, Hoefgen R, Krajinski F** (2013) The arbuscular mycorrhizal symbiosis influences sulfur starvation responses of *Medicago truncatula*. *New Phytol* **197**: 606-616
- Smith FA, Read DJ** (2008) Mycorrhizal symbiosis. Academic Press, New York
- Smith SE, Read DJ** (2003) Mycorrhizal symbiosis, Ed 2. Academic Press, London, pp 11-3145
- Smith SE, Smith FA** (2012) Fresh perspectives on the roles of arbuscular mycorrhizal fungi in plant nutrition and growth. *Mycologia* **104**: 1-13
- Stockinger H, Walker C, Schussler A** (2009) '*Glomus intraradices* DAOM197198', a model fungus in arbuscular mycorrhiza research, is not *Glomus intraradices*. *New Phytol* **183**: 1176-1187
- Strack D, Fester T, Hause B, Schliemann W, Walter MH** (2003) Arbuscular mycorrhiza: biological, chemical, and molecular aspects. *J Chem Ecol* **29**: 1955-1979
- Strack D, Fester T, Hause B, Walter MH** (2001) Die arbuskuläre Mykorrhiza. *Biologie in unserer Zeit* **5**: 286- 295
- Strehmel N, Hummel J, Erban A, Strassburg K, Kopka J** (2008) Retention index thresholds for compound matching in GC-MS metabolite profiling. *J Chromatogr B Analyt Technol Biomed Life Sci* **871**: 182-190
- Tadege M, Wen J, He J, Tu H, Kwak Y, Eschstruth A, Cayrel A, Endre G, Zhao PX, Chabaud M, Ratet P, Mysore KS** (2008) Large-scale insertional mutagenesis using the *Tnt1* retrotransposon in the model legume *Medicago truncatula*. *Plant J* **54**: 335-347
- Tejeda-Sartorius M, Martinez de la Vega O, Delano-Frier JP** (2008) Jasmonic acid influences mycorrhizal colonization in tomato plants by modifying the expression of genes involved in carbohydrate partitioning. *Physiol Plant* **133**: 339-353
- Tian C, Kasiborski B, Koul R, Lammers PJ, Bucking H, Shachar-Hill Y** (2010) Regulation of the nitrogen transfer pathway in the arbuscular mycorrhizal symbiosis: gene characterization and the coordination of expression with nitrogen flux. *Plant Physiol* **153**: 1175-1187
- Tisserant E, Kohler A, Dozolme-Seddas P, Balestrini R, Benabdellah K, Colard A, Croll D, Da Silva C, Gomez SK, Koul R, Ferrol N, Fiorilli V, Formey D, Franken P, Helber N, Hijri M, Lanfranco L, Lindquist E, Liu Y, Malbreil M, Morin E, Poulain J, Shapiro H, van Tuinen D, Waschke A, Azcon-Aguilar C, Becard G, Bonfante P, Harrison MJ, Kuster H, Lammers P, Paszkowski U, Requena N, Rensing SA, Roux C, Sanders IR, Shachar-Hill Y, Tuskan G, Young JP, Gianinazzi-Pearson V, Martin F** (2012) The transcriptome of the arbuscular mycorrhizal fungus *Glomus intraradices* (DAOM 197198) reveals functional tradeoffs in an obligate symbiont. *New Phytol* **193**: 755-769
- Trouvelot A, Kough JL, Gianinazzi-Pearson V** (1986) Mesure du taux de mycorrhization VA d'un système racinaire. Recherche des méthodes d'estimation ayant une signification fonctionnelle. *In* V Gianinazzi-Pearson, S Gianinazzi, eds, *The Mycorrhizae : Physiology and Genetic*. INRA Presse, Paris, pp 217-221
- Usadel B, Poree F, Nagel A, Lohse M, Czedik-Eysenberg A, Stitt M** (2009) A guide to using MapMan to visualize and compare Omics data in plants: a case study in the crop species, Maize. *Plant Cell Environ* **32**: 1211-1229

- Walder F, Niemann H, Natarajan M, Lehmann MF, Boller T, Wiemken A** (2012) Mycorrhizal networks: common goods of plants shared under unequal terms of trade. *Plant Physiol* **159**: 789-797
- Walker TS, Bais HP, Grotewold E, Vivanco JM** (2003) Root exudation and rhizosphere biology. *Plant Physiology* **132**: 44-51
- Wang H, Qi M, Cutler AJ** (1993) A simple method of preparing plant samples for PCR. *Nucleic Acids Res* **21**: 4153-4154
- Wright DP, Read DJ, Scholes JD** (1998) Mycorrhizal sink strength influences whole plant carbon balance of *Trifolium repens* L. *Plant Cell & Environment* **21**: 881-891
- Zhang Q, Blaylock LA, Harrison MJ** (2010) Two *Medicago truncatula* half-ABC transporters are essential for arbuscule development in arbuscular mycorrhizal symbiosis. *Plant Cell* **22**: 1483-1497

7 SUPPLEMENTARY

7.1 Oligonucleotides used in this study

Table S1.1: Promoter amplification of AM-regulated *M. truncatula* transporter candidate genes.

Name	Binds to promoter region of (Mt3.5)	Sequenz 5' – 3'	Reference
pMtNRT1-fwd	Medtr2g017750.1	CACCTAAAAGTGTACCACATATCCAGCTG	This work
pMtNRT1-rev	Medtr2g017750.1	GGACAAAAATGAAAAAAAAAGGACATAATAAGC	This work
pMtPTR1-fwd	Medtr8g087780.1	CACCTGTTGGTGGTTTCACTTCAAAC	This work
pMtPTR1-rev	Medtr8g087780.1	TGTTCTTGAGAAAAATGTATTGAGTG	This work
pMtNIP1-fwd	Medtr8g087710.1	CACCGCCCGATTACGTTGTTTGTGGTTC	This work
pMtNIP1-rev	Medtr8g087710.1	AAGTGATAGAGAACAAGGAACTATTTAG	This work
pMtABC15-fwd	Medtr8g022270.1	CACCTCTGGCCAAAAATAGGAAGAACATT	This work
pMtABC15-rev	Medtr8g022270.1	GGCTAGCTAGCTACCTAGCAG	This work
pMtPTR4-fwd	Medtr8g087810.1	CACCACATCTTACCATTACCGGCAA	This work
pMtPTR4-rev	Medtr8g087810.1	AATATTAATAATTAATTAAGTAGCTTGT	This work
pMtDIT2-fwd	Medtr2g009220.1	CACCGAGCCATTTGATTATGATGGTG	This work
pMtDIT2-rev	Medtr2g009220.1	TGGAACAACAGAACAACAACAATTG	This work
pMtNIP4-fwd	Medtr5g063930.1	CACCCTCGTATGTTATATGATTTTATTGT	This work
pMtNIP4-rev	Medtr5g063930.1	GTTATAGGTTGAATGCCAAAC	This work
pMtPTR3-fwd	Medtr7g098040.1	CACCTCGCCGGAAATTTTCTTAATG	This work
pMtPTR3-rev	Medtr7g098040.1	GATGCTGGACAAGAAAACTATT	This work
pMtSUT4-1-fwd	Medtr5g067470.1	CACCGTAGTAAATTAATAAGTGCTTATAA	This work
pMtSUT4-1-rev	Medtr5g067470.1	CGTGATGCCGACGCCGAAT	This work
pMtHXT1-fwd	Medtr1g104780.1	CACCTCCCCAATACAATTTTGTGATTC	This work
pMtHXT1-rev	Medtr1g104780.1	GGTTAGTTATTTCTGTCTTCAAC	This work
pMtPGP18-fwd	Medtr3g086430.1	CACCTGAAAAAGTGAGTATTGAGTGAC	This work
pMtPGP18-rev	Medtr3g086430.1	ATTCTTAGCAGCACAGCATG	This work

Table S1.2: qRT-PCR

Name	Binds to (Mt3.5)/ (Ri contig ID)	Sequence 5' – 3'	Reference
MtPt4-fwd		CAAGAAAGATTAGACGCGCAA	Harrison <i>et al.</i> (2002)
MtPt4-rev		GTTCCGTCACCAAGAACGTG	Harrison <i>et al.</i> (2002)
Ef1alpha-fwd	Medtr6g021800.1	GACAAGCGTGTGATCGAGAGATT	Kakar <i>et al.</i> (2008)
EF1alpha-rev	Medtr6g021800.1	TTTCACGCTCAGCCTTAAGCT	Kakar <i>et al.</i> (2008)

Pdf2-fwd	TC107161	GTGTTTTGCTTCCGCCGTT	Kakar <i>et al.</i> (2008)
Pdf2-rev	TC107161	CCAAATCTTGCTCCCTCATCTG	Kakar <i>et al.</i> (2008)
GapDH-fwd	Medtr3g085850.1	TGCCTACCGTCGATGTTTCAGT	Kakar <i>et al.</i> (2008)
GapDH-rev	Medtr3g085850.1	TTGCCCTCTGATTCTCTCTTG	Kakar <i>et al.</i> (2008)
UbiExon-fwd	Medtr3g091400.1	GCAGATAGACACGCTGGGA	Kakar <i>et al.</i> (2008)
UbiExon-rev	Medtr3g091400.1	AACTCTGGGCAGGCAATAA	Kakar <i>et al.</i> (2008)
UbiIntron-fwd		GTCCTCTAAGGTTTAATGAACCGG	
UbiIntron-rev		GAAAGACACAGCCAAGTTGCAC	
RiRNA-fwd		GTATGCCTGTTTGAGGGTCAGTATT	Isayenkov <i>et al.</i> (2004)
RirRNA-rev		AAACTCCGGAACGTCCTAAAGAG	Isayenkov <i>et al.</i> (2004)
RiTef-fwd		TGTTGCTTTCGTCCCAAT	Helber <i>et al.</i> (2011)
RiTef-rev		GGTTTATCGGTAGGTCGA	Helber <i>et al.</i> (2011)
qRT_MtNRT1-fwd	Medtr2g017750.1	TGCTTTGCTCATGCTAGTCACACTTGG	This work
qRT_MtNRT1-rev	Medtr2g017750.1	AGTTGGTGAGCATGTTAGCAGCATCTT	This work
qRT_MtABC15-fwd	Medtr8g022270.1	TGACGACCGTTCATGGCAGGG	This work
qRT_MtABC15-rev	Medtr8g022270.1	CGATTGGCGAAACACGCGGC	This work
qRT_MtNIP1-fwd	Medtr8g087710.1	ATGGCTAATGATAATTCAGCAAGAA	This work
qRT_MtNIP1-rev	Medtr8g087710.1	CTTTTGCAAGAAAGGGACAGAGACA	This work
qRT_MtPTR4-fwd	Medtr8g087810.1	TGCTCGTACTAGGGGCGTTTGC	This work
qRT_MtPTR4-rev	Medtr8g087810.1	ACCATGTTAGCTGCATCTGCTAGTTC	This work
qRT_MtMPT1-fwd	Medtr7g083790.1	TGTCAGTCACCCTGCAGACACCT	This work
qRT_MtMPT1-rev	Medtr7g083790.1	GCCGAGTCTCGCCACAACC	This work
qRT_MtDIT2-fwd	Medtr2g009220.1	TGCTGTATACTATGGAGCTGGCTATGT	This work
qRT_MtDIT2-rev	Medtr2g009220.1	AGAGCCAACCTCTCCCAGATGA	This work
qRT_MtAAP1-fwd	Mtr.44555.1.s1_at	TCAGCTTGGGCTACACCTTCCTTGT	This work
qRT_MtAAP1-rev	Mtr.44555.1.s1_at	GGCAGTGAAGGCACTGAAGACCC	This work
qRT_MtPGP18-fwd	Medtr3g086430.1	TGCAGAAAGACAACTTCGCGGATG	This work
qRT_MtPGP18-rev	Medtr3g086430.1	TGGTGGCAATTACTTGAAGGTTGT	This work
qRT_MtAMT2-fwd	Medtr8g095040.1	CCGGTAGCATACCAAGCATGGACAAG	This work
qRT_MtAMT2-rev	Medtr8g095040.1	TGGCATGCTTTGAATTCCAACAAGGGT	This work
RiMFS2-qRT-fwd	comp2270_c0	TAATATCCAAGCAGATGCGGGTAC	This work
RiMFS2-qRT-rev	comp2270_c0	GTGCTTGCAAATATAACAAGTCA	This work
RiGLCT1-qRT-fwd	comp2866_c0	AGAAACCGAAGATTTGGGGCGTA	This work
RiGLCT1-qRT-rev	comp2866_c0	TTCTCCTCTCCTCTTTTGTACC	This work
RiMFS3-qRT-fwd	comp4884_c0	TGGGAACGATCTGTTTTCAATTC	This work
RiMFS3-qRT-rev	comp4884_c0	ACCATTCCATATTTGCCTCCATCT	This work
RiMFS1-qRT-fwd	comp8571_c0	GTTATACTCCTGAAGTTTTGGGACT	This work
RiMFS1-qRT-rev	comp8571_c0	TGCCTCCTCTTGTCTATTGGT	This work

RiSUT1-qRT-fwd	comp11677_c0	ACACAACCTGGATTTACAACAGCT	This work
RiSUT1-qRT-rev	comp11677_c0	ACACAAAAGTACTCAGCAAAAGCT	This work
RiYVC1-qRT-fwd	comp19601_c0	GGACAATGATGCTAAGCGATTATGA	This work
RiYVC1-qRT-rev	comp19601_c0	TGGTACAGGGAAAGAACTCCTCGT	This work
RiPT-qRT-fwd	comp29_c0	TCACTATTATGGGAACCGTTCCTG	This work
RiPT-qRT-rev	comp29_c0	ACTTCCCCTGGAACGATGAATGT	This work

Table S 1.3: MtHxt1 Tnt1 screening

Name	Binds to (Mt3.5)	Sequence 5' – 3'	Reference
NF3151HXT1-fwd (P1)	Medtr1g104780.1	CAGTGGATAAACTTGGTCGTCG	This work
NF3151HXT1-rev (P2)	Medtr1g104780.1	CTCATCTCAATATAATCATTTTCAAC	This work
Tnt1-R2 (P3)	<i>Tnt1</i>	TCAACAAAGTTGGCTACCAATCCAACA AGGA	Dr. Igor Kryvoruchko (Ardmore, OK, USA)
Tnt1-F2 (P4)	<i>Tnt1</i>	TCTTGTTAATTACCGTATCTCGGTGCT ACA	Dr. Igor Kryvoruchko (Ardmore, OK, USA)

Table S 1.4: CDS amplification of *M. truncatula* sugar transporter genes.

Name	Binds to (Mt3.5)	Sequence 5' – 3'	Reference
MtSUT4-fwd	Medtr5g067470.1	CACCATGCCGAATCCCACTACAACA	This work
MtSUT4NoStop-rev	Medtr5g067470.1	TATGCGGACTCGAGGCTTTTG	This work
MtSUT4-rev	Medtr5g067470.1	TCATATGCGGACTCGAGGCTTTTG	This work
MtMSS1-AttB1-fwd	Medtr1g104780.1	GGGGACAAGTTTGTACAAAAAAGCAG GCTATGACGGGAGGAGGCTTCAGC	This work
MtMSS1-fwd	Medtr1g104780.1	CACCATGACGGGAGGAGGCTTC	This work
MtMSS1NoStop-rev	Medtr1g104780.1	CAACTGAGAAACAAGATCATTTTC	This work
MtMSS1-AttB2-rev	Medtr1g104780.1	GGGGACCACTTTGTACAAGAAAGCTG GGTTTACAACCTGAGAAACAAGATCATT	This work

Table S 1.5: *R. irregularis* full CDS amplification

Name	Binds to (contig ID)	Sequence 5' – 3'	Reference
RiMFS2-CDS-fwd	comp2270_c0	ATGAGTAACAAGAATAATGCCG	This work
RiMFS2-CDS-rev	comp2270_c0	TTAGGCCATGCTTATAGCTTCG	This work
RiMFS1-CDS-fwd	comp8571_c0	ATGAATTCTAAAAAAATTTTCGTTC	This work
RiMFS1-CDS-rev	comp8571_c0	TTATGCCTGCCTTCCTCTTGT	This work
RiSUT1-CDS-fwd	comp11677_c0	ATGGAGGAGCTTAATCAACC	This work
RiSUT1-CDS-rev	comp11677_c0	TTAAATATCTTTTATGGTAACCGC	This work
RiMFS3-CDS-fwd	comp4884_c0	ATGGCTACACGATCTTC	This work
RiMFS3-CDS-rev	comp4884_c0	TTAATTAATATAATTAAGAATAACAC	This work

Table S 1.6: Contol/ sequencing primer

Name	Binds to (Mt3.5)	Sequence 5' – 3'	Reference
Donr-F	pENTR/D-TOPO, pDONR201 (Invitrogen)	TCGCGTTAACGCTAGCATG	LGC Genomics
SeqL-E	pENTR/D-TOPO, pDONR201 (Invitrogen)	GTTGAATATGGCTCATAACAC	LGC Genomics
M13-24F	pCR2.1 (Invitrogen)	CCAGGGTTTTCCCAGTCACG	LGC Genomics
M13-24R	pCR2.1 (Invitrogen)	CGGATAACAATTCACACAGG	LGC Genomics
M13 fwd (-20)	pCR2.1 (Invitrogen)	GTAAACGACGGCCAG	Invitrogen
M14 rev	pCR2.1 (Invitrogen)	CAG GAA ACA GCT ATG AC	Invitrogen
293 RNAi_Intron_Fwd	pK7GWIWG2 (I)	AGAAAGCCGTAAGAAGAGGC	Dr. Emanuel Devers, ETH Zürich, Switzerland
294 RNAi_Intron_Rev	pK7GWIWG2 (I)	TTAACGTGTTTGCAGGTCAGC	Dr. Emanuel Devers, ETH Zürich, Switzerland
1346 pK7WseqFwd	pK7GWIWG2 (I)	TGCGGACTCTAGCATGGC	This work
RNAi_pMtPT4-fwd	316p9RFP-PT4-RNAi	TCTCCTAAGCTAACTTAGGACTAAACGTC ACATTG	Silvia Bortfeld, MPI- MP Golm
RNA_Tnos-rev	316p9RFP-PT4-RNAi	ATAGGCGTCTCGCATATCTCATTAAAGC AGGG	Silvia Bortfeld, MPI- MP Golm

7.2 *M. truncatula* transporter genes

Table S 2.1: Identifiers and *A. thaliana* homologs of AM-regulated *M. truncatula* transporter candidate genes.

Annotation	IMGAG ID Mt3.0	IMGAG ID Mt3.5	Affymetix GeneChip	Best <i>A. thaliana</i> homolog (% nucleotide identity)
Copper transporter MtCot			mtr.37110.1.s1_at	
Low-affinity nitrate transporter, MtNRT1	Medtr2g021270.1	Medtr2g017750.1	mtr.36985.1.s1_at	AtNRT1;2 (41 %)
Mitochondrial phosphate transporter, MtMPT1	Medtr7g096810.1	Medtr7g083790.1	mtr.39705.1.s1_at	mitochondrial phosphate transp. (78 %)
Dicarboxylate transporter, MtDIT2	Medtr2g009260.1	Medtr2g009220.1	mtr.13956.1.s1_at	AtDIT2;1 (87 %)
Amino acid transporter, MtAAP1			mtr.44555.1.s1_at	amino acid permease-like protein (82 %)
Ammonium transporter, MtAMT2	Medtr4g144250.1	Medtr8g095040.1	mtr.25576.1.s1_at	AtAMT2 (69 %)
Nucleobase-ascorbate transporter MtNAT2	Medtr4g134900.1	Medtr8g086520.1	mtr.28814.1.s1_at	AtNAT2 (86 %)
Sucrose/H ⁺ symporter MtSUT4	Medtr5g076420.1	Medtr5g067470.1	mtr.21349.1.s1_s_at	AtSUT4 (69 %)
Hexose transporter MtHXT1	Medtr1g132750.1	Medtr1g104780.1	mtr.433.1.s1_at	AtSTP13 (77 %)
Oligopeptide transporter, MtPTR1	Medtr4g136300.1	Medtr8g087780.1	mtr.17764.1.s1_at	AtPTR1 (39 %)
Oligopeptide transporter, MtPTR3	Medtr7g116510.1	Medtr7g098040.1	mtr.37112.1.s1_at	AtPTR3-B (59 %)
Oligopeptide transporter, MtPTR4	Medtr4g136330.1	Medtr8g087810.1	mtr.46057.1.s1_at	H ⁺ -dependent oligopeptide transport (POT) family protein (42 %)
ABC transporter/MDR, MtABC15	Medtr8g025810.1	Medtr8g022270.1	mtr.46524.1.s1_at	AtABC15 (61 %)

ABC transporter/ MDR, MtPGP18	Medtr3g102650.1	Medtr3g086430.1	mtr.1103.1.s1_at	P-Glycoprotein (69 %)
Major intrinsic protein, MtNIP1	Medtr4g136190.1	Medtr8g087710.1	mtr.37525.1.s1_at	AtNIP1;2 (71 %)
Major intrinsic protein, MtNIP4	Medtr5g072770.1	Medtr5g063930.1	mtr.7596.1.s1_at	AtNIP4;2 (48 %)

Table S 2.1: Identifiers of AM-regulated *M truncatula* genes associated with carbohydrate metabolism

Annotation	Affymetix GeneChip	IMGAG ID Mt3.0	IMGAG ID Mt3.5
Fructose-1,6-bisphosphatase	Mtr.22592.1.S1_at	Medtr2g008160.1	Medtr2g008030
Glucose-1-phosphate adenyltransferase	Mtr.22751.1.S1_at	Medtr7g134380.1	Medtr7g111020
Alpha-amylase	Mtr.18116.1.S1_at	Medtr3g150290.1	Medtr3g099510
Neutral invertase, putative	Mtr.40256.1.S1_at	Medtr1g122200.1	Medtr1g096140
Neutral invertase, putative	Mtr.18500.1.S1_at	Medtr1g121820.1	Medtr1g096110
Vacuolar invertase	Mtr.43881.1.S1_at	Medtr8g106250.1	Medtr4g101630
Sucrose synthase, SUS6	Mtr.43776.1.S1_at	Medtr6g090340.1	Medtr6g081120

7.2.1 *hxt1* phenotype

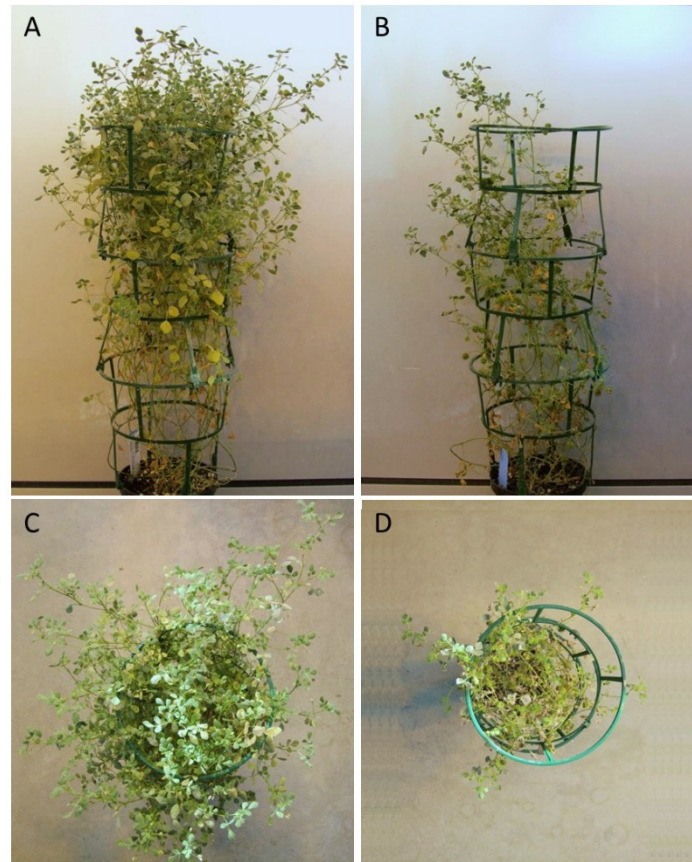


Figure S 1: Biomass production of *hxt1* and WT *M. truncatula tnt1* insertion plants. 12 weeks-old non-mycorrhizal plants, P-fertilized. A, C: *hxt1*; B, D: WT.

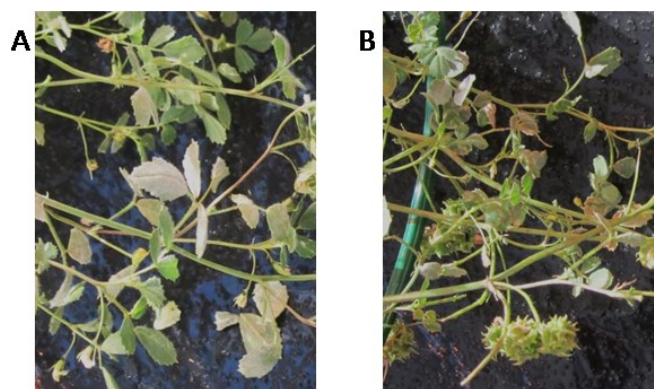


Figure S 2: Flowers and seed Pods on *hxt1* and WT *M. truncatula tnt1* insertion plants. 12 weeks-old non-mycorrhizal plants, P-fertilized. A: *hxt1*; B: WT.

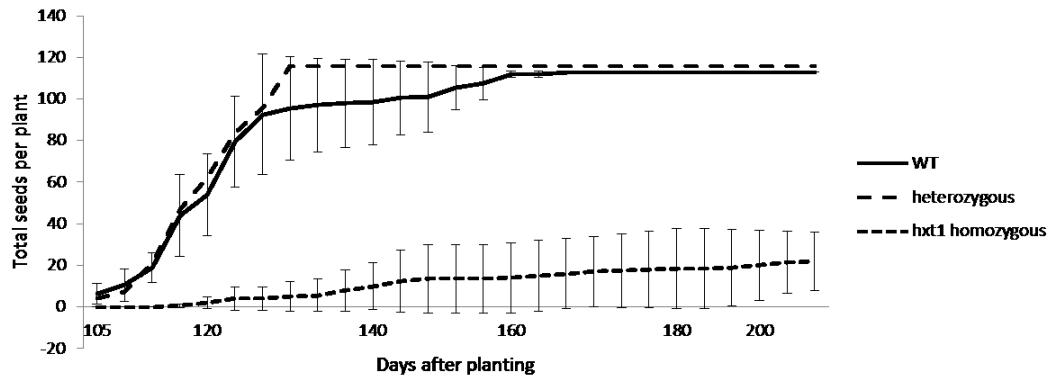


Figure S3: Seed production of *M. truncatula* *hxt1*, WT, and heterozygous plants.

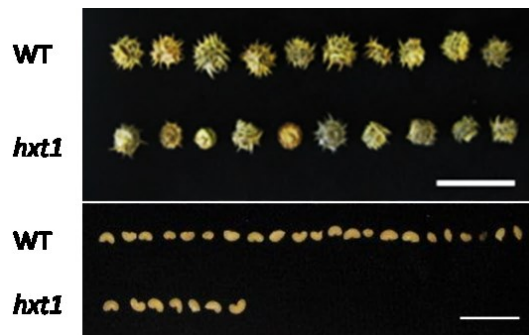


Figure S4: Pods and seeds of *M. truncatula* *Mthxt1 Tnt1* knock-out and WT plants. The seeds shown are those removed from the pods above. Scale bar: 2 cm.

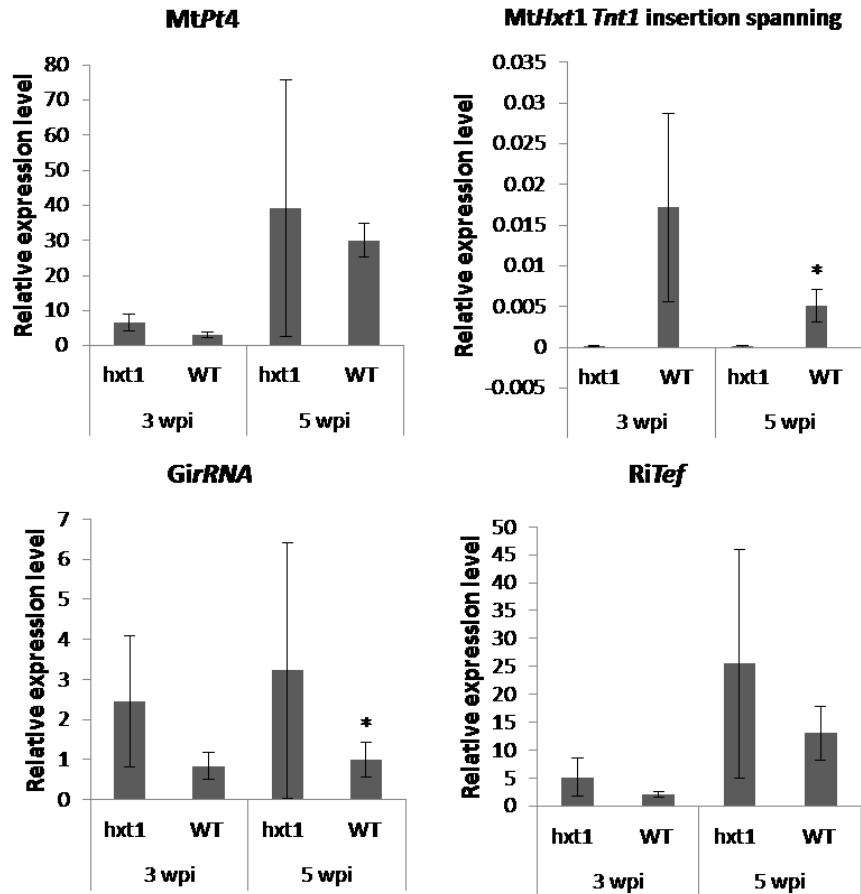


Figure S 5: Relative expression levels (2^{-dCt} values) of AM marker genes in *M. truncatula* *hxt1* and WT roots determined by qRT-PCR. Roots were harvested 3 and 5 wpi with *R. irregularis*. A housekeeping gene index (*UbiExon*, *Pdf2* and *EF1 α*) was used for normalization. Values shown are mean \pm standard deviation of two to four biological replicates with two technical replicates of each PCR reaction. *: p-value \leq 0.05.

7.3 *R. irregularis* sequencing

Table S3.1: Known *R. irregularis* genes with at least one read in one of the samples in the Illumina sequencing. The raw reads mapping to each gene were normalized to total read amount of each sample, the log₂-fold changes or the ratio of the normalized reads in each sample and the GenBank identifier and annotation are given.

GenBank accession	Description	LFC (arb/ ERM)
AB114298.1	Glomus intraradices GiALP mRNA for alkaline phosphatase, complete cds	-2.65
AF110197.1	Glomus intraradices MYC2 (myc2) mRNA, partial cds	0/4 ^x
AF359112.1	Glomus intraradices phosphate transporter mRNA, complete cds	-6.73
AF420481.1	Glomus intraradices plasma membrane proton ATPase (HA5) mRNA, partial cds	-5.35
AF503447.1	Glomus intraradices glycogen branching enzyme mRNA, complete cds	-4.17
AJ315337.1	Glomus intraradices ORF1	4.90
AJ319763.1	Glomus intraradices partial bip gene for binding protein, sequence 29	0.29/0 ^x
AJ319766.1	Glomus intraradices partial bip gene for binding protein, sequence 20	-3.96
AJ319767.1	Glomus intraradices partial bip gene for binding protein, sequence 42	-3.90
AJ319768.1	Glomus intraradices partial bip gene for binding protein, sequence 44	-4.19
AJ319769.1	Glomus intraradices partial bip gene for binding protein, sequence 36	1.27
AJ319770.1	Glomus intraradices partial bip gene for binding protein, sequence 47	0.22
AJ319771.1	Glomus intraradices partial bip gene for binding protein, sequence 43	-4.08
AJ319772.1	Glomus intraradices partial bip gene for binding protein, sequence 10	0.92
AJ319773.1	Glomus intraradices partial bip gene for binding protein, sequence 45	-3.89
AJ319774.1	Glomus intraradices partial bip gene for binding protein, sequence 56	0.45
AJ319776.1	Glomus intraradices partial bip gene for binding protein, sequence 30	-5.78
AJ319777.1	Glomus intraradices partial bip gene for binding protein, sequence 38	0/5 ^x
AJ574787.1	Glomus intraradices mRNA for zinc transporter 1 (znt1 gene)	0.22
AJ584702.1	Glomus intraradices partial bip1 gene for binding protein	-3.36
AJ584703.1	Glomus intraradices partial bip2 gene for binding protein	-3.94
AJ584704.1	Glomus intraradices partial bip3 pseudogen	0.29/0 ^x
AJ606126.1	Glomus intraradices mitochondrial coxVI gene for cytochrome oxidase subunit VI, isolate DAOM 181 602	-4.25
AJ606127.1	Glomus intraradices mitochondrial coxVI gene for cytochrome oxidase subunit VI, Swiss isolate H	-5.53
AJ717308.1	Glomus intraradices partial atub gene for alpha-tubulin, exons 1-2	-2.82
AJ841805.1	Glomus intraradices mitochondrial partial LSU gene for large subunit ribosomal RNA and LAGLIDADG homing endonuclease, clone 814_1	0/2 ^x
AJ841806.1	Glomus intraradices mitochondrial partial LSU gene for large subunit ribosomal RNA and LAGLIDADG homing endonuclease, clone 814_9	0/3 ^x
AJ841807.1	Glomus intraradices mitochondrial partial LSU gene for large subunit ribosomal RNA and LAGLIDADG homing endonuclease, clone 814_10	0/1 ^x
AJ880327.1	Glomus intraradices mRNA for ammonium transporter 1 (AMT1 gene)	-7.88
AJ973192.1	Glomus intraradices mitochondrial partial lsu gene for large subunit ribosomal RNA and putative LAGLIDADG homing endonuclease, clone 867_5	0-1
AJ973193.1	Glomus intraradices mitochondrial partial lsu gene for large subunit ribosomal RNA and putative LAGLIDADG homing endonuclease, clone 867_6	0/1 ^x
AM040753.1	Glomus intraradices mRNA for metallothionein 1 (nMT1 gene)	-9.33
AM049264.1	Glomus intraradices mRNA for 14-3-3 protein	-2.95
AM118102.1	Glomus intraradices ena1 gene for P-Type II D ATPase, exons 1-9	2.26
AM118103.1	Glomus intraradices ena2 gene for P-type II D ATPase, exons 1-9	3.80/0 ^x
AM118104.1	Glomus intraradices partial ena1 gene for P-type IID ATPase, exons 1-4, isolate C3	1.17/0 ^x

AM118106.1	Glomus intraradices partial ena1 gene for P-type II D ATPase, exons 1-4, isolate C2	2.04/0 ^x
AM118108.1	Glomus intraradices partial ena3 gene for P-Type II D ATPase, exons 1-4, isolate C2	0.58/0 ^x
AM118112.1	Glomus intraradices partial nk1 gene for P-Type IIC ATPase	-6.05
AM118113.1	Glomus intraradices partial nk2 gene for P-type IIC ATPase	0.92
AM118117.1	Glomus intraradices partial pmca1 gene for P-Type II B ATPase	-4.21
AM118121.1	Glomus intraradices partial serca gene for P-type II A ATPase, exons 1-2	-3.96
AM284973.1	Glomus intraradices partial RPB1 pseudogene for RNA polymerase II large subunit, isolate BEG158	-1.19
AM284974.1	Glomus intraradices partial RPB1 gene for RNA polymerase II largest subunit, isolate DAOM197198	-3.36
AM932873.1	Glomus intraradices grx1 gene for glutaredoxin 1, exons 1-4	-4.13
AM947047.1	Glomus intraradices mRNA for Ste12-like transcription factor (ste12 gene), isolate DAOM181602	-4.33
AM947048.1	Glomus intraradices mRNA for Ste12-like transcription factor (ste12 gene), isolate BEG141	-5.61
AM949787.1	Glomus intraradicesm RNA for vitamin B6 biosynthesis protein (PDX gene), culture collection DAOM:197198	-6.42
AM950203.1	Glomus intraradices mitochondrial partial lsu gene for large subunit ribosomal RNA and LAGLIDADG homing endonuclease, clone DCBF1164_5	0/1 ^x
AM950217.1	Glomus intraradices mitochondrial partial lsu gene for large subunit ribosomal RNA and LAGLIDADG homing endonuclease, clone NBh2_2	0/2 ^x
AY033936.1	Glomus intraradices probable acyl-CoA dehydrogenase mRNA, complete cds	-6.64
AY033937.1	Glomus intraradices putative fatty acid CoA ligase mRNA, partial cds	-5.26
AY037894.1	Glomus intraradices phosphate transporter mRNA, partial cds	-9.74
AY326320.1	Glomus intraradices beta tubulin (BTub1) gene, partial cds	0.58/0 ^x
AY326321.1	Glomus intraradices beta tubulin (BTub2) gene, partial cds	0.55
AY326322.1	Glomus intraradices H+ ATPase (HA1) gene, partial cds	-3.23
AY326323.1	Glomus intraradices H+ ATPase (HA2) gene, partial cds	-3.29
AY326324.1	Glomus intraradices H+ ATPase (HA3) gene, partial cds	-2.73
AY326325.1	Glomus intraradices H+ ATPase (HA4) gene, partial cds	-3.34
AY326326.1	Glomus intraradices H+ ATPase (HA5) gene, partial cds	0.29/0 ^x
AY326328.1	Glomus intraradices H+ ATPase (HA7) gene, partial cds	0.58/0 ^x
AY326329.1	Glomus intraradices H+ ATPase (HA8) gene, partial cds	0.58/0 ^x
AY787134.1	Glomus intraradices neutral trehalase (NTH1) mRNA, complete cds	-6.49
AY830086.1	Glomus intraradices trehalose-6-phosphatase (TPS2) mRNA, partial cds	-1.08
DQ063587.1	Glomus intraradices glutamine synthase mRNA, partial cds	-3.99
DQ087527.1	Glomus intraradices Ras2-like protein mRNA, partial cds	-5.20
DQ282611.1	Glomus intraradices isolate AFTOL-ID 845 elongation factor 1-alpha (EF1-alpha) gene, partial cds	-4.37
DQ294603.1	Glomus intraradices isolate AFTOL-ID 845 RNA polymerase II largest subunit (RPB1) gene, partial cds	-2.36
DQ302794.1	Glomus intraradices isolate AFTOL-ID 845 RNA polymerase II second largest subunit (RPB2) gene, partial cds	-4.79
DQ383980.1	Glomus intraradices heat shock protein 60 (hsp60) mRNA, complete cds	-4.09
DQ383981.1	Glomus intraradices heat shock protein 60 (hsp60) gene, complete cds	-4.16
DQ499469.1	Glomus intraradices clone NtGi2 urease accessory protein G mRNA, partial cds	0/4 ^x
EF488828.1	Glomus intraradices DNA binding protein (BP1) mRNA, complete cds	-12.07
EU232637.1	Glomus intraradices isolate DAOM181602 Cu-Zn superoxide dismutase gene, partial cds	0.29/0 ^x
EU232643.1	Glomus intraradices isolate B1 Cu-Zn superoxide dismutase gene, partial cds	0.29/1 ^x
EU232644.1	Glomus intraradices isolate B13 Cu-Zn superoxide dismutase gene, partial cds	0.29/2 ^x
EU232649.1	Glomus intraradices isolate C5 Cu-Zn superoxide dismutase gene, partial cds	0.29/3 ^x
EU232651.1	Glomus intraradices isolate C7 Cu-Zn superoxide dismutase gene, partial cds	0.29/4 ^x
EU232652.1	Glomus intraradices isolate B4 Cu-Zn superoxide dismutase gene, partial cds	0.58/0 ^x

EU281994.1	Glomus intraradices glutamine synthetase (Gln) mRNA, partial cds	-4.97
EU478725.1	Glomus intraradices glucose-6-phosphate dehydrogenase mRNA, partial cds	0/86
EU931681.1	Glomus intraradices AGP-like protein 1 precursor (AGL1) mRNA, complete cds	-7.58
EU931682.1	Glomus intraradices AGP-like protein 2 (AGL2) mRNA, partial cds	0/93 ^x
FJ161948.1	Glomus intraradices germinating spore putative ATP-sulfurylase mRNA, partial cds	1.55
FJ161949.1	Glomus intraradices putative cystathionine gamma-lyase mRNA, partial cds	-3.19
FJ161950.1	Glomus intraradices putative cystathionine beta-synthase mRNA, partial cds	-4.66
FJ174299.1	Glomus intraradices isolate NB102C beta-tubulin (btub) gene, exons 1 through 4 and partial cds	-6.25
FJ554631.1	Glomus intraradices culture-collection MUCL:43194 C-4 sterol methyl oxidase (SMO) mRNA, complete cds	-1.99
FJ861239.1	Glomus intraradices aquaporin 1 (AQP1) mRNA, complete cds	0/21 ^x
FM207964.1	Glomus intraradices mnSOD gene for mitochondrial Mn-superoxide dismutase, exons 1-7	-6.22
FM993985.2	Glomus intraradices mRNA for ammonium transporter 2 (amt2 gene)	-3.14
FR744743.1	Glomus intraradices amt2 gene for ammonium transporter 2, culture collection DAOM 197198	-4.83
GN117614.1	Sequence 510 from Patent WO2009037329	-4.49
GN118668.1	Sequence 1564 from Patent WO2009037329	-6.81
GN119064.1	Sequence 1960 from Patent WO2009037329	-7.99
GN129354.1	Sequence 12250 from Patent WO2009037329	-9.12
GQ249346.1	Glomus intraradices ATP-binding cassette transporter 1 (ABC1) mRNA, complete cds	-7.55
GQ303446.1	Glomus intraradices strain DAOM 225240 mitochondrial F-ATPase beta subunit (atp2) gene, partial cds	-2.78
GQ303447.1	Glomus intraradices strain DAOM 225240 elongation factor 1-alpha (EF1-alpha) gene, partial cds	0/1 ^x
GU111909.1	Glomus intraradices glutamine synthetase 1 mRNA, complete cds	-4.06
GU111910.1	Glomus intraradices glutamine synthetase 2 mRNA, complete cds	-5.21
GU111911.1	Glomus intraradices argininosuccinate synthase mRNA, complete cds	-6.15
GU111912.1	Glomus intraradices ornithine aminotransferase mRNA, complete cds	-4.21
GU111913.1	Glomus intraradices arginase mRNA, complete cds	1.62
GU111914.1	Glomus intraradices ornithine decarboxylase mRNA, complete cds	0/53 ^x
GU111915.1	Glomus intraradices urease mRNA, complete cds	-1.37
GU111916.1	Glomus intraradices NADH-glutamate synthase mRNA, partial cds	-11.48
GU111917.1	Glomus intraradices carbamoyl-phosphate synthase mRNA, partial cds	-8.99
GU111918.1	Glomus intraradices arginosuccinate lyase mRNA, partial cds	-5.60
GU111919.1	Glomus intraradices nitrate transporter mRNA, partial cds	-2.61
HM143864.1	Glomus intraradices culture-collection DAOM:197198 sugar transporter (MST2) mRNA, complete cds	-0.06
HM998615.1	Glomus intraradices secreted protein SP7-v.0.9Kb (SP7) mRNA, complete cds, alternatively spliced	-13.35
HM998616.1	Glomus intraradices secreted protein SP7-v.0.8 Kb (SP7) mRNA, complete cds, alternatively spliced	-12.19
HM998617.1	Glomus intraradices secreted protein SP7-v.1.2 Kb (SP7) mRNA, complete cds, alternatively spliced	-11.25
HQ848965.1	Glomus intraradices sugar transporter (MST4) mRNA, complete cds	-5.29
HQ848966.1	Glomus intraradices sugar transporter (SUC1) mRNA, complete cds	-6.38
HQ896039.1	Glomus intraradices strain BEG158 phosphate transporter (PT) gene, partial cds	-11.40
L77908.1	Glomus intraradices chitin-UDP acetyl-glucosaminyl transferase 1 (CHS) gene, partial cds	-5.61

^x: Log₂-fold changes could not be calculated if 0 reads were found in either of the libraries. If that was the case, the normalized reads are given.

7.3.1 The coding sequence of the following *R. irregularis* genes have been confirmed:

Green: transcontigs assembled from the Illumina reads.

Red: corrections to the genomic Sequence given in the *R. irregularis* genome DB.

The contig IDs, the genome IDs and the transcript names/ annotations are given.

comp8571_c0/ e_gw1.2824.2.1/ *RiMFS1*

ATGAATTCTAAAAAAATTTTCGTTTCGTCTGAAGAAAATATACGAATTCGGAGGAGGAACGAGAACGTTTTCTGTACCA
TCAAGTCCAGATAATATTACTAAAAGGAATCTTTTTCGGATGATGATGATAATGCGGATATTATAATACGTGAAGAA
AATGATGATATTGATTCTAATTTATTGGCAGATATTGAAATTGTAAAAGATCAATACGAAGAATTGGATAATATTATTCA
AGCATCGGAATGGGAAATTTTCAAAAACGATTATTGGTACTTTGTGGATTGGTTGTTATCAGATGCTTTGTGGATGATG
GTACATTAATATTTAGGATTTAGTGCCTTATTTATATATTGTTTCTTAATGTTTTACTTTCAAATTCAAATATTTAATAATTT
TCAGTGCCTAGCAATAATATTACCTCGAGTTCAAGTTCACCTTCAAGTACCAAATTCATTATTGGATTACTTTCAAGTTCA
CAATATTTTGAATGATGTTTGGAGCCGTGTTTTGGGAATAATTTTCAGATACATATGGACGCAAACAGGCGTTCAGCTG
GACACTAGGATTGTCCGATTTTTTGGTTATATTGCAAGTCTTCTCAAAGCTTTGAACAATTATGTTTTCTATTTTTCATGTT
AGGATTTGGTGTGGAGGAAATTTACCAGTAGATGGAGCGATATTTTTGGAATTTGTACAAAAGAGAATCAATATCTTCT
TACTTTGTTATCAGTTTTCTTTGAATTTGGAGCTGCATTACAGCTTTAGTTGGATATTTAATTTTACCTTCATATAGTTGTTT
TAAAGAAGGTTGTGATGTTTATAAAGAAAATAATGGTTGGAGATACGTAATAATGATTCTTGGAACTTGCACGTTAATTAT
GTTGATCATCAGAATCTTTTCTTTAGACTTTTGAATCACCTAAATTTTTATTATCACATAATCGAAAACAAGAAGCAATTT
TTGTATTTCAAGAAATGCAAGAATTAATGGAAATGAAATTCATCTTGATAATTTATCATCACCTAAACATTCAA
CGTATCACCAGAATCAAATAGAAATTTCAATAAATCTAGCATTCTTTCAACACAAAAATTTAGTTCATTATTTAATGATTTG
AAATATTTATTTAAGAAGCAATGGATAACAACAACAATGATTGTATGGAGTATGTGGGGAGTAATATCATTGGAAGTGT
AATGTTAATCTTTATCTTCTAAATATCTTGAAACTGTGAGTAAAGAAGAAAATAAAGAACATAGTGAAGGTGGCGAAG
CTATTAGGAAAGGTTGAAGGGTTTTATGATTTTTCAATATGGGGAGCTCCGGGTGCTATAATTGCATCATATTTAATTG
AAACGATTTTAGGTAGAAAAGGTGCAATGATTATAGCGGCAACCGGAGTTTCTTTATCAACATTTTTATTGCGAATTTTC
ATCATCATTATAGTGTAGTTCTATTTTCAATGATTATTGGTATTTAAAATCTGTTAATTGGTCCGTAATTTATTGTTATACTC
CTGAAGTTTTGAGACTAAAATAAGGGGAACTGCTTGTGGAATCTCTTCTGTTTTGCTAGAATTACCGGTATGATTTGCTCC
TATTATTACCGAACTTTAATTTCTCTGAGTGTCTGCACCATTATATGTAACCTCATTGTTTTTGGTATATTGGCAATTTT
AGTATTTATGTTACCAATAGAAAACAAGAGGAAGGCAGGCATAA

comp11677_c0/ gm1.11960_g/ *RiSut1*

The contig was 100% in agreement with the corrected sequence (i.e. the sequencing results of the amplified cDNA)

ATGGAGGAGCTTAATCAACCTCCCTCGAAAATGCTTCAAAAAGTACCGCAACAGCTGATCTGGAATCAAATCAAGAAA
TAAAAATATAGAGTTAATGCTCAAAATCCGTGGAAATTATTAACCTCGATTAATAAACAACAAGGACTTACTTTTGTCTGC
AGCATTTTTAGGATGGACATTAGATGCTTTTGTATTTTTACTGTGGTATTATCTGTACCTTATATTGCAAAAAGAAATTCGAA
CGGAACCATCTGTAATTACTGGAAGTATAACGATTACGTTGTGTTACGTCCATTGGGGCAGCAATATTTGGTCTGTTAG
CAGATCGTTATGGTAGAAGATATCCATTAATGGCAGATATTATTCTTTATAGTGTTATGGAATTAGCTTCAGGGTTTGTCTC
AAATTTTTTGGTCTCTTTATCTTAAGAGCAATTTTTGGAATGCTATGGGAGGTGAATGGGGATTAGGCACGGCATTGGC
GATGGAAGTCTTACCACCAGAACTCGCGGATTTTTCCGGTATTTGAAACAAGGTTATGCTGTAGGATTTCTTTTAGCAT
CAATTTTATATTATGTTGTGATAGAAAATATTGGATGGAGGGCAATGTTTTGGATAGGTTCAATTCGGCTCTTTTGGTTGT
TTAATTCGTTTCTTTGTACCGAATCACCCGTTTGGAAAGCTCATCGAATGCTAGAAAATCAGGTGGCAAAAATTTTCTG

TCTAGCACTAAATTAGCGTTAAA **G**CATCATTGGAAAAAGTTCATATATTGTGTTCTATTAATGTCTGTTTTAGTTTTATGA
 GTCAT **GGTACACAGGATTTATATCCAACCTTCTTAAAAACACA**CTTGGATTACACAGCTCAAGTTACAATTCTTACAGT
AGTAGCAAATATAGGAGCTATAATTGGAGGCTCGATTTGTGGATTTTGTCACAATTATTTGGTCGTAGGAAAATTTTT
CATTTTCGGTTGTTTTAGCAGCATGTTTTATGCCATTATATATATTACCAAAGAATTTTGGATTATTGATTGTTGGAGCTTTTG
CTGAGTACTTTTGTGTTCCAGGGGGCATTGGGAATCGTCCAGCGCACTTAAACGAACCTTACCACCAGAATTTCTGGGCA
 CGTCCCAGGATTAACCTATCAATTGGGTACTTTAGTAGCGTCATCATCAGCACAAGTTGAAGCAAATTAGGAGAAATAT
 TAAAAAAAATGGAA **T**ATATAATTATGG **GAT**AGTTATTGTT **G**TGTTATCTCTTATTGTTATGACGTTGTAGCACTGTTAA
 TATACTGGG **T**AAAGAAAATAAAGATGCAAATTCATCGAACAAAGTTGAAATCGTCGAACAAATTACGGTTAATGATAAGA
GTAAAGAAAAGGAACTGAACAGGATGAAAAAGTAGCGGTTACCATAAAAAGATATTTAA

comp2270_c0/ gm1.366_g/ RiMFS2

ATGAGTAACAAGAATAATGCC **A**CGATACTACCTTCTCTCATGATGAGAAACATAATATTACCATGTTTCATTATAGG **T**ATCA
 TGTGCTT **C**AAATTTGCCTTT **G**AGAGTCTTAGTTCATCCATTTCTTT **C**CTAGCTCAGGAAAAGTTTGCGAAATCTATAGCTCTT
 ACT **A**TGAC **A**CCCGTTTT **A**ACATCATGTTTTAATAATGCAATGATTTG **C**TCTATTGGAGCTGCACAACCTTT **T**GGTACGATT
 TCGGACAAACGTTATATTAGCGTTCAGTATGTTTTGTTTCGGAGCACTTGCTCT **A**ATTCTCATTATTGTTGATGC **G**CAACT
 GGTGGTAAATTTGAAAGTCAAGGTAATTGGACCCCTTGATCCTTTTCCCAATATACCTTCTATGGGAGGCTGTCTTGGA
 GTTTTGGAGCTCGTTAGGCGTGTCTT **A**CCCTCGTATATCGTTGGTGAAAATCCAGAAAA **C**TAAAAAAAATGGACGCACA
 CGTACAT **A**TCTTTTATGAAATTGCTGGAACCTTCTGGAGCTTTCGCAACTACTCCCTCGTTAAGAAGATGGGCCCGTTTAC
 GCTT **A**ATGCTTATTCCAATTCTGTTCACTGT **T**GCTGGTTTTAT **C**TGGCT **A**AGAATTAACATAA **C**CC **A**AAT **G**CACCTTCAGA
 TATCAATAGAAATAAAGAAA **T**TGATAGTT **C**AGATCGAAAGAA **C**ATTTTCTACTTATATTTTTACTCCGTAAAACGTGG **C**GC
 ACAAATCGTTTTTTCGGAACGTCGATTATCTGGCTTATGGGAGGCTATGTTTT **A**CTTTTCGTCTTCCACAGATTCAATGAG
 AACGTTATCTTCCAACATTTGCAAATCAAGTTCTCAAAGAAAAGTCTTACTTATATCCTTCTTAGGAGCATCTAA **T**TTTGG
 AGAACTTCTGGTGCA **C**TTGTCGTTCTCTTATTGCT **G**CAAAAGTTGCCACCCCTCTACCTTGGGTTG **C**TTTGACGCCGTT
 GCTT **A**ATGACTCTGGATATTTCCCTTTTACCCGTTAAAT **C**CGCACTTTCATGGGCTTTGAGTGC **A**CTT **C**CACTTATGAT
 CGTTCTTTC **A**TGGGATGGGCAGCTGGTGA **C**GTTTCTCTCGTGGCCTATAT **A**CAATCTAGATTGCATT **C**AGTTAATAT **C**CAA
GCAGATGCGGGTACTT **C**ACCACCTTGGATGTGTCATGGCTTTCTTTATTCTTCATATATCATCGTCTTTACA **G**TTCTCTCAAT
TCC **G**CTTGAAGAGTTTTT **G**ATGCATATAAGG **C**ACT **G**TAATATAAATCA **A**GC **G**TTTTTATATATTGCAGGA **A**TTATGAT
AACTGTTGGTGCA **G**TTGTTAT **A**TTTGAAGCACTTTT **A**TACCAAGGCACTCGTGGGCTTTAATCCAAGGTTGATCCTGAT
GATGA **A**ATAGCAGCTAGTGAAGAAGAAGTTAAAGGAGAAAAAGAAAAGG **C**ACTGTCAATCTCGTCGAAGCTATA
AGCATGGCCTAA

The altered nucleotides resulted in a slightly changed amino acid sequence of the translated sequence:

MSNKNNA **H**DTTFSHDEKHNITMFIIGIMCFKFAFESLSSSIFLAQEKFAKSIALTMTPVLTSCFNIMQCICSIGAAQLLVRFRNTV
 ILAFSMFCFGALALI **L**IIVDA **T**TGGKFESQGNWTPWILFPIYLP **M**GGCLGVLELVRRVLP **R**DIVGENPEKLLKMDAHVHIFYEIA
 TSGAFATTPLVKKMG **P**VYALMLIPILFT **V**AGFIWLRIKHNP **N**APSDINRNKEI **D**SSDRKNIFYLYFYSVKRGAQIVFSERRFIWLM
 GGYVLPFV **F**HRIENVIFPTFANQVLKEKSYI **L**LGASNFGELLGAL **L**VLLFA **A**KVATPLPWV **R**FDAVALMTLWIFPFLPVKSALS
 WALSALPLMIVLSMGWAAGDVSLVAYIQSRLHSVNIQADAGTSP **L**GCVMFLYSSYIIVFT **V**LSIPLGRVFDAYKA **T**GNINQAF
 YIAGI **M**ITVGAVVIFASTFI **P**RHSWAFNPKVDP **D**EIAASEEEVKEKEK **G**TVN **L**VEAISMA

8 ACKNOWLEDGEMENTS

DANKSAGUNG

An erster Stelle möchte ich mich bei Frau Prof. Dr. Franziska Krajinski für die Bereitstellung dieses Themas und die tolle Betreuung bedanken. Vielen Dank für die Unterstützung und Hilfsbereitschaft und für das Vertrauen - von meiner Bachelorarbeit über die Masterarbeit bis zur Promotion!

Vielen Dank an Herrn Prof. Dr. Ralph Bock für die Übernahme des Erstgutachtens und an Prof. Dr. Daniel Wipf, Prof. Dr. Francis Martin und Prof. Dr. Thomas Boller für die Bereitschaft, diese Arbeit zu begutachten.

Vielen Dank an die Mitglieder meines Thesis Komitees Prof. Dr. Ralph Bock, Prof. Dr. Lothar Willmitzer und Dr. Dirk Walther für die hilfreichen Anregungen und ausführlichen Diskussionen!

Ein riesengroßes Dankeschön geht an alle aktuellen und ehemaligen Mitglieder der AG Krajinski für die allerbeste Arbeitsatmosphäre, die Unterstützung im Laboralltag, entspannte und lustige Mittagspausen, Suppentage, Schokolade und den gemeinsamen Spaß bei der Arbeit. Anja, Amelie, Christoph, Dani, Dany, Derek, Emanuel, Julia, Nicole, Silvia und Vinz: Ihr wart super! Mein Besonderer Dank geht an Dani Sieh und Nicole Gaude, meine liebsten und weltbesten Labor- und Büronachbarinnen! Danke dafür, dass ihr mir immer mit Rat und Tat zur Seite gestanden habt, für jeden entspannten ersten Morgen-Kaffee, für die Unterstützung beim Schreiben und das Korrekturlesen dieser Arbeit!

Vielen Dank auch an alle anderen (ehemaligen) Mitarbeiter des MPI-MPs, die mich im Laufe dieser Arbeit unterstützt haben. Mein besonderer Dank geht an Dr. Dirk Walther und Dr. Samuel Arvidsson für die großartige Hilfe bei der Auswertung meiner RNA Seq Daten und Dr. Joachim Kopka, Alexander Erban und Ines Fehrlé für die Metabolit Messungen! Danke für eure Geduld!

Darüber hinaus geht mein besonderer Dank an meine Freunde! An alle Potsdamer- Danke für die Ablenkung nach langen Arbeitstagen und dass ihr dafür gesorgt habt, dass ich mich hier zu Hause fühle. Und an meine Hannoveraner, dafür dass ihr schon seit Jahren immer da seid und für die allerbeste Ablenkung, die man sich an den Wochenenden zu Hause nur wünschen kann ;) ...oder bei Urlauben und Kurztrips ;)

Mein allergrößter Dank geht an meine Familie! Ihr habt es ermöglicht, dass ich es bis hier her geschafft habe! Ganz besonders möchte ich mich bei meinen Eltern und meiner Schwester für die permanente Unterstützung bedanken und dafür, dass ihr mich aufgebaut, angetrieben und an mich geglaubt habt! Und danke, Papa und Julle, fürs Korrekturlesen!

9 EIDESSTATTLICHE ERKLÄRUNG

Ich versichere hiermit, die vorliegende Arbeit selbstständig angefertigt und keine anderen als die angegebenen Quellen und Hilfsmittel verwendet zu haben. Ich versichere ebenfalls, dass die Arbeit an keiner anderen Hochschule als der Universität Potsdam eingereicht wurde.

27.05.2013

Nina Duensing